

Chapter 1

LIQUID CRYSTALS FOR ELECTRO-OPTIC APPLICATIONS

S. M. Kelly

Department of Chemistry, University of Hull, Hull HU6 7RX, UK

M. O'Neill

Department of Physics, University of Hull, Hull HU6 7RX, UK

Contents

Introduction	2
1. Electro-Optic Response of Liquid Crystals	3
2. The Liquid Crystalline State	4
3. Physical Properties of Liquid Crystals	5
3.1. Optical Anisotropy (Birefringence)	5
3.2. Dielectric Anisotropy	7
3.3. Elastic Constants	8
3.4. Viscosity	8
3.5. Spontaneous Polarization	8
4. Liquid Crystal Display Devices	10
5. Addressing Methods for LCDs	11
5.1. Direct Addressing	11
5.2. Multiplex Addressing	11
5.3. Active Matrix Addressing	12
6. Alignment Layers	12
7. Compensation Films for LCDs	13
8. Electrically Controlled Birefringence LCDs	15
9. ECB-LCD Configuration	15
9.1. Off State	15
9.2. On State	15
10. Nematic Materials of Negative Dielectric Anisotropy	16
11. Twisted Nematic LCDs	18
12. TN-LCD Configuration	19
12.1. Off State	20
12.2. On State	20
13. Nematic Materials of Positive Dielectric Anisotropy	21
13.1. Nematics for Direct Addressing	22
13.2. Nematics for Multiplex Addressing	25
13.3. Nematics for Active Matrix Addressing	30
14. Supertwisted Nematic LCDs	34
15. STN-LCD Configurations	34
15.1. Bistable Liquid Crystal Twist LCDs	34
15.2. Supertwisted Nematic Guest-Host LCDs	35
15.3. Superbirefringent Effect LCDs	35
15.4. Supertwisted Nematic LCDs	37
15.5. Optical Mode Interference LCDs	37

*Handbook of Advanced Electronic and Photonic Materials and Devices, edited by H.S. Nalwa
Volume 7: Liquid Crystals, Display and Laser Materials*

Copyright © 2000 by Academic Press

All rights of reproduction in any form reserved.

16. Electro-Optic Performance of STN-LCDs	37
16.1. General Electro-Optic Performance of STN-LCDs	38
16.2. Temperature Dependence of Electro-Optic Performance of STN-LCDs	38
17. Interference Color Compensation	38
17.1. Double-Layer Supertwisted Nematic LCDs	38
17.2. Film-Compensated STN-LCDs	38
18. Nematic Materials for STN-LCDs	38
18.1. Polar Nematic Materials for STN-LCDs	39
18.2. Apolar Nematic Materials for STN-LCDs	42
19. Surface-Stabilized Ferroelectric LCDs	46
20. SSF-LCD Configuration	46
20.1. Dark State	46
20.2. Bright State	46
21. Smectic C* Materials	47
21.1. Ferroelectric Smectic C* Mixtures of Optically Active Components	47
21.2. Ferroelectric Guest-Host Chiral Dopant-Smectic C Host Mixtures	51
22. Conclusions	59
References	61

INTRODUCTION

Liquid crystals have found wide commercial application over the last 25–30 years in electro-optical flat panel display (FPD) devices for consumer audiovisual and office equipment, such as watches, clocks, stereos, calculators, portable telephones, personal organizers, notebooks, and laptop computers. There are many other applications for liquid crystal displays (LCDs), such as information displays in technical instruments and in vehicle clocks, speedometers, and navigation and positional aids. They are also used in low-volume, niche products, such as spatial light modulators and generally as very fast light shutters. More importantly, they have come to dominate the displays market in portable instruments due to their slim shape, low weight, low-voltage operation, and low power consumption. LCDs are now starting to win market shares from cathode ray tubes (CRTs) in the computer monitor market. The market share of LCDs in the total market for displays is expected to significantly increase over the next decade. There are a number of existing competing FPD technologies, such as plasma displays (PDs), vacuum fluorescence displays (VFDs), inorganic light-emitting diodes (LEDs), and micro mirrors (MM). However, these have relatively small shares of the overall displays market. There are also a series of promising technologies in development, such as organic light-emitting diodes (OLEDs), light-emitting polymers (LEPs), and field emission displays (FEDs). The first production lines for LEP technology were recently commissioned. However, the value of LCDs is still expected to exceed that of the CRT tube in the near future. Manufacturing facilities for FPDs are very capital intensive. For example, a plant for twisted nematic LCDs with active matrix addressing can cost upward of \$1 billion. As a consequence of the capital already invested in LCD plants, it will take many years for competing technologies to gain a significant market share in the displays market in general. In particular, LCDs can be expected to maintain a dominant position in portable applications.

The successful development of LCD technology was dependent on parallel developments and progress in an unusual combination of scientific disciplines such as synthetic organic chemistry, physics, electronics, and device engineering. These include improvements in batteries, polarizers, electrodes, complementary metal-oxide semiconductor (CMOS) drivers, spacers, alignment layers, and nematic liquid crystals. These developments were made in response to a clear market requirement for a low-voltage, low-power-consuming flat panel display screen for portable, battery-operated instruments

to display graphic and digital information of ever increasing volume, speed, and complexity. In this chapter, we attempt to illustrate this development using the three most important types of LCDs currently in large-scale manufacture. We also describe ferroelectric LCDs, which have the potential to become a major commercial product, to illustrate the problems to be overcome before an LCD technology can be successfully established in the displays market. All of these technologies can be incorporated in gels and polymer-dispersed LCDs. Therefore, they will not be dealt with here in any detail, because the general principles of operation are essentially the same.

The historical development of these types of LCDs is illustrative of the general dependence of consistent improvement in the performance of LCDs as a consequence of the invention, laboratory preparation, evaluation, scale-up, and then large-scale manufacture of liquid crystal components and mixtures. This development is described in detail herein.

Light shutters with very fast response times ($<1 \mu\text{s}$) that utilize the orientation of an organic material in an electric field applied perpendicular to an incident beam of light do not need to use liquid crystals. The Kerr effect relies upon the macroscopic alignment of polarizable molecules in an electric field to produce an induced birefringence Δn from the isotropic liquid. The magnitude of the induced birefringence depends upon the strength of the applied field, E according to

$$\Delta n = \lambda B E^2 \quad (1)$$

where λ is the wavelength of incident light and B is the Kerr constant. The amount of light transmitted through a cell with crossed polarizers is dependent on the optical retardation δ induced by the organic medium under the action of the applied electric field, and is given by

$$\delta = \frac{2\pi\Delta n d}{\lambda} \quad (2)$$

This effect is based upon a field-dependent birefringence and can also be found for calamitic liquid crystals above the clearing point in the isotropic liquid. However, the birefringence produced in the liquid crystalline state with similar permanent dipole moments can be up to 4 orders of magnitude greater, due to the stabilizing effect associated with the shape anisotropy. An effect similar to the Kerr effect, but utilizing the dielectric interaction of an applied electric field with an organic medium in the nematic phase (rather than the

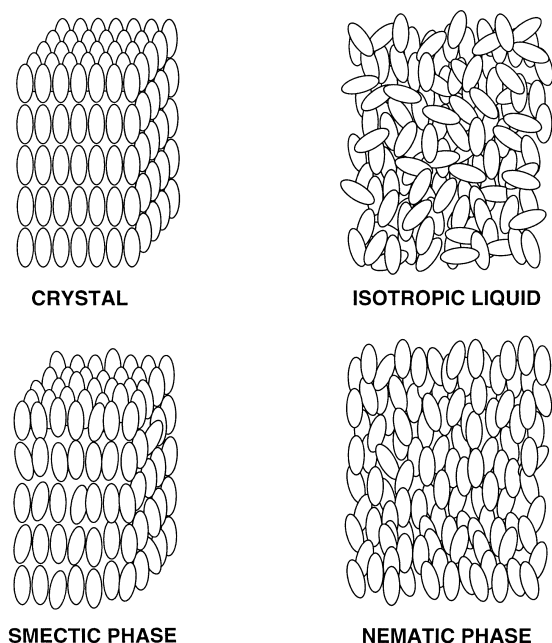


Fig. 1. Schematic representation of the structures of a solid, a smectic phase, the nematic phase, and the isotropic liquid state formed by calamitic organic molecules with a large length-to-breadth ratio.

isotropic liquid) is the basis of the vast majority of liquid crystal displays manufactured at the present time.

A whole range of materials exist in some form of liquid crystalline state under certain conditions [1–3]. Small molecules with rodlike “calamitic” liquid crystals with a relatively large length-to-breadth ratio tend to exhibit nematic and smectic phases (See Fig. 1). Only organic calamitic materials that exhibit the nematic or smectic phases as a function of temperature are considered here. Lyotropic liquid crystallinity produced by the action of a solvent on a solid material, such as carbohydrates in water, are not be dealt with here [4–9]. Lyotropic phases also exhibit a temperature dependency, and some materials may be amphoteric; that is, they exhibit thermotropic and lyotropic phases, such as certain phospholipids [9]. Furthermore, the electro-optic applications of liquid crystalline polymers have been described in depth elsewhere [10–14] and are not discussed here. Laser-addressed displays that incorporate side-chain liquid crystal polymers for high-information-content displays (such as maps and ferroelectric side-chain liquid crystal polymers for lightweight displays, including heads-up displays for pilots) have been developed for military customers. However, liquid crystalline polymers have yet to find wide commercial acceptance in the consumer displays marketplace. The vast majority of electro-optical instruments that incorporate flat panel displays utilize LCDs that incorporate a thin film of a nematic liquid crystal, whose optical properties are modulated by an electric field [15]. These form the main part of the discussion here [16–25]. However, LCDs based on some unique properties of smectic liquid crystals have the potential to overcome some of the limitations [25], and these will also be discussed here, although they are not manufactured in bulk despite decades of intense research and development.

1. ELECTRO-OPTIC RESPONSE OF LIQUID CRYSTALS

Three distinct physical phenomena [26–28] associated with the nematic state can be manipulated by an electric field in different

LCD geometry to modulate the intensity of light passing through the cell in the activated (select) and nonactivated (nonselect) states. (This will be discussed further later.) A very wide variety of commercial and prototype LCDs have been developed based on these three related, but different, effects. Although the utilization of liquid crystals in flat panel display devices began in the late 1960s, the effects of magnetic and electric fields on nematic liquid crystals have been investigated since the beginning of the 20th century [16–19]. The first practical electro-optical flat panel LCD that used any kind of liquid crystal as the switchable light valve device was reported by Heilmeyer, Zanoni, and Barton [29, 30] at the RCA Laboratories in Princeton, New Jersey in 1968. The switching is due to the movement, under the action of an electric field, of a small number of ions within the nematic liquid crystal that gives rise to electrohydrodynamic instabilities [31, 32]. The stirring effect of an electric field on nematic liquid crystals had already been observed in the 1930s [17] and lead to the formation of visible domains, known as Williams domains, at low voltages and light scattering above a higher threshold voltage [19]. The RCA display appears black when there is no applied voltage. The interaction of the electric field with the ions gives rise to turbulence in the liquid crystalline medium [32], resulting in the movement of areas of liquid crystal in alternate directions to produce visible stripes referred to as Williams domains [19, 33]. The shear produced by this electrohydrodynamic effect is counterbalanced by the elastic and dielectric torques under steady state conditions. At higher fields, these stripes are replaced by a homogeneous scattering of incident visible light, so the display is bright. Although liquid crystals are generally regarded as dielectrics (i.e., nonconductive, insulating organic materials), the conductivity required for the formation of electrohydrodynamic instabilities is relatively low ($10^{-9} \Omega^{-1} \text{cm}^{-1}$).

For the vast majority of calamitic nematic liquid crystals of high resistivity, the application of an electric field results in an orientation of the nematic director either parallel or perpendicular to the field, depending on the sign of the dielectric anisotropy of the nematic medium [15, 34, 35]. The molecules align themselves with the molecular axis of greatest polarization parallel to the field. The dielectric realignment of the nematic phase caused by an electric field can be described by the same equations used to define the effect of magnetic field on a nematic liquid crystal, with appropriate modifications to allow for the different nature of the field. This realignment is due to dielectric coupling between permanent and induced dipoles in the liquid crystal molecules with the electric field, and corresponds to the Kerr effect manifested in the nematic state, but is of much higher magnitude. This concept is the basis of most LCDs manufactured at the current time and includes the majority of LCDs [20–28] that use nematic liquid crystals.

The third physical property manifested by calamitic nematic liquid crystals is flexoelectricity, which corresponds to piezoelectricity in crystals. It is postulated that banana-shaped or wedge-shaped liquid crystals give rise to a bulk curvature electric effect under certain boundary conditions. Although this effect was predicted in the late 1960s [36] and experimentally confirmed many years ago [37], LCDs that utilize this effect (such as the bistable nematic displays [38–40]) are only just now being developed for the flat panel displays market. As such, they will not be discussed here.

Smectic liquid crystals have been used in commercial LCDs to a much lesser extent. They are based on different physical phenomena, which are associated with the layer structure of smectic liquid crystals, to generate an electro-optical effect. The most important of these physical properties is ferroelectricity [41–46]. This can be manifested by optically active rodlike molecules organized in fluid layers, such as a chiral smectic C^* phase, where the molecular long axis is tilted with respect to the layer normal (See Sects. 3.5 and 19). Soon after the initial discovery [41] of ferroelectricity in chiral smectic liquid crystals, it was predicted [42] that the suppression of the helix of a smectic C^* phase by surface forces in very thin layers between two glass electrodes would pin the molecules in their positions and allow

switching between two energetically equivalent polarization directions, thereby giving rise to an electro-optic memory effect. This is the basis of the electro-optic display device called the surface-stabilized ferroelectric liquid crystal device (SSF-LCD) [43], which uses ferroelectric liquid crystals (See Sect. 1.19). In the SSF-LCD, the helix is suppressed by surface forces if the cell gap is considerably lower than the pitch of the smectic C* helix. Therefore, long-pitch smectic C* materials are used. Compounds that exhibit the smectic C* phase are chosen due to the low rotational viscosity (γ) of this phase compared with that of the more ordered tilted smectic phases. Deformed helix LCDs [44] and antiferroelectric LCDs [45] also have great promise, because prototypes exhibit improved shock stability and the absence of ghost images associated with SSF-LCDs. The smectic A* phase exhibited by optically active materials can be used in an electroclinic effect [46] which is very similar to electrically controlled birefringence (See Sect. 8). It is of great interest for spatial light modulators in optical computing. However, these types of LCDs, that utilize smectic liquid crystals are not discussed here, due to space constraints.

Anisotropic gels are (at least) two component systems derived from a polymer LC network matrix and lower-molar-mass liquid crystals [47–49]. They are produced by the *in situ* polymerization of an oriented nematic or smectic liquid crystal mixture consisting of a small amount (e.g., < 5 wt.%) of liquid crystalline monomers with at least two polymerizable groups, such as diacrylates, in the presence of nonpolymerizable, low-molar-mass liquid crystals without reactive units, typically cyanobiphenyl mixtures [50–53]. These liquid crystalline gels are much more stable to external shocks and, therefore, the textures are also stabilized. Droplets of liquid crystal can be formed by phase separation at higher concentrations of polymer. The droplets then respond to an external electric field in what is referred to as polymer-dispersed LCDs [54–56]. In principle, all LCD types can be reproduced as a gel-stabilized or polymer-dispersed LCD.

2. THE LIQUID CRYSTALLINE STATE

There are a number of very early reports in the literature [3, 4] of the strange melting behavior and appearance of some naturally occurring compounds—either as pure compounds or as gels in water—that have now been shown to be thermotropic or lyotropic liquid crystals. The former are formed under the action of heat (See Fig. 1) and

the latter in conjunction with a solvent such as water. However, the true nature of these materials was not suspected at the time. Therefore, the discovery of the liquid crystalline state is usually attributed to the botanist Reinitzer [57] from the Institute for Plant Biology of the German University of Prague in 1888. He was attempting to determine the exact chemical formula of cholesterol extracted from plant sources, so he synthesized the acetate and benzoate derivatives of cholesterol isolated from human gallstones. While determining their melting points in capillary tubes, he noticed the reflection colors of their melts, as had others before him for other cholesterol derivatives. However, he also noted that samples of cholesteryl benzoate (**1**) seemed to melt at 145.5 °C and form a cloudy opaque liquid, which then appeared to melt again at 178.5 °C and form a clear transparent liquid (See Fig. 2). This second melting point was found to be reversible within a few degrees, whereas the first transition showed a substantial degree of supercooling. The liquid crystalline state Reinitzer observed is now known to be the chiral nematic state (i.e., the helical equivalent, formed by some optically active materials, of the usual nematic state; See Fig. 3). This state was referred to as the cholesteric state for many years, due to its origin. Reinitzer sent a sample to the German physicist Otto Lehmann, who had developed a series of optical polarization microscopes. Lehmann [58] recognized that he was looking at a different state of matter than that of classical solids, liquids, and gases, so he introduced the term *fließende Kristalle*—flowing crystals, or liquid crystals—to describe the materials that gave rise to it. He soon found that some synthetic organic compounds, such as the azoxy compounds shown in Table I, also exhibited liquid crystallinity.

Since the turn of the 20th century, many new synthetic liquid crystals have been prepared, especially in Germany and mostly at the Martin Luther University in Halle [59–61], and since the late 1940s in the United Kingdom at the University of Hull [62–64]. This research was purely academic, because no commercial applications for liquid crystals were known at this time. Many systematic studies soon established the relationships between central linkages, terminal groups, lateral substituents, number of rings, and type of mesophase and transition temperatures, which are still valid today [59–64]. A typical liquid crystal possesses a linear structure with a central core that contains several collinear rings, a linear unsaturated linkage and two terminal chains, as exemplified by the chemical structures [65–73] for compounds 2–16 collated in Table I. It was known that short chains favored the formation of the nematic state. The combination of one short alkyl chain on one ring and a polar substituent on the other

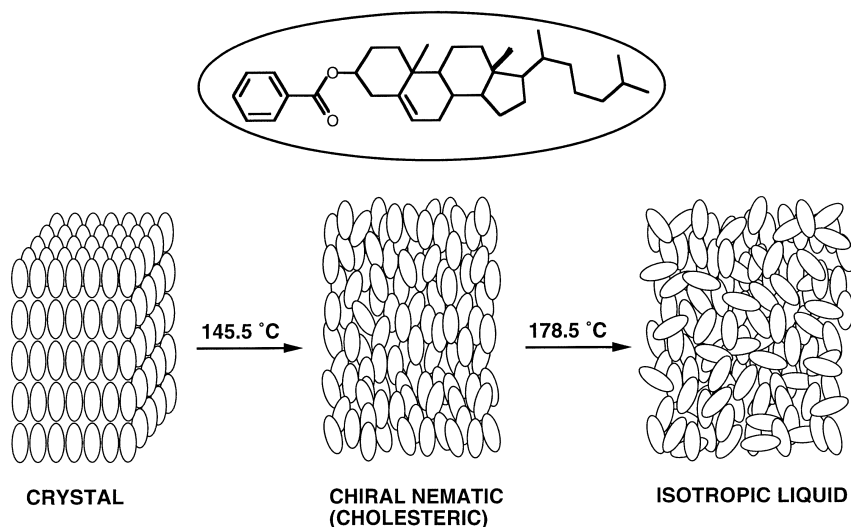


Fig. 2. The chemical structure of cholesteryl benzoate and a schematic representation of the melting of crystalline cholesteryl benzoate **1** [57, 58] at 145.5 °C to form a chiral nematic (cholesteric) phase, which, in turn, forms an isotropic liquid on further heating to 178.5 °C.

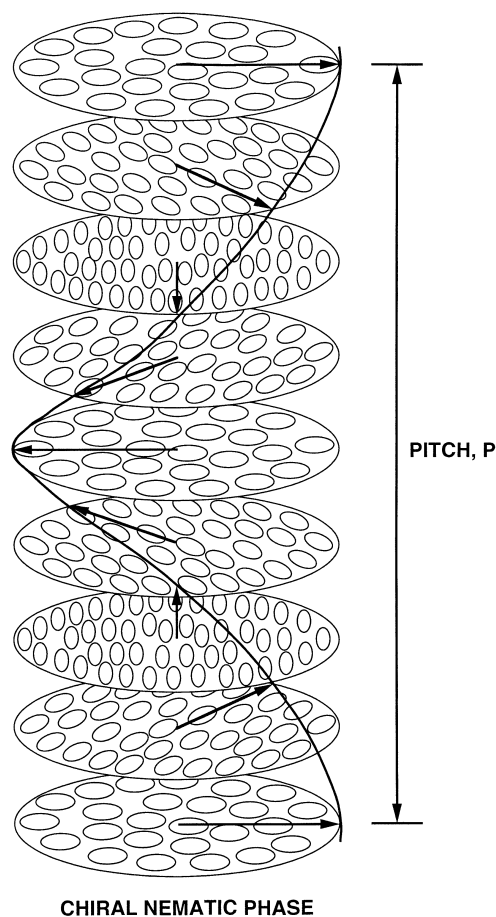


Fig. 3. Schematic representation of the periodic helical structures of the chiral nematic (cholesteric) phase. The pitch of the helix corresponds to the rotation of the director through 360° . There is no layered structure in a chiral nematic N^* phase.

was also known to be favorable for nematic phase formation, and an order of efficiency for these terminal polar substituents was reported [62–64]. Therefore, all of the compounds reported in Table I are aromatic with two phenyl rings joined by an unsaturated central linkage to maximize the degree of conjugation and anisotropic polarizability of electron density. The fundamental theories [74–85] that describe the nematic state were developed well before the advent of LCDs. The synthesis of these materials provided physicists with the liquid crystals required to investigate and to determine the anisotropic nature of their physical properties [15, 34, 35], which determine the complex response of the liquid crystalline state to an electric field in LCDs [16–25].

The liquid crystalline state represents an intermediate state of matter between that of a crystalline solid with three-dimensional order at one extreme and a completely disordered liquid at the other. A liquid crystal may exhibit order in one or two dimensions. In the nematic state formed by calamitic organic compounds, with a rodlike or lathelike molecular structure, where the length-to-breadth ratio is much greater than unity, there is a parallel orientation of the long molecular axis of individual molecules. This results in a long-range orientational order, but no positional order. This is the prime factor that differentiates the nematic state from an isotropic liquid. This is shown schematically in Figure 1 and described generally by continuum theory [74–80], which postulates that the director of the nematic state changes continually and gradually throughout the bulk of the

nematic material, although there are many alternative theories for specific interactions and phenomena in liquid crystals [81–85].

The average direction of these long molecular axes at any one point is defined as the director n , where n is identical to $-n$; that is, there is an inversion symmetry axis at any one point along the director. The order parameter S is a scalar quantity and it represents the average orientation of the molecules in the liquid crystal relative to the director and is a macroscopic property [81] defined as

$$S = \langle \frac{1}{2} (3 \cos^2 \theta - 1) \rangle, \quad (3)$$

where θ is the angle between the long molecular axis of an individual molecule and the director. In a completely disordered liquid made up of rodlike molecules, $\cos \theta = 1/3$ and $S = 0$. Conversely, in an ideal macroscopically ordered nematic liquid crystalline state, $\cos \theta = 1$ and $S = 1$. Usually, S lies between 0.5 and 0.7 for a typical compound in the nematic state at a temperature relatively far away from the clearing point (i.e., the temperature at which the compound ceases to exhibit the liquid crystalline state and forms the isotropic liquid). According to the Maier–Saupe theory, S at a temperature T depends only on the reduced temperature T_{red} and is not a molecular property,

$$T_{\text{red}} = \frac{T}{T_{N-I}} \quad (4)$$

where T_{N-I} is the nematic clearing point (See Fig. 4).

3. PHYSICAL PROPERTIES OF LIQUID CRYSTALS

The rodlike shape of liquid crystals means that their physical properties [1, 15, 34, 35] also possess a degree of anisotropy; that is, they exhibit different values when measured parallel or perpendicular to the director [15] (See Fig. 5). Free rotation around the long molecular axis gives an axis of symmetry parallel to the director, so that the values of the physical properties measured perpendicular to the director (i.e., along the y and z axes) are identical; however, they do differ from those measured parallel to the director (i.e., along the x axis). The anisotropic nature of the physical properties of liquid crystals, due to their shape anisotropy, combined with the ability of magnetic and electric fields to influence the bulk spatial orientation of these molecules renders them of such importance to electro-optic display devices. Their fast reorientation under the influence of a moderate electric field is a result of their fluid nature. The physical properties also depend on temperature and pressure, as well as the type of liquid crystal state (e.g., nematic, smectic, columnar) and the degree of ordering in the liquid crystalline state. The anisotropic properties of relevance to LCDs [86, 87] are described in general in the next section. Table II provides an example of typical physical properties.

3.1. Optical Anisotropy (Birefringence)

Aligned calamitic liquid crystals are uniaxial, due to their shape and polarization anisotropy, and are therefore birefringent, exhibiting different properties for light traveling with the electric field propagating parallel and perpendicular to the director or optic axis. Birefringence is a property usually associated with transparent crystals with a non-centrosymmetrical lattice structure (e.g., calcite). The free rotation in liquids averages out any asymmetry of molecular shape and renders the optically isotropic. The electric vector of incident plane polarized light entering a birefringent medium is split into two mutually perpendicular components called the ordinary (o) and extraordinary (e) rays. The electric field of the o-ray is always perpendicular to the optic axis, so its refractive index n_o is a constant independent of propagation direction. The electric field of the e-ray lies in a plane that

Table I. Transition Temperatures (°C) for Compounds (2–16)^a

Compound	Molecular structure	Crystal	Nematic	Isotropic	Ref.
2		• 69	—	•	68
3		• < 25	—	•	68
4		• 49	(• 37)	•	68, 70
5		• 145	—	•	68
6		• 61	(• 25)	•	69
7		• 40	(• 25)	•	69
8		• 118	• 121	•	68, 69
9		• 32	• 47	•	69, 71
10		• 108	(• 70)	•	68

continues

contains the optic axis, so its refractive index $n_e(\theta)$ varies with the ray propagation angle θ with respect to the optic axis according to

$$n_e(\theta)^2 = \left(\frac{\cos^2 \theta}{n_o^2} + \frac{\sin^2 \theta}{n_e^2} \right)^{-1} \quad (5)$$

This relationship is illustrated by the refractive index ellipsoid shown in Figure 6. The birefringence of the medium, $\Delta n(\theta)$, depends on the propagation direction and is defined as

$$\Delta n(\theta) = n_e(\theta) - n_o \quad (6)$$

The maximum birefringence occurs when $\theta = 90^\circ$ (i.e., when the electric field of the e-ray is parallel to the optic axis) and is given by

$$\Delta n = n_e - n_o \quad (7)$$

where $n_e = n_e(\theta = 90^\circ)$. Δn is defined as the difference between the refractive indices for the o- and the e-rays of a fully oriented nematic phase [88] propagating parallel and orthogonal, respectively, to the optic axis of the nematic medium. Most nematic liquid crystals have

positive birefringence ($\Delta n > 0$), meaning that the e-ray is delayed with respect to the o-ray on passage through the material.

Birefringence is responsible for the appearance of interference colors in LCDs operating with plane-polarized light. Interference between the extraordinary ray and the ordinary ray, which have traveled through the medium with different velocities, gives rise to the colored appearance of these thin films. For a wave at normal incidence, the phase difference in radians between the o- and e-rays caused by traversing a birefringent film of thickness d and birefringence Δn is referred to as the optical retardation δ given by

$$\delta = \frac{2\pi\Delta nd}{\lambda_v} \quad (8)$$

where λ_v is the wavelength of light in a vacuum. The retardation is wavelength dependent, so that positive and destructive interference occur at different wavelengths, resulting in the suppression of some part of the visible spectrum, and, therefore, a nonwhite color. Moreover, the birefringence is also wavelength and temperature dependent, because the refractive indices also vary with these parameters

Table I. (continued)

Compound	Molecular structure	Crystal	Nematic	Isotropic	Ref.
11		• 113	(• 53)	•	68, 72
12		• 42	• 77	•	68, 72
13		• 41	• 74	•	68
14		• 46	• 49	•	72
15		• 20	• 47	•	73
16		• 28	—	•	68

^aThe parentheses [()] represent a monotropic transition temperature.

(See Fig. 7). Above the nematic clearing point in the isotropic liquid, the material is no longer birefringent ($n_e = n_o$) and an isotropic refractive index n_i is observed.

3.2. Dielectric Anisotropy

The interaction between a liquid crystal and an electric field is dependent on the magnitude of the dielectric permittivity measured parallel ε_{\parallel} and perpendicular ε_{\perp} to the director and to the difference between them [i.e., the dielectric anisotropy $\Delta\varepsilon$; See Eq. (9) and Fig. 8]. The dielectric permittivity measured along the x axis is unique, whereas the dielectric permittivities measured along the y and z axes are identical. Therefore,

$$\Delta\varepsilon = \varepsilon_{\parallel} - \varepsilon_{\perp} \quad (9)$$

where the dielectric permittivity ε of a material is defined as the ratio of the capacitance C_{mat} of the parallel plate capacitor that contains the material to the capacitance C_{vac} , of the same capacitor that contains a vacuum:

$$\frac{C_{\text{mat}}}{C_{\text{vac}}} = \varepsilon \quad (10)$$

The dielectric constants are dependent on the temperature and the frequency of the applied field up to the transition to the isotropic liquid. Above the clearing point, the dielectric constants measured along all three axes are equal due to the isotropic nature of a liquid and, therefore, the dielectric anisotropy decreases to zero. The

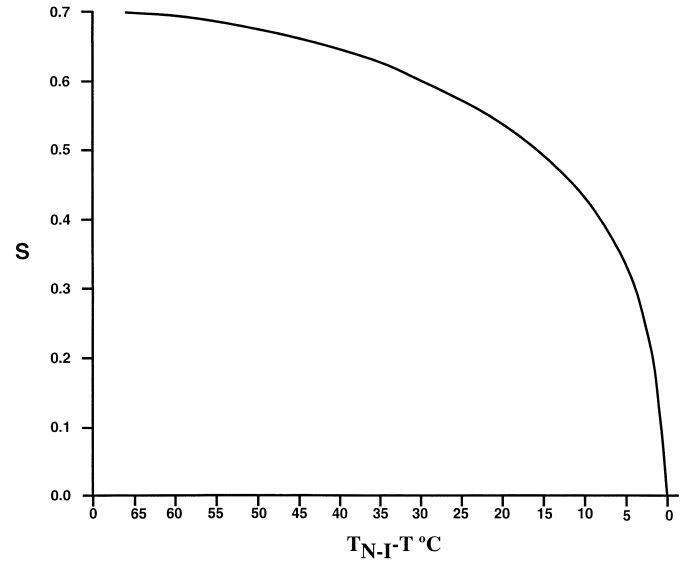


Fig. 4. The dependence of the order parameter S on the reduced temperature $T_c - T$, where T_c is the transition from the liquid crystalline state to the isotropic liquid (i.e., the clearing point) and T is the actual temperature [81].

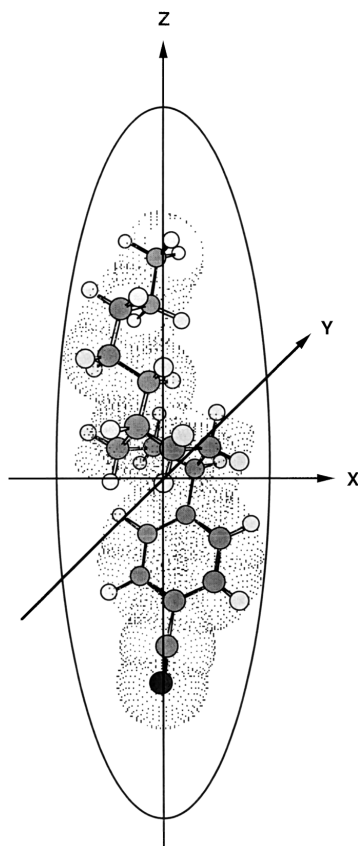


Fig. 5. The molecular structure of a typical nematic liquid crystal with a large length-to-breadth ratio. The breadth of the molecule measured in the x - y plane is symmetrical about the z axis, due to very rapid rotation about the molecular long axis.

resultant dielectric constant ϵ_i is the dielectric constant of the liquid (See Fig. 8). The sign and magnitude of the dielectric anisotropy are dependent on the anisotropy of the induced polarizability, $\Delta\alpha$, and the anisotropy and direction of the permanent polarization attributable to the resultant of permanent dipole moments.

3.3. Elastic Constants

The elastic behavior [76] of a liquid crystal phase under a distorting force, such as an electric field or at an interface with a solid surface is determined by the three elastic constants, k_{11} , k_{22} , and k_{33} that are associated with splay, twist, and bend deformations, respectively (See Fig. 9). The elastic constants are molecular parameters and describe the restoring forces on a molecule within a liquid crystalline phase in response to an external force that distorts the medium from its lowest energy configuration. The elastic constants co-determine the spatial and temporal response of the director to applied external electrical and magnetic fields. They are also obviously important for surface-stabilized electro-optic displays displaced from their equilibrium states by dielectric interaction with an applied electric field. The equilibrium position is then restored upon removal of the field by elastic forces that originate at the surface between the liquid crystal and the orientation layers that cover the device substrates.

3.4. Viscosity

The flow viscosity [89, 90] of the liquid crystalline state is also an anisotropic property, depending on the direction of flow of an

Table II. Typical Values and Symbols for Some Physical Properties [86] of 4-(*trans*-4-Pentylcyclohexyl)benzonitrile **17** [87] determined at 20 °C



Property and symbol	Value and units
Melting point (Cr-N)	30 °C
Clearing point (N-I)	55 °C
Melting point enthalpy	21.35 kJ mol ⁻¹
Clearing point enthalpy	0.96 kJ mol ⁻¹
Density (ρ)	0.9706 g cm ⁻³
Bulk viscosity (η)	22.5 mm s ⁻¹
Rotational viscosity (γ_1)	0.1507 Pa s
Refractive index of the extraordinary ray (n_e) ^a	1.6173
Refractive index of the ordinary ray (n_o) ^a	1.4924
Birefringence (Δn)	0.1249
Dielectric constant parallel to the long axis (ϵ_{\parallel}) ^b	17.5
Dielectric constant orthogonal to the long axis (ϵ_{\perp}) ^b	4.8
Dielectric anisotropy ($\Delta\epsilon$) ^b	12.7
Splay elastic constant (k_{11})	9.6×10^{-12} N
Twist elastic constant (k_{22})	6.5×10^{-12} N
Bend elastic constant (k_{33})	19.4×10^{-12} N
Bend/splay elastic constant ratio (k_{33}/k_{11})	2.03
Bend/twist elastic constant ratio (k_{33}/k_{22})	3.0
Diamagnetic anisotropy (χ)	4.0×10^{-8}

^a Measured at 546 nm.

^b Measured at 1 kHz.

individual molecule with respect to the director at any one point within the medium. Three parameters are required to characterize the viscosity of the nematic state, due to the shape anisotropy of its constituent molecules. These are η_1 , which is perpendicular to the direction of flow, but parallel to the velocity gradient; η_2 , which is parallel to the direction of flow, but perpendicular to the velocity gradient; and η_3 , which is perpendicular to the direction of flow and to the velocity gradient. The bulk viscosity of an unaligned nematic liquid crystal is an average of these three viscosity coefficients [89]. However, individual viscosity coefficients influence the optical response times in an electro-optic display device, due to the constrained anisotropic environment imposed by the boundary conditions and the unidirectionality of any applied electric field. Such an environment is represented by the rotational viscosity γ_1 , which, in the nematic phase, is associated with the movement of a molecule from a homogeneous planar conformation parallel to the cell surfaces to a homeotropic conformation with the long molecular axis (director) perpendicular to the cell walls and parallel to the applied electric field.

3.5. Spontaneous Polarization

In the smectic C phase, the molecules are tilted at an angle θ from the axis normal to the plane of the layer, forming a mirror plane (See Fig. 10). This tilt angle is a molecular property and is the same for all molecules of the same compound in the pure state, although it is a temperature-dependent physical parameter. However, the molecules are free to rotate around the layer normal (i.e., around the zenithal axis) on the surface of cone. The direction of tilt makes an angle ϕ in the azimuthal plane parallel to the layer. The symmetry group is C_{2h} , because of the C_2 axis, which is perpendicular to the molecular axis, and the mirror plane. In the corresponding tilted chiral smectic layers exhibited by a compound with an optically active center,

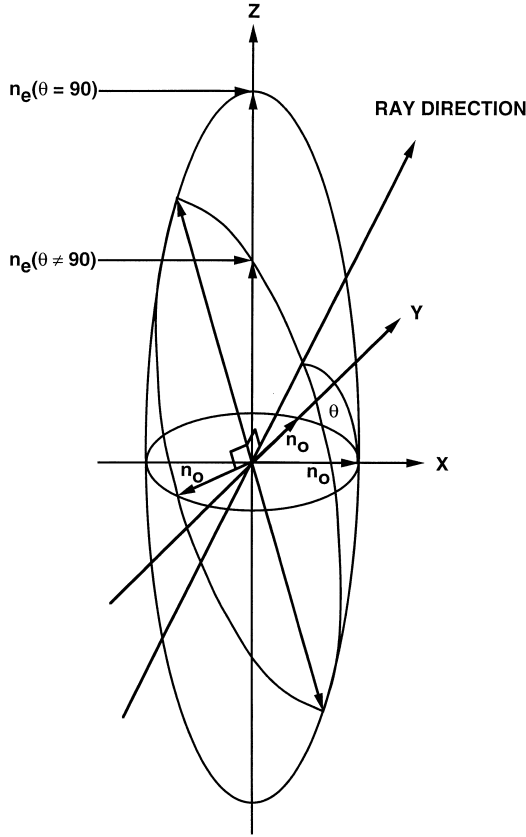


Fig. 6. The refractive index ellipsoid of a uniaxial liquid crystal phase with the optic axis parallel to the x axis. The refractive index n_o of the ordinary ray is independent of propagation. The refractive index n_e of the extraordinary ray is larger than n_o for a liquid crystalline material of positive birefringence [15].

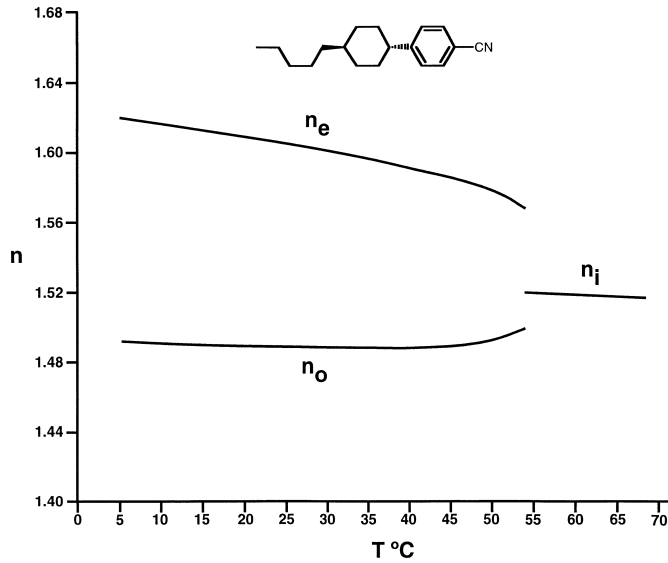


Fig. 7. The dependence of the refractive indices n_o and n_e of the ordinary and extraordinary rays, respectively, on the temperature T for a typical nematic liquid crystal. Above the clearing point T_c (the transition to the isotropic liquid), the birefringence has disappeared and only one refractive index (n_i) is observed [86].

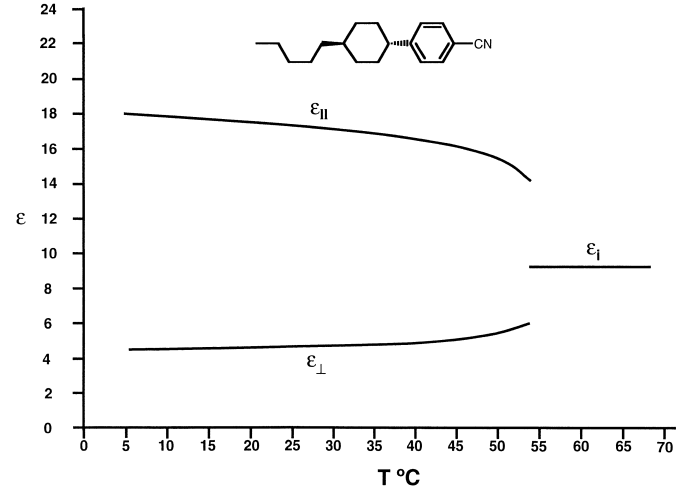


Fig. 8. The dependence of dielectric constants ϵ_{\perp} and ϵ_{\parallel} measured perpendicular and parallel, respectively, to the director, on the temperature T for a typical nematic liquid crystal. Above the clearing point T_c (the transition to the isotropic liquid), the dielectric anisotropy $\Delta\epsilon = \epsilon_{\parallel} - \epsilon_{\perp}$ disappears, and only one dielectric constant, ϵ_i the permittivity (of the isotropic liquid), is observed [86].

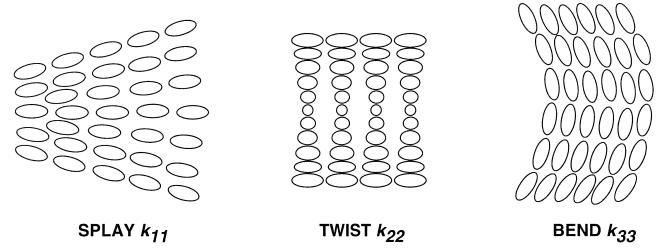


Fig. 9. Schematic representation of the Frank elastic constants k_{11} , k_{22} , and k_{33} for splay, twist, and bend, respectively, of a nematic phase [76].

the chiral and polar nature of the individual molecules give a local C_2 symmetry without a mirror plane. This is in spite of a considerable degree of molecular reorientation about the long axis [41–43, 90–92]. The consequence of this time-dependent alignment of the dipoles along the C_2 twofold axis is a spontaneous polarization (P_o) with a large component parallel to the layer planes and orthogonal to the layer normal. The spontaneous polarization is averaged out macroscopically to zero by the helical superstructure of the chiral smectic C (C^*) phase, with a temperature-dependent pitch p caused by torsional twist and splay deformations, due the chiral nature of the molecules (See Fig. 11). The azimuthal angle ϕ varies linearly with distance along the normal to the layers. However, a permanent polarization arises in a homogeneous monodomain if the helix is unwound by an electric field applied parallel to the layer normal or suppressed by elastic forces, due to the interaction of thin smectic C^* films with flat surfaces. The spontaneous polarization P_o is a molecular property characteristic for the dopant. However, the observed polarization P_s is dependent on the tilt angle according to

$$P_s = P_o \sin \theta \quad (11)$$

For a smectic C phase, an effective viscosity γ_{eff} can be defined [90] by

$$\gamma_{\text{eff}} \frac{d\phi}{dt} + P_s E \sin \phi = 0 \quad (12)$$

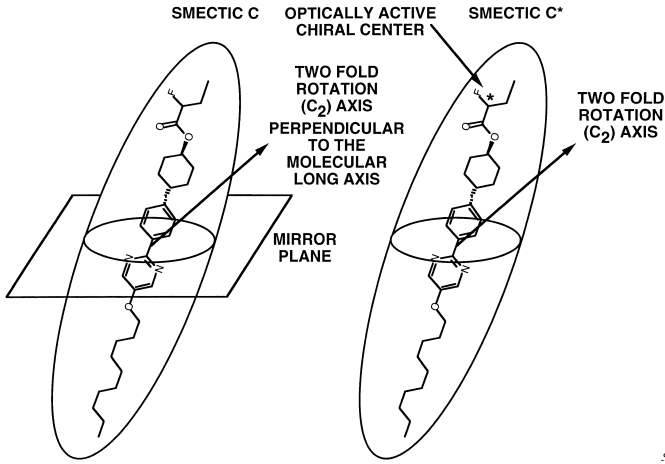


Fig. 10. Molecular structure and symmetry considerations in the smectic C and ferroelectric smectic C* phases for a typical chiral dopant [41–43, 92].

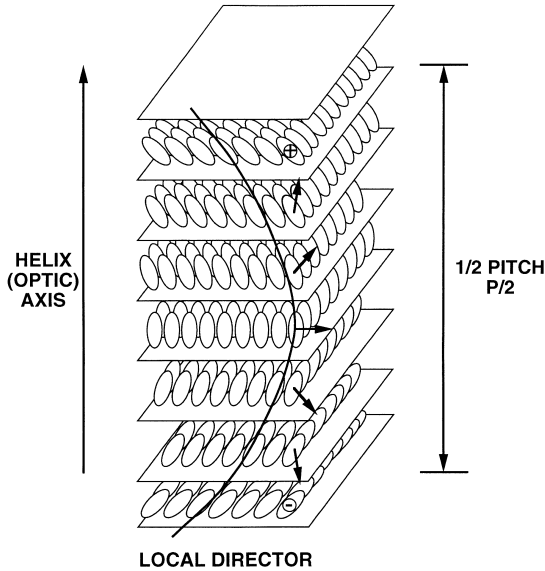


Fig. 11. Schematic representation of the periodic helical structures of layers in the smectic C* phase. The pitch of the helix corresponds to the rotation of the director through 360° . The direction of the spontaneous polarization indicated by arrows is orthogonal to the local director. The spontaneous polarization of a bulk, inhomogeneously oriented smectic C* phase is zero, due to the helical local structure [41–43, 92].

where φ is the angle of rotation on the chiral smectic C cone and E is the applied electric field. Equation (12) allows the definition of a characteristic time τ

$$\tau = \frac{\gamma_{\text{eff}}}{P_s E} \quad (13)$$

The experimental switching time is proportional to τ . Geometrical considerations indicate that γ_{eff} is related to θ by

$$\gamma_{\text{eff}} = \gamma_o \sin^2 \theta \quad (14)$$

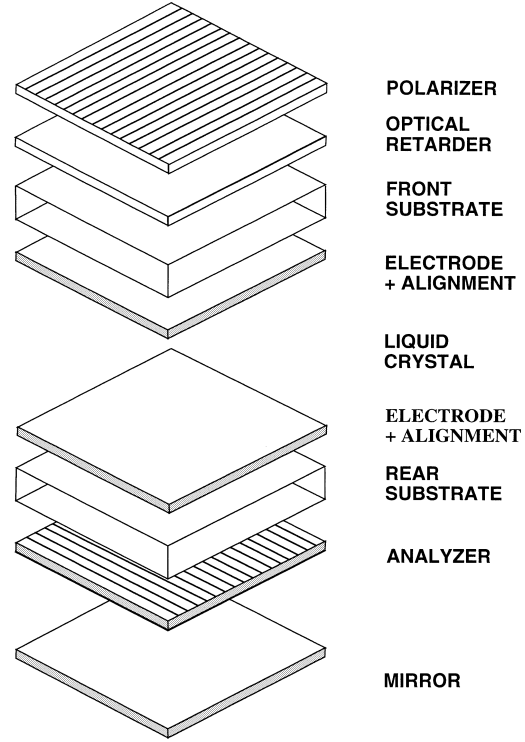


Fig. 12. Generalized schematic representation of the major optical and electrical components of a liquid crystal display.

where γ_o is independent of θ and represents the rotational viscosity of a hypothetical nematic-like smectic C structure with a tilt angle of 90° .

4. LIQUID CRYSTAL DISPLAY DEVICES

Displays that use liquid crystals [16–28] generally consist of a very thin layer of a nematic or smectic liquid crystal mixture enclosed between two transparent parallel glass substrates hermetically sealed around the edges (See Fig. 12). The glass plates are held apart by solid spacers (fibers, strips, or beads) to form a uniform cell gap ($\approx 2\text{--}10\ \mu\text{m}$), which should be as uniform as possible across the visible area of the display. Thicker cells are generally not used, because they are turbid, due to light scattering, as well as exhibit much longer response times. The inner surfaces of the glass substrates are coated with a whole series of thin, transparent layers with different functions. The first coating is often a barrier layer (e.g., silica) to prevent leaching of ions from the glass substrates into the liquid crystal, which should be a dielectric with a high resistivity. Color LCDs often incorporate a regular pattern of red, green, and blue color filters that correspond to the pixel pattern. However, the absorption of the other colors at each pixel gives rise to insufficient brightness for LCDs driven in reflection. Therefore, LCDs with color filters are driven in transmission or transfection (transmission and reflection) with a powerful backlight. The next layer is a transparent conducting material, most often indium–tin oxide (ITO), between which the electric field is applied; early displays often used NESA.

There are three basic methods for generating the appropriate electric field responsible for the modulation of light transmission at a particular picture element (pixel) of the LCD. These are direct addressing, multiplex addressing, and active matrix addressing (See Sects. 5.1, 5.2, and 5.3, respectively). In directly addressed LCDs, the

desired pixel pattern is obtained by using patterned electrodes on one surface and a nonpatterned back electrode on the second surface. Passively addressed LCDs with multiplexed addressing utilize electrodes in a series of rows on one electrode surface and columns on the other electrode surface that are arranged orthogonal to each other. Actively addressed LCDs use a silicon substrate with a series of thin film transistors combined with a (structured or unstructured) back electrode on the other glass substrate. On top of the electrode surface, there may be another thin protective layer to prevent migration of ions into the liquid crystal mixture. The last layer is an alignment layer that is in direct contact with the liquid crystal mixture and is used to induce a homogeneous, uniaxial orientation of the local optic axis, which is usually coincident with the director in the azimuthal plane of the device. The alignment layer should induce the desired direction of the director at both of the substrate surfaces, depending on the type of LCD. In directly addressed or multiplexed addressed LCDs, the two glass substrates are offset to some extent to allow physical contact with the drive electronics. The contacts usually are composed of plastic sheets with alternate strips of conducting and insulating polymers, whose dimensions correspond to the width of the electrodes on the substrate. In high-information-content displays, electrical contact is often achieved by using patterns of conducting adhesives attached directly to the motherboard.

Once the cell has been constructed, it is evacuated through a small hole to produce a vacuum and then filled with the appropriate liquid crystal mixture under an inert atmosphere. The area around the hole is cleaned to remove excess liquid crystal and then hermetically sealed (e.g., with epoxy resin or even gold). The chosen direction of alignment at the glass substrates is dependent on the optics of the type of LCD. For many types of LCDs, a sheet of polarizer is then attached to the outer surface of one or both substrates—usually by contact bonding. The polarization direction makes angles, α and β to the direction of rubbing at each surface and, therefore, the optic axis (director) of the liquid crystal mixture. Sheets of optical retarders also may be placed between the glass substrates and the polarizers. External plastic sheets, which scatter more transmitted light through a wider viewing angle cone, also may be attached.

5. ADDRESSING METHODS FOR LCDs

The addressing of any display device [24] converts the image or information to be displayed into a sequence of sequential voltage pulses to activate individual pixels. These applied voltages result in a modulation of the light intensity at the array of pixels, thus generating the image or information on the display. Each pixel has to be switched on and off individually by applying and then removing an electric field or by applying a voltage of opposite polarity. There are three main methods by which this can be achieved; (1) direct addressing, (2) multiplex addressing, and (3) active matrix addressing.

5.1. Direct Addressing

In simple, low-information-content displays, such as digital clocks and some basic calculators, each pixel is driven directly with a dedicated electrical contact and a driver for each segment of the digit (See Fig. 13). The first commercial LCDs were constructed with direct addressing. With this type of addressing, the off voltage can be zero, and the on voltage can be several times the threshold voltage for switching. Therefore, in a twisted nematic (TN) LCD, where the electro-optical characteristic is relatively flat, a good contrast can be attained, as well as low power consumption. However, the need for displays with higher information content (e.g., sophisticated calculators, personal organizers, notebooks, and portable computers) requires more complex addressing schemes, due to the high cost of using many drivers and the absence of sufficient space for the profusion of electrical contacts.

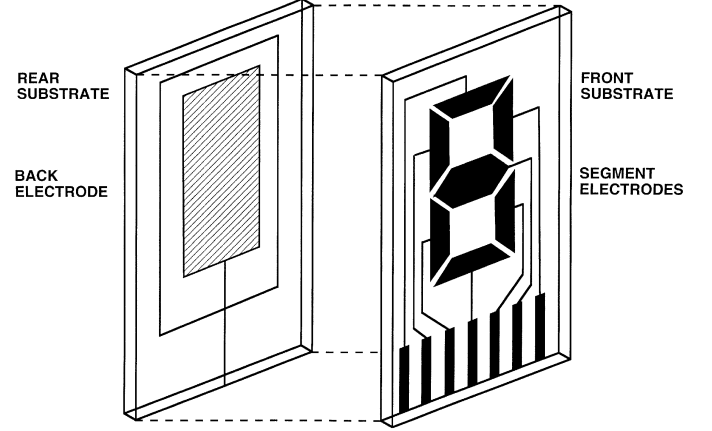


Fig. 13. Schematic representation of a simple, low-information-content, alphanumeric TN-LCD with direct addressing made up of segmented electrodes.

5.2. Multiplex Addressing

A high-information-content display contains a very large number of pixels, each of which has to be addressed [24]. Individual connections to each element would require $M \times N$ connections. There is a limit above which it is impossible to physically connect all the pixels. Multiplex addressing, however, with M electrode columns and N electrode rows allows $M \times N$ pixels to be driven by $M + N$ connections, thereby significantly reducing the number of electrode connections (See Fig. 14). This renders it possible to address more lines, thereby allowing larger flat panel displays with good optical properties to be produced (See Sects. 11 and 14).

In an LCD with multiplex addressing, parallel lines of electrodes are etched onto both glass substrates and then positioned so that they are perpendicular to one another, resulting in a matrix of rows and columns. Each row is sequentially scanned by a scan or select pulse (V_s), whereas the columns are addressed by data pulses (V_d), which contain the information to be displayed. As voltage is applied sequentially to each row, voltage pulses are applied to the corresponding columns. When the combination of row and column voltages in phase with each other is greater than the threshold voltage, the liquid crystal responds to the applied voltage and the pixel is turned on. An appropriate reduction in the voltage applied to one electrode turns the pixel off. For most nematic LCDs, the root mean square (rms) voltage is the relevant switching parameter, because the response of the liquid crystal is caused solely by an induced polarization of the nematic medium that varies with the square of the applied electric field. Unfortunately, the number of addressable lines in a multiplexed LCD with good legibility is limited, albeit to a much lesser extent than direct addressing. Alt and Pleshko [93] showed that the maximum number of addressable lines (N) is given by the equation

$$\frac{V_{ns}}{V_s} = \sqrt{\frac{\sqrt{N-1}}{\sqrt{N+1}}} \quad (15)$$

where V_s and V_{ns} are the select and nonselect voltages, respectively (See Fig. 15). For 64 addressable lines, there is only a difference of about 11% between the select and nonselect voltages. Therefore, the more lines there are to be addressed, the smaller the permissible voltage change becomes. This results in lower contrast, due to the inadvertent activation of neighboring pixels (i.e., cross-talk). To increase the number of addressable lines without reducing the contrast, it is essential that the electro-optical response curve exhibit a very steep or, indeed, infinite slope. However, a steep electro-optic

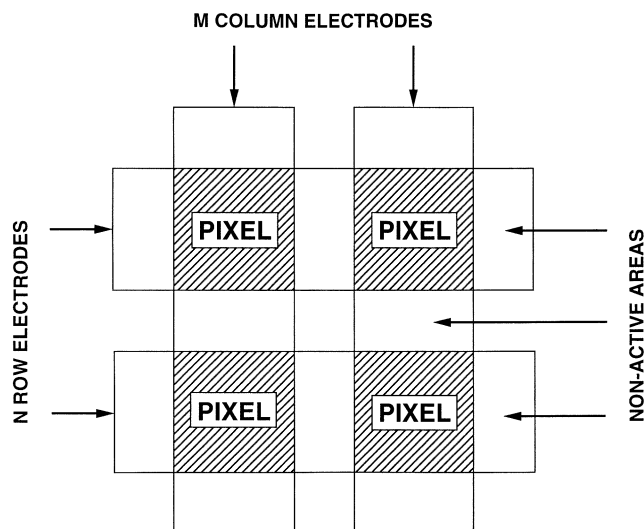


Fig. 14. Schematic representation of the pixels of a LCD with multiplexed addressing made up of a pattern of orthogonal rows and columns of electrodes [24].

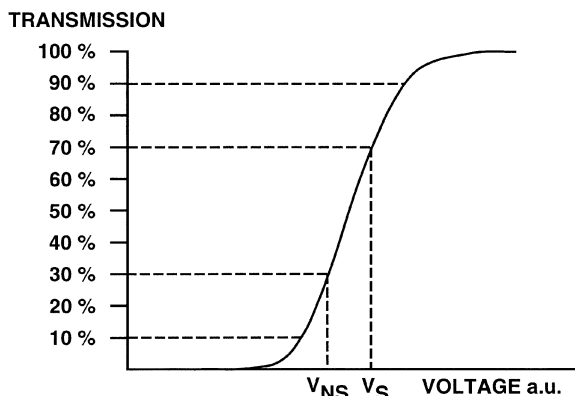


Fig. 15. Schematic representation of the transmission versus applied voltage for a LCD with multiplexed addressing. V_{ns} and V_s are the non-select and the select voltages, respectively [24].

characteristic reduces the scope for generating gray scale and, therefore, full color [94]. Gray scale allows the intensity of light (i.e., brightness) at a pixel to be controlled almost linearly by varying the applied voltage (See Fig. 15). Therefore, multiplexed LCDs are only capable of displaying a limited amount of information at the same time as good contrast and legibility, unless the electro-optic transmission curve is very steep [e.g., for supertwisted nematic LCDs; see Sect. 14]. LCDs with a relatively flat electro-optic transmission curve are incapable of displaying a high information content with good contrast, short response times, and acceptable viewing-angle dependency. In practice, a duty cycle of 1 : 64 is the upper limit for TN-LCDs; that is, 64 rows can be addressed in one frame.

5.3. Active Matrix Addressing

A large number of pixels for high-information-content LCDs are presently achieved commercially by using versions of passively addressed TN-LCDs and STN-LCDs [24] with in-plane switching multiplexed addressing, or active matrix electrically controlled birefringence (ECB) LCDs, IPS-LCDs, or TN-LCDs (See Sects. 8–14) [95–98]. Most commercial LCDs with active matrix addressing use a discrete thin film transistor (TFT) [96] or diode [97] at each

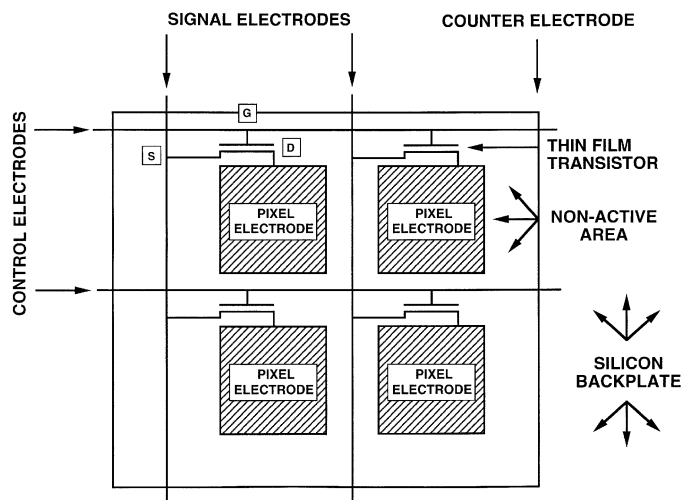


Fig. 16. Schematic representation of the electrode pattern and thin film transistors at each pixel of a high-information-content LCD with active matrix addressing [24].

individual pixel that is formed on an amorphous silicon backplate [98] (See Fig. 16 for a TN-TFT-LCD and Sect. 11). This arrangement does away with the requirement for rows and columns and removes the stringent size constraints imposed by multiplexed addressing. Thin film transistors that use cadmium selenide (CdSe) were developed in the early 1960s to address several kinds of display devices [99], and there are very many variants and combinations of LCDs with active matrix addressing on the market [100]. This diversity is attributable to the significant advantages of this technology, which include high contrast ratio, almost complete absence of cross-talk, adequate gray scale, fast response times, high-information-content, and large area. Major disadvantages include low luminosity and high power consumption, but, more importantly, the high production cost associated with the silicon substrate and the low production yield, due to pixel damage and subsequent repair. However, more efficient manufacturing methods, improved technology, and specially designed production equipment are constantly improving the yield, increasing the size, and lowering the cost of LCDs with active matrix addressing.

Active matrix addressing of LCDs essentially corresponds to a memory effect; that is, the addressing pulse switches the TFT, which maintains a constant charge on the pixel capacitor until it is addressed again in the subsequent frame. Leakage of charge away from the pixel e.g., into the nematic liquid crystal decreases the effective voltage across the pixel, which, in turn, leads to lower contrast. Hence, nematic materials with high resistivity are required.

6. ALIGNMENT LAYERS

Most LCDs based on field effects are, in effect, surface stabilized in one way or another [101]. Organic polymers such as polyimides and polyamides, mechanically rubbed to create microgrooves [102], obliquely deposited inorganic oxides such as SiO_2 [103], or long-chain aliphatic siloxanes [104] are the most common orientation layers. Although it is capable of generating the desired orientation of the optic axis of the liquid crystal mixture reproducibly in the azimuthal and zenithal planes, the production technique for inorganic alignment layers is intrinsically expensive and not very compatible with continuous production processes. Aliphatic siloxanes usually generate homeotropic alignment with small pretilt angles measured from the normal to the plane of the cell. Therefore, buffing of organic polymers has become the standard alignment technique for homogeneous (planar) alignment with a defined pretilt

angle in commercial TN-LCDs, STN-LCDs, and LCDs with active matrix addressing (e.g., TN-TFT-LCDs) [105–112]. However, rubbing can cause pixel damage and generate static electricity which leads to dielectric breakdown or the reduced resistivity of the liquid crystal layer. These consequences are especially important for LCDs with active matrix addressing, where the presence of even very small amounts of dust particles or static surface charges can lead to an unacceptable deterioration in display performance with subsequent lower production yields and higher costs.

Noncontact alignment layers, which use plane-polarized light to generate a surface anisotropy and, thus, uniform alignment of the liquid crystal director, have the potential to eliminate problems caused by buffing organic layers. A variety of related methods [113–121] that utilize the cis–trans photoisomerization of azo dyes to produce an orientation effect have been developed. However, all these methods use the same basic effect that is, the cooperative influence of configuration changes of the azo-dye molecules (cis–trans photoisomerization) produced by the absorption of polarized light on the spatial arrangement of neighboring liquid crystalline molecules. The dye may be dissolved directly into a standard orientation layer (e.g., polyimide) [113] or the LC mixture [114, 115], or covalently bonded to polymers either spun onto the substrate surface [116–118] or arranged in Langmuir–Blodgett monolayers [119–121]. Noncontact alignment layers that use azo chromophores require the use of intense laser light for relatively long periods (e.g., 1–2 h), to induce the isomerization of the dye molecules. The high concentration of dye required (e.g., 2 wt%) may induce an unwanted colored appearance. The thermal and ultraviolet light stability of the orientation layers or the azo dyes themselves may also be insufficient for commercial applications, due to relaxation effects or degradation over time.

Photoinduced anisotropic cross-linking of side-chain polymers is among the most promising of the various noncontact alignment technologies [122–140]. It was found that poly(vinylcinnamate) (PVC) films exposed to linearly polarized ultraviolet light yield homogeneous liquid crystal alignment perpendicular to the polarization direction of the light [122–128]. Alignment results from an anisotropic depletion of the cinnamate side chains because of (2+2) cycloaddition reactions (See Fig. 17), although some authors suggest that cis–trans isomerization is also involved at low fluences [124]. A low azimuthal surface anchoring energy of $\approx 4 \times 10^{-6} \text{ J m}^{-2}$ has been measured [125], but better alignment is found when PVC derivatives are used [126–128]. Small liquid crystal pretilt angles ($\approx 0.3^\circ$), measured from the surface, have been generated in PVC by means of a double exposure of the alignment layer [128]. However, the pretilt angle is more easily varied by exposure at nonnormal incidence, when the alignment direction is parallel to the polarization direction of the ultraviolet light. These conditions were reported with a coumarin side-chain polymer [129, 130] (See Fig. 18). Subpixelated, multidomain devices with improved viewing-angle dependence of the contrast have been produced using this material [131, 132]. The mechanism of photoalignment was investigated in some detail [133–138]. Anchoring energies comparable to rubbed polyimide have been determined. This technique can be used to improve the viewing-angle dependence of TN-LCDs and STN-LCDs by photolithographic generation of multidomain pixels, in which the subdomains exhibit different microscopic alignment directions. The anisotropic photodegradation of polyimide layers using plane-polarized ultraviolet light can also give rise to good alignment [137, 138]. However, the process generates a lot of chemical debris, which must be completely removed for commercial applications.

7. COMPENSATION FILMS FOR LCDs

Compensation films for LCDs are essentially optical retarders [139]. They are used in attempts to compensate for the very strong viewing-angle dependency of the optical properties, such as contrast,

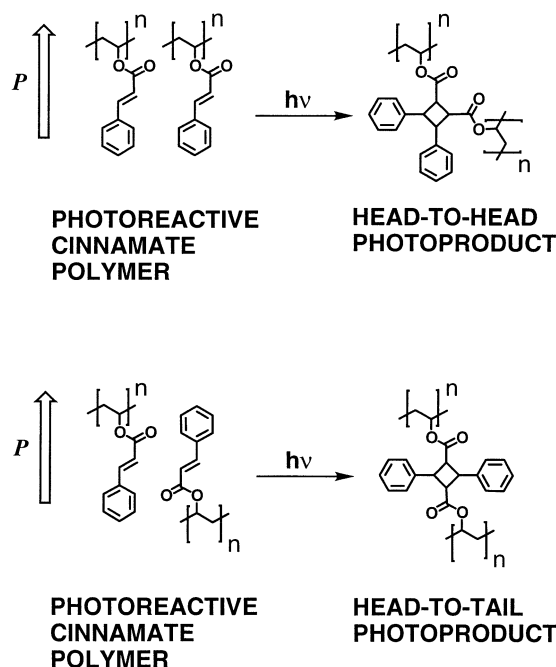


Fig. 17. Schematic representation of the anisotropic cross-linking of a photoreactive cinnamate polymer by the action of polarized ultraviolet light to produce a stable anisotropic network as a noncontact alignment layer [133–135].

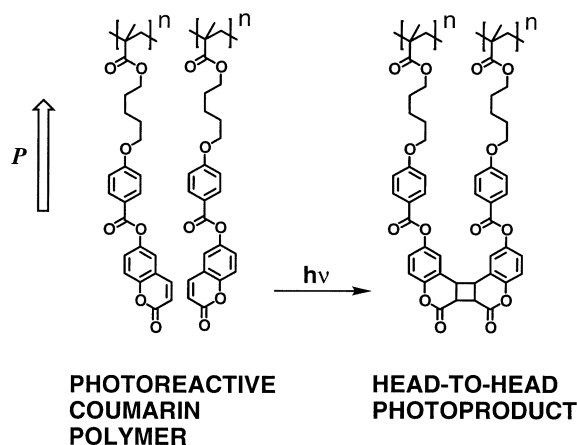


Fig. 18. Schematic representation of the anisotropic cross-linking of a photoreactive coumarin polymer by the action of polarized ultraviolet light to produce a stable anisotropic network as a noncontact alignment layer [133–135].

luminosity, gray scale, and color, which are caused by the anisotropic nature of the birefringent polarizers and the nematic layer in the cell. These optical properties degrade as the angle of view increases from normal to the plane of the cell (See Fig. 19). However, the viewing-angle dependency of these properties is asymmetric, that is, different in the zenithal and azimuthal planes. These problems are particularly acute for the ECB, TN, and STN LCDs due to wave-guiding and interference effects. The basic mode of operation of a compensation film is to match the optical symmetry of the compensation layer to the optical pattern of the liquid crystal layer, but with an inverse sign of birefringence.

Many kinds of compensation films in many different combinations have been reported [140–153]. They may be layers of positive

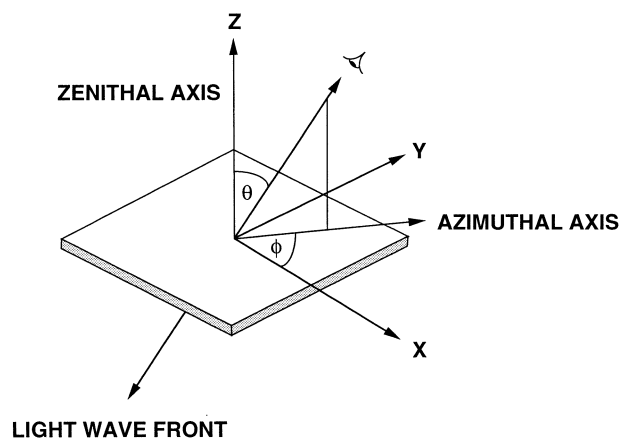


Fig. 19. Schematic representation of viewing angles θ and ϕ in the zenithal and azimuthal planes for light traversing a LCD [24].

or negative birefringence, whose optic axis makes an angle to the plane of the cell, which may be fixed or increased by a splay of the nematic director. The optic axis of these layers may be parallel to the nematic director or the major axis of absorption of the polarizer or make some angle to either of them. One, two, or a stack of compensation layers may be fixed above and below the cell inside the polarizers. These practical combinations are often far from simple. For example, it was found that compensation layers of negative birefringence on either side of a TN-LCD cell with the optic axes in the plane of the cell led to an improvement in the horizontal plane, but did not improve the viewing-angle dependency in the vertical plane. However, tilting the optic axis of the compensation layer with respect to the plane of the cell resulted in better optical properties in the vertical direction. The relationship between these factors is complex. Therefore, computer programs, such as the Jones or Berreman programs [151], are used to predict the effect on the optics of a given display of a compensation layer of a given birefringence, thickness, and orientation. The Jones program is simpler than the Berreman program and, therefore, marginally less accurate. However, it is much quicker to run and is sufficient for most purposes.

Organic films of optical retarders are often preferred by LCD manufacturers and systems integrators of displays, because pre-

formed compensation films can simply be laminated to commercial displays, using a pressure-sensitive adhesion layer, to improve their optical properties to meet a given set of specifications. These organic optical retarders can be formed in a number of ways. Standard compensation films are formed by mechanically stretching films of aromatic main-chain polymers that incorporate polarizable aromatic units (e.g., a polycarbonate polymer). The stretching procedure aligns the long polymer chains parallel to each other in the direction of mechanical stress. This alignment induces an anisotropy of polarizability, because the polarizability parallel to the long polymer axis is greater than that orthogonal to the direction of stretching. Therefore, n_e is greater than n_o , and the retardation film has positive birefringence [See Eq. (7)]. A styrene polymer [140] treated in the same way will have negative birefringence, because the refractive index measured orthogonal to the oriented polymer axis is larger than that parallel to the polymer axis; that is, n_e is less than n_o , (See Fig. 20).

Optical compensation layers are generally produced as anisotropic networks from photoreactive liquid crystalline precursors [141–153]. Nematic liquid crystals are preferred to smectic liquid crystals, due to their low viscosity and good alignment properties. However, columnar networks of negative birefringence are used commercially, despite their high intrinsic viscosity. Anisotropic networks are generally formed by spin casting a polymerizable nematic liquid crystal onto a substrate, evaporating off the solvent, and then polymerizing and cross-linking the reactive nematic precursors with ultraviolet light (See Fig. 21) to produce a solid three-dimensional network (See Fig. 22).

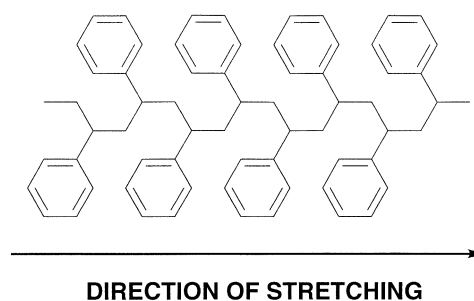


Fig. 20. Schematic representation of the linear structure of a stretched polystyrene component of an optical retardation sheet.

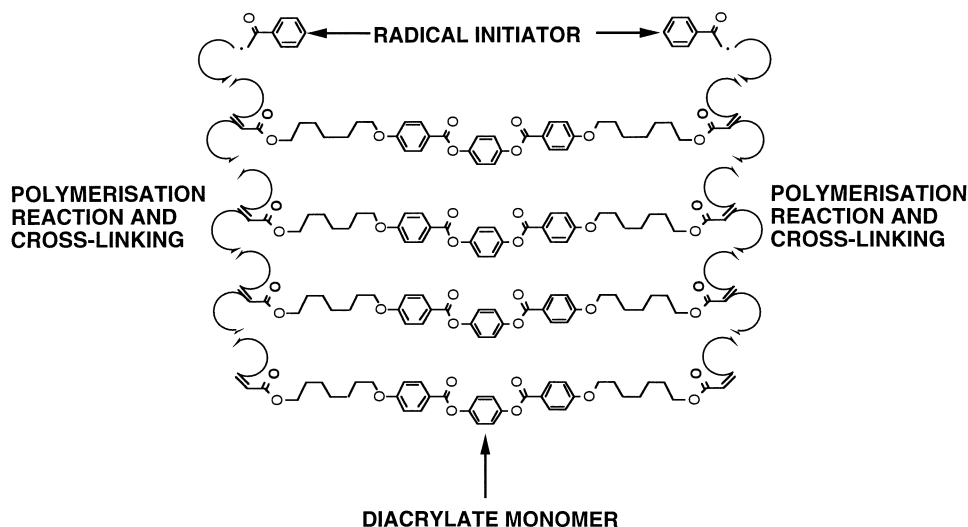


Fig. 21. Schematic representation of the process of radical polymerization and cross-linking in the nematic phase of a diacrylate to produce an anisotropic polymer network [49].

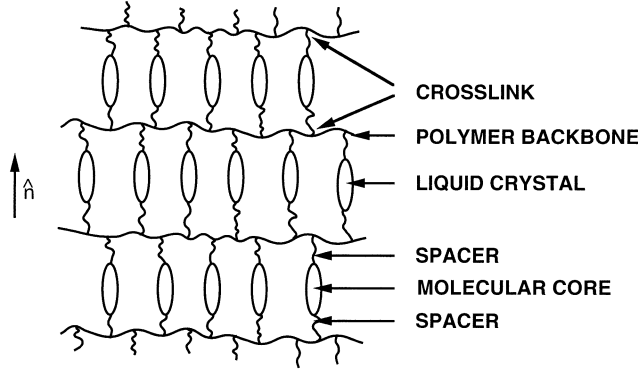


Fig. 22. Schematic representation of the structure of a nematic polymer network [49].

Optically anisotropic photoalignment films produced by cross-linking induced by polarized ultraviolet light are birefringent and can be used to generate photopatterned, high-resolution optical retarders, polarization converters, and interference filters [122, 123]. However, the birefringence value is generally very low, and thick films have to be used. Therefore, they are used in combination with anisotropic networks formed from reactive mesogens [123, 126, 127]. If some of the molecules in a liquid crystals mixture contain at least two reactive groups, which can be either photochemically or thermally polymerized, then cross-linked, anisotropic networks can be produced in a relatively simple fashion. Macroscopic, uniaxially oriented forms or films can be formed by orientation of the sample on the photoalignment layer and then cross-linked to form a patterned optical retarder as an anisotropic network.

8. ELECTRICALLY CONTROLLED BIREFRINGENCE LCDs

There are many different variants (e.g., deformation of vertically aligned phases and homeotropic nematic) of LCDs that utilize electrically controlled birefringence [154–159]. However, they all have the same basic cell setup as shown in Figure 23 and are essentially based on the Fréedericksz effect [160] described in the early

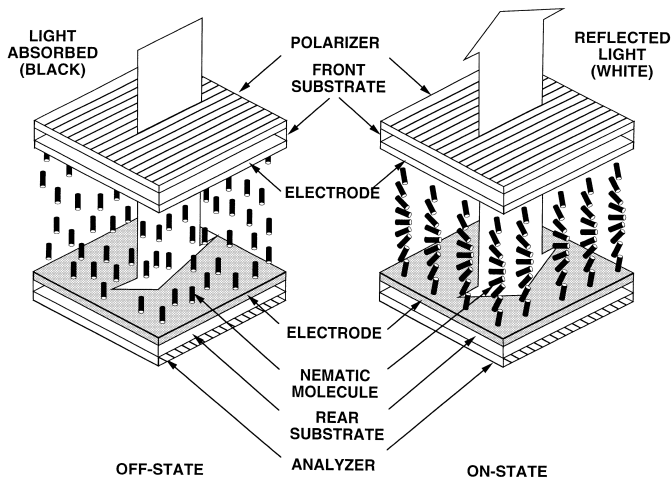


Fig. 23. Schematic representation of an electrically controlled birefringence LCD [154–159].

1930s. Interest in ECB-LCDs has ebbed and flowed over the last 30 years without any large-scale commercial breakthrough primarily due to their unsuitability for high-information-content displays with passive, multiplexed addressing. The brightness is low ($\approx 20\%$), the gray scale is poor, the contrast is also relatively low (25 : 1), and the color is angle dependent. However, LCD products that incorporate ECB-LCDs with active matrix addressing are starting to appear on the market, due to their capacity to generate full color using gray scale and relatively rapid response times. This renewed interest is also due to the availability of stable nematic mixtures of negative dielectric anisotropy, high birefringence, and low viscosity.

9. ECB-LCD CONFIGURATION

A nematic liquid crystal of negative dielectric anisotropy is aligned orthogonally to the cell walls by means of a surfactant orientation layer, and the bulk alignment is modulated by dielectric coupling with an electric field applied between the two electrodes. One or two polarizers (linear, elliptical, or circular [159]) are required, depending on whether the cell is operated in the transmissive or reflective mode.

9.1. Off State

If the cell is positioned between crossed polarizers, then, in the off state, polarized light produced by the first polarizer travels through the homeotropically aligned nematic medium unchanged and is subsequently absorbed by the second polarizer. Therefore, extinction occurs and the cell appears dark (See Fig. 23).

9.2. On State

An electric field applied between the electrodes causes the nematic director to tilt away from the normal with increasing field above a threshold voltage [161]

$$V_{th} = \sqrt{\frac{\pi^2 k_{33}}{(\epsilon_{\perp} - \epsilon_{\parallel}) \epsilon_o}} \quad (16)$$

where $\epsilon_{\perp} - \epsilon_{\parallel} < 0$. This induces birefringence Δn_i and allows some of the incident light to traverse the cell in the on state. The optical effect is produced by interference between the extraordinary and the ordinary rays and, therefore, at voltages above the threshold voltage, white incident light is often converted into colored light by interference. Theoretically, this conversion allows the production of colored displays. However, as explained subsequently there is virtually no change in color at voltages near the threshold voltages. Therefore, the display is usually operated in the threshold voltage region using color filters. The optical retardation δ is proportional to the induced birefringence, $\Delta n = n_e - n_o$, which, for a given cell gap d and wavelength of light λ is given [162] by

$$\delta = \frac{2\pi \Delta n d}{\lambda} \quad (17)$$

when operated in the transmission mode.

The value for the refractive index of the ordinary ray (n_o) passing through the cell is unaffected by the applied field, but the value for the extraordinary ray (n_e) increases with voltage (due to dielectric coupling of the director with the field) if the liquid crystal mixture is of negative dielectric anisotropy. Thus, the effective birefringence increases with applied electric field strength. Therefore, the intensity I of light traversing the cell depends on the optical retardation (phase difference) δ , as well as on the angle of incidence of light (ϕ),

$$I \propto I_o \sin^2(2\phi_o) \sin^2\left(\frac{\delta}{2}\right) \quad (18)$$

where I_o is the intensity of the incident plane-polarized light. This produces bright information on a black background. The intensity I of transmitted light is a maximum when

$$\Delta nd = (2m + 1) \frac{\lambda}{2} \quad (19)$$

where m is an integer. Usually, Eq. (19) is satisfied at an operating voltage with $m = 0$ and $\lambda \approx 550$ nm, the central wavelength of the visible spectrum. This gives a black and white display with good uniform transmission across the visible spectrum. Whereas the induced birefringence depends on the electric field strength, the amount of light transmitted can be modulated to produce a tunable birefringence (i.e., gray scale). Because the magnitude of the displacement of the director is not large enough for an optical effect to be observed, the switch-on times of this display type are intrinsically short (≈ 20 μ s), although they occur at relatively high operating voltages. The switch-off time t_{off} is dependent on a viscosity coefficient, η , a curvature elastic modulus κ and the thickness of the cell d [161]:

$$t_{\text{off}} \propto \frac{\eta d^2}{\kappa} \quad (20)$$

Therefore, because no field effect is involved, switch-off times are often 3 or 4 orders of magnitude larger than switch-on times, although special addressing techniques can produce short frame times (≈ 50 μ s) [163, 164]. The nematic director should be inclined in one specific direction (e.g., 1° pretilt) to produce a uniform optical appearance. In this case, there may be no sharp threshold voltage [165].

10. NEMATIC MATERIALS OF NEGATIVE DIELECTRIC ANISOTROPY

LCDs based on electrically controlled birefringence require a sharp threshold voltage and a steep electro-optic contrast curve [166]. To meet these conditions, the nematic mixture used should fulfill a number of conflicting specifications. A high negative value of $\Delta\epsilon$ and high positive values of k_{33}/k_{11} , Δn , and δ are required. However, high values of Δn , which allow thin cells and, therefore, shorter response times [See Eq. (19)] also give rise to birefringence in the off state, because of the finite pretilt, interference colors, and, consequently, lower contrast ratio. A large cell gap leads automatically to longer response times according to Eq. (20). The parameter $\Delta\epsilon/\epsilon_{\parallel}$ should also be low; that is, both ϵ_{\perp} and ϵ_{\parallel} should be high. However, high operating voltages, which are already relatively high for operation with standard, low-cost CMOS drivers, are observed if $\Delta\epsilon/\epsilon_{\parallel}$ is too low.

The first LCDs based on electrically controlled birefringence used readily available nematic Schiff bases of negative dielectric anisotropy, such as *N*-(4-methoxybenzylidene)-4-butyraniline (MBBA) or mixtures of Schiff bases, such as MBBA and *N*-(4-ethoxybenzylidene)-4-butyraniline (EBBA). These compounds possess a nematic phase, a high clearing point, and a melting point at or below room temperature (See Table I). However, the dielectric anisotropy of these Schiff bases is low ($0 > \Delta\epsilon > -1$). Therefore, the operating voltages of prototypes such as the ECB-LCDs [154], now often referred to as deformation of vertically aligned phases (DAP) LCDs, were relatively high (7–8 V). The effect on the threshold voltage of the elastic constants could not be ascertained, because they were not known at that time.

Subsequent LCD types using electrically controlled birefringence, such as homeotropic nematic (HN) LCDs [159] or electrically controlled birefringence (ECB) LCDs [156, 158], utilized liquid crystal mixtures of relatively strong negative dielectric anisotropy. These mixtures incorporated components that possessed a polar substituent,

such as a halogen or a cyano group (e.g., F, Cl, Br, and CN), in a lateral position. In this way, the vector of the dipole moment associated with this lateral substituent perpendicular to the long molecular axis was greater than that parallel to the long molecular axis [167–175]. (See Table III). The cyano group was utilized most of all, because of its large dipole moment (4 D) [167–175].

The large van der Waals volume of the cyano group induces substantial clearing point depressions and a high viscosity, whereas the induced negative dielectric anisotropy is only moderate ($-2 > \Delta\epsilon > -4$). This situation is illustrated by the data collated in Table III for compounds **18–23** [169]. The nematic clearing point decreases linearly with increasing radius of the lateral substituent for compounds **20–22**, except for the fluorine derivative (**19**). This is due to a shielding effect associated with the large rotation volume of the 1,4-disubstituted bicyclo[2.2.2]octane ring. The clearing point of the fluoro-substituted derivative (**19**) with the lateral substituent in position 2 is much higher than that of the corresponding ester (**23**) with the fluoro substituent in position 3. This indicates that a lateral substituent in position 3 is no longer shielded or is shielded to a much lesser extent than the same substituent in position 2. The viscosity increases proportionately with increasing size of the lateral substituent. Therefore, a lateral substituent should be next to the carboxy group (i.e., in position 2) to minimize steric effects on the nematic clearing point and the viscosity. Furthermore, the component of the dipole moment of the lateral substituent parallel to the long molecular axis tends to cancel out that of the carboxy group, while the orthogonal contributions reinforce each other. Therefore, the cyano group in position 2 of compound **22** induces a negative value (-2) for the dielectric anisotropy of the nematic phase. This is too low for LCDs based on ECB effects, because it results in high operating voltages.

Materials that incorporate two cyano groups in lateral positions (e.g., compound **24** exhibit a much greater negative value for the dielectric anisotropy ($-12 > \Delta\epsilon > -20$) because the resultant dipole moment (≈ 7 D) is directed perpendicular to the long axis of the molecules, because the dipole vectors parallel to the long molecular axis cancel each other out. The viscosity does not increase proportionately for dicyano-substituted derivatives, compared with corresponding mono-cyano-substituted derivatives, although the resulting viscosity is high, whereas the clearing point may be even higher. This observation is probably due to the shielding effect of the first nitrile group, because the molecular rotation volume remains almost constant. Therefore, the degree of molecular separation is not increased.

In the case of the two-ring compounds (**18–24**), the large rotation volume of the 1,4-disubstituted bicyclo[2.2.2]octane ring reduces the steric effect of the lateral substituent on the clearing point, and the viscosity, although bicyclo[2.2.2]octane derivatives are generally very viscous. Three-ring materials are generally necessary to retain mesomorphism in compounds that incorporate the nitrile function in a lateral position, e.g., compound **25** [167] (See Table IV). The increased molecular length and polarizability of such three-ring compounds also contribute to the high observed viscosity. The Chisso Corporation made nematic mixtures of high negative dielectric anisotropy for LCD applications available in the late 1970s. These mixtures contained liquid crystalline ester derivatives of 4-*n*-alkoxy-2,3-dicyanophenol such as compound **26** [168]. However, these mixtures suffered from a degree of photochemical instability, which limited the effective lifetime of displays in which they were incorporated. The substitution of a methylene group for the terminal oxygen atom of 4-*n*-alkoxy-2,3-dicyanophenol to produce analogous 4-*n*-alkyl-2,3-dicyanophenyl ester derivatives, such as compound **27**, resulted in materials that were sufficiently stable for commercial applications [172, 173]. Although the magnitude of the dielectric anisotropy of dicyano-substituted materials is sufficiently great to allow the use of small concentrations, mixtures that incorporate these substances are still very viscous and result in long response times. Attempts to reduce the viscosity by incorporating two cyclohexane

Table III. Transition Temperatures (°C), van der Waals Radius (V) of C–X (Å), Viscosity (cSt measured at 20 °C), Dipole Moment of C–X (μ D), and Dielectric Anisotropy ($\Delta\epsilon$ measured at $0.95 \times T_{N-1}$) for Nematic Liquid Crystals **18–24**^a

Compound	X ₁	Crystal	Nematic	Isotropic	V	η	μ	$\Delta\epsilon$	Ref.
18		• 31.0	• 64.5	•		34 ^b		–0.6	169
19		• 26.0	• 65.0	•	5.8	44	1.47	–1.1	169
20		• 35.5	• 41.0	•	12.0	100 ^b	1.59		169
21		• 14.5	• 27.0	•	14.4		1.57		169
22		• 27.5	• 29.5	•	14.7		4.05	–2.0	169
23		• 44.5	(• 38.5)	•					169
24		• 84	(• 36)	•				–12.0	172

^aThe parentheses [()] represent a monotropic transition temperature.^bValue for a 1:1 mixture of 3/5 and 5/5 homologues.

rings (e.g., compound **28** [170]) or replacing the carboxy function by an ether link (e.g., compound **29** [170]) or by an ethyl group (e.g., compound **30** [176]) resulted in almost insoluble, nonmesomorphic compounds with very high melting points. The incorporation of only one cyano group in three-ring materials without carboxy groups, but with sp^2 bonding on aromatic rings (**31**) [177] and sp^3 bond angles in central linkages or terminal chains (**32**) [178] resulted in low negative values of the dielectric anisotropy.

A variety of liquid crystalline 3,6-disubstituted pyridazines, such as compound **33**, whose lone pair electrons, which are situated at the electronegative nitrogen atoms give rise to a large dipole moment perpendicular to the long molecular axis, were then prepared [178–181] (See Fig. 24). The lone pair electrons do not increase the breadth of the molecule. Therefore, due to the absence of steric effects associated with lateral substituents, two-ring 3,6-disubstituted pyridazine derivatives exhibit nematic phases of high negative dielectric anisotropy ($-6 > \Delta\epsilon > -10$) and low viscosity. Unfortunately, they also suffer from the serious disadvantages for commercial LCD applications of photostability over time and insufficient resistivity.

The *trans,trans*-4,4'-dialkyl-1,1'-dicyclohexyl-4'-carbonitriles, such as compound **34**, contain only one cyano group. However, the axial position of this nitrile function on one of the cyclohexane rings locates the dipole moment almost exactly perpendicular to the long molecular axis [182–184] (See Fig. 25). The axial hydrogen atoms on the same side of the cyclohexane ring shield the axial cyano

group to some extent. Thus, these chemically, thermally, and photochemically stable materials exhibit wide-range enantiotropic nematic phases whose viscosity is much lower than that of the aromatic, monocyano-substituted compounds. However, the very low birefringence of axially substituted bicyclohexanes renders them unsuitable for electro-optic displays based on electrically controlled birefringence; related derivatives that incorporate two benzene rings and one axially substituted cyclohexane ring are more appropriate.

The most promising approach to the synthesis of nematogens of negative dielectric anisotropy and low viscosity involves 2,3-difluorobenzene derivatives, such as compound **35** [185] (See Table IV). The small van der Waals volume of the fluorine atom (5.8 Å) and its relatively small dipole moment (1.47 D) lead to materials of relatively low viscosity and weak to moderately strong negative dielectric anisotropy in the nematic phase. If diether derivatives of 2,3-difluoroquinone are prepared, the resultant dipole moment perpendicular to the long molecular axis is enhanced, and, thus, relatively large values of the dielectric anisotropy ($-4 > \Delta\epsilon > -6$) are induced. Fluoro-substituted pyridines, such as compound **36**, also exhibit negative dielectric anisotropy, due to the resultant dipole moment orthogonal to the long molecular axis [186]. However, they do not appear to exhibit properties superior to the corresponding 2,3-difluorophenyl derivatives, and the synthesis is more complex. Attempts to improve the properties of 2,3-difluorophenyl derivatives involved synthesizing and evaluating compounds with different central linkages [187]. It is evident from the data in Table V for

Table IV. Molecular Structures, Transition Temperatures (°C), and Dielectric Anisotropy ($\Delta\epsilon$ measured at 20 °C) for Nematic Liquid Crystals **25–36**^a

Compound	Molecular structure	Crystal	Smectic	Nematic	Isotropic	$\Delta\epsilon$	Ref.
25		• 59	—	• 113	•	−3.8	167
26		• 138	—	• 148	•	−19.0	168
27		• 106	—	(• 102)	•	−11.5	172–175
28		• 88	154 ^b	• 169	•		170
29		• 230	—	—	•		170
30		• 224	—	—	•		176
31		• 63	(• 43)	• 79.5	•		177
32		• 71.5	• 162	• 173	•		178
33		• 59.5	—	(• 0)	•	−6.0	179–181
34		• 25	• 30 ^c	• 66	•	−8.0	182–184
35		• 74	• 86 ^c	• 171	•	−4.1	185
36		• 112	(• 105) ^c	• 190	•	−5.3	186

^aThe parentheses [()] represent a monotropic transition temperature.

^bSmectic A.

^cSmectic B.

compounds **37–42** that two oxygen atoms ($Z = \text{CH}_2\text{O}$, $\text{C}_3\text{H}_6\text{O}$, and $\text{C}_3\text{H}_4\text{O}$) are required to produce even a moderately strong negative dielectric anisotropy ($\Delta\epsilon = -6$). A range of diether derivatives of 2,3-difluoroquinone are manufactured commercially (by E. Merck) for several types of LCDs, which require nematic mixtures of negative dielectric anisotropy.

11. TWISTED NEMATIC LCDs

The twisted nematic (TN) liquid crystal display (TN-LCD) [105] was invented at Hoffman–La Roche in Basel, Switzerland, as part of a wider collaboration with Brown Boveri (Baden, Switzerland) and Ebauche (Neuchatel, Switzerland) to develop flat panel displays e.g.,

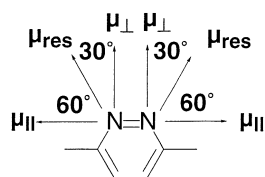


Fig. 24. Schematic representation of the resultant transverse dipole moment across the molecular long axis of a 3,6-disubstituted pyridazine derivative.

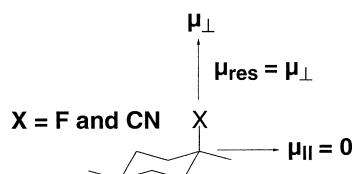


Fig. 25. Schematic representation of the resultant transverse dipole moment across the molecular long axis of an axially 4'-fluoro-substituted or 4'-cyano-substituted *trans,trans*-4,4'-dialkyl-1,1'-dicyclohexane derivative.

for watches. Brown Boveri constructed the first TN-LCD factory at Videlec in Lenzburg, Switzerland, in the mid 1970s. Since its invention, the TN-LCD has established itself as the dominant electro-optic display in portable instruments. Directly addressed or multiplex addressed TN-LCDs are found in low-information-content electro-optic devices, such as digital clocks, watches, computer games, and

calculators. Active-matrix addressed TN-LCDs are slowly replacing multiplexed STN-LCDs [24] (see Sect. 14) in the high-information-content segment of the displays market (e.g., in notebooks, personal organizers, and laptop computers). The dominance of TN type LCDs with these different types of addressing is due to an advantageous combination of properties, such as low power consumption, low threshold and operating voltages, adequate optical contrast (at least for narrow viewing angles), relatively efficient multiplexing at least at low ratios, (e.g., a 1 : 32 duty cycle), long operating lifetime, and low cost. The main disadvantages of the TN-LCD are long response times (especially at low temperatures), poor brightness, and limited contrast, as well as large variation of contrast with viewing angle, especially in passive matrix applications.

12. TN-LCD CONFIGURATION

A typical TN-LCD consists of a nematic liquid crystal mixture enclosed in a cell with rubbed polyimide alignment layers, crossed polarizers, and a cell gap of 5–10 μm (See Fig. 26). The nematic director is aligned in the azimuthal plane of the device parallel to the direction of rubbing. The alignment layer usually induces a small pretilt angle ($\theta \approx 1\text{--}3^\circ$) in the zenithal plane. The direction of alignment at the upper glass substrate is orthogonal to that at the lower glass substrate. This configuration generates an overall twist of 90° across the liquid crystal layer, due to elastic forces in the off state. The polarization direction of the crossed polarizers is usually arranged parallel to the director of the nematic mixture at each surface. Sometimes, the polarizers are parallel to one another to generate a dark off state and a bright on state with a wider viewing angle cone, between the on state and off state.

Table V. Transition Temperatures ($^\circ\text{C}$) and Dielectric Anisotropy ($\Delta\epsilon$) for 4-Ethoxy-2,3-difluorophenyl-Substituted Nematic Liquid Crystals 37–42^a

Compound	Z	Crystal	Smectic B	Smectic A	Nematic	Isotropic	$\Delta\epsilon$	Ref.
37		• 68	• 109	—	• 160	•	−3.7	185
38		• 62	—	—	• 154	•	−6.0	185
39		• 76	• 79	—	• 186	•	−4.4	185
40		• 87	(• 81)	• 98	• 222	•	−4.1	185
41		• 59	—	—	• 136	•	−5.1	187
42		• 65	—	—	• 135	•		187

^aThe parentheses [()] represent a monotropic transition temperature.

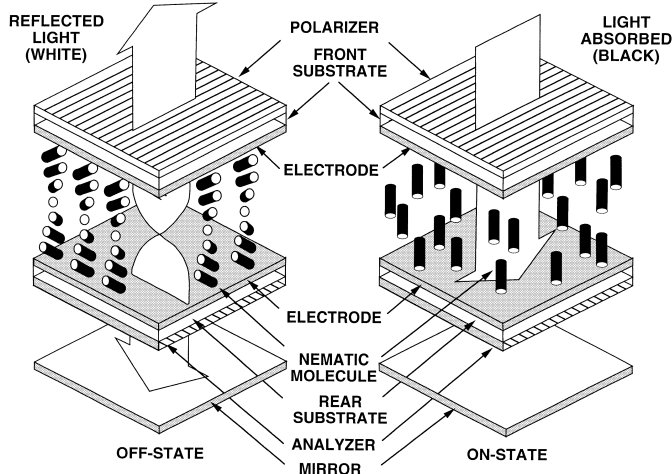


Fig. 26. Schematic representation of a twisted nematic liquid crystal display [24].

12.1. Off State

The twisted nematic medium rotates the plane of the polarized light generated by passage through the first polarizer by 90° through the twisted nematic medium, due to a wave-guiding action. This rotation occurs because the wavelength of visible light ($380\text{--}780\text{ nm}$) is much less than the thickness ($5\text{--}10\text{ }\mu\text{m}$) of the nematic layer [188]. This wave-guiding action allows the plane-polarized light to pass through the second polarizer (analyzer), because the direction of plane-polarized light is now parallel to the transmission direction of the second polarizer. In the reflection mode, this light is then reflected back along its original path by a mirror. Thus, the off state, or transition state, appears white. The off state is often referred to as the open mode or white mode.

To avoid the production of elliptically polarized light rather than plane-polarized light from a TN-LCD, it is necessary to meet certain conditions with respect to the cell thickness d , the birefringence of the nematic medium, Δn , and the wavelength of light in a vacuum λ , according to the equation

$$d\Delta n \gg \frac{\lambda}{2} \quad (21)$$

TN-LCDs often operate with small values of d ($\approx 5\text{ }\mu\text{m}$), because the response time of TN-LCDs is proportional to the square of the cell gap. The first commercial TN-LCDs had to operate at greater values of d ($\approx 8\text{ }\mu\text{m}$) to compensate for an inability to accurately control the cell gap homogeneously across the whole of the cell. A disadvantage of smaller cell gaps is that the transmitted light is more elliptically polarized, due to the small pitch of the twisted nematic medium. Thus, TN-LCDs can be tinged with color, especially for nonorthogonal viewing angles, due to interference between the extraordinary and ordinary rays. However, for certain wavelengths of light, interference at the analyzer can inhibit the production of elliptically polarized light to some degree. This gives rise to linearly polarized light according to the equation

$$u = \frac{2d\Delta n}{\lambda} \quad (22)$$

where the coefficient u is much larger than unity, which is the Mauguin limit [189]. Thus, for the center of the spectral range ($\approx 550\text{ nm}$) of visible light ($\approx 380\text{--}780\text{ nm}$), the wavelength at which the eye is most sensitive, a series of maxima and minima in transmission are produced for discrete values of the coefficient u (i.e.,

$\sqrt{3}, \sqrt{15}, \sqrt{35}, \sqrt{63}$, etc.). These are often referred to as the first, second, and so forth Mauguin [189] or Gooch and Tarry, [188] minima. Thus, for a TN-LCD with ideal parallel polarizers and neglecting light absorbed by the first polarizer,

$$I \propto \sin^2 \left[\frac{\pi/2(1+u^2)^{1/2}}{1+u^2} \right] \quad (23)$$

Whereas the amplitude of transmission decreases with increasing values of u , it is advantageous to operate in the first minimum or, at most, the second minimum to maximize the brightness, contrast, and acceptable viewing angle. The curve is inverted for crossed polarizers, and, therefore, the minima become maxima and vice versa. A bright TN-LCD can be achieved by utilizing a nematic liquid crystal mixture with a low birefringence ($\Delta n < 0.10$) in a TN-LCD with a cell gap of $6.55\text{ }\mu\text{m}$ operated in the first minimum [21, 190] (See Fig. 27). Higher birefringence values correspond to different Gooch and Tarry minima with consequent lower transmission in the off state. A nematic mixture of low viscosity is used to achieve fast response times. A certain amount of light still leaks through all TN-LCDs, due to a variety of factors, such as nonperfect polarizers, nonuniform nematic alignment, cell thickness, variation, temperature and wavelength dependence of Δn , and the polychromaticity of visible light itself. A combination of these factors results in a lower contrast

12.2. On State

When a voltage above the threshold voltage, V_{th} , is applied across a TN cell, the molecules in the center of the cell and, therefore, the optic axis, start to tilt to realign themselves in the direction of maximum polarization (i.e., parallel to the electric field) if the nematic phase is of positive dielectric anisotropy. This realignment results in a decrease in the effective average birefringence. A high voltage leads to a tilt angle of 90° at the center of the cell, where the twist is then completely unwound. The effective birefringence is then nearly zero, and, consequently, the plane of the polarized light is no longer rotated. Therefore, the plane-polarized light strikes the analyzer in a crossed polarizer configuration and is absorbed. Thus, the TN-LCD in this configuration exhibits positive contrast (i.e., displays black figures on a white background). However, there are residual transition regions of bend and splay at the cell boundaries, where the director is rigidly fixed. Near the threshold voltage, the deformation of the director gives rise to sinusoidal perturbations that have the longest wavelength compatible with the boundary conditions [74, 75, 81, 191]. The elastic energy required and the dielectric energy

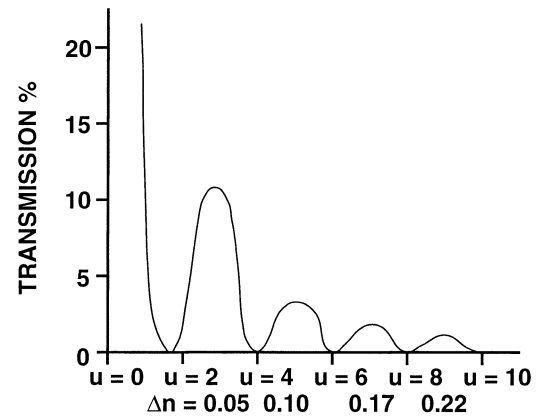


Fig. 27. Gooch and Tarry plot of transmission versus the coefficient u and the corresponding birefringence values Δn for a TN-LCD of thickness $6.55\text{ }\mu\text{m}$ operating between parallel polarizers [21, 189, 190].

released by this deformation depend on the square of the amplitude of these perturbations. The instability threshold is attained when the two quadratic terms are equal, and the threshold voltage for a twisted nematic cell is then defined [105] by the equation

$$V_{th} = \pi \left[\frac{1}{\varepsilon_o \Delta \varepsilon} \left(k_{11} + \frac{k_{33} - 2k_{22}}{4} \right) \right]^{1/2} \quad (24)$$

where k_{11} , k_{22} , and k_{33} are the Frank elastic constants [76], ε_o is the dielectric constant of a vacuum, and $\Delta \varepsilon$ is the dielectric anisotropy of the nematic mixture. Upon removal of the applied field, surface and elastic forces [34, 76, 192] restore the twist, which allows plane-polarized light to be transmitted once more. The response times, t_{on} and t_{off} , are defined [105] as

$$t_{off} \propto \frac{\eta d^2}{\Delta \varepsilon E - \kappa \pi^2} \quad (25)$$

$$t_{on} \propto \frac{\eta d^2}{\kappa \pi^2} \quad (26)$$

where

$$\kappa = \left[k_{11} + \left(\frac{k_{33} - 2k_{22}}{4} \right) \right] \quad (27)$$

η is the rotational viscosity, (γ_1) and E is the applied field. The response of the director is not identical throughout the cell and depends on the strength of the anchoring at the substrate surfaces. The molecules of the nematic mixture closest to the inner surfaces probably do not respond at all to an applied field.

The optical contrast of a TN-LCD is highest along a direction parallel to the director in the middle of the cell and is lowest at right angles to this direction. Therefore, the observed contrast for a TN-LCD is asymmetric and depends not only on the viewing angle, but also on the direction of view with respect to the director. Molecules in a twisted nematic structure can give rise to areas, or domains, of reverse twist upon application of an electric field. Disclination lines between neighboring domains reduce the observed contrast. This reduction can be eliminated by adding a small amount of an optically active material (dopant) [192], which induces a uniform direction or handedness of twist in the nematic medium that coincides with the twist in the cell. If the ratio of the pitch and cell gap (p/d) is too small, areas of reverse twist can form. Therefore, the pitch p induced in the nematic medium by the chiral dopant should be long and result in a relatively large ratio for p/d (≈ 7). Larger values for the pitch can fail to inhibit the formation of domains with reverse twist. A consequence of the addition of a chiral dopant is that the medium is also no longer a twisted nematic phase, but a chiral twisted nematic phase. This results in a higher threshold voltage according to the equation

$$V_{th} = \sqrt{\frac{k_{11} \pi^2 + \{k_{33} - k_{22}(1 - 4d/p)\}(\pi/2)^2}{\varepsilon_o \Delta \varepsilon}} \quad (28)$$

where the pitch of the chiral nematic mixture is also a term [105]. Initially, derivatives of cholesterol such as cholesteryl nonanoate [193] were added to induce the desired handedness of twist. However, such derivatives are hygroscopic and not particularly stable, so they were quickly supplanted by optically active derivatives of cyanobiphenyls such as 4-cyano-4'-[(S)-2-methylbutyl]biphenyl [194, 195].

The activated on states of a TN-LCD leak more light than desired, due to the nonideal behavior of the nematic director in the cell. Even at high applied voltages, some nematic molecules in the bulk of the cell are not completely parallel to the applied field [21]. Furthermore, at the surface of the cell, a layer of nematic molecules probably does not move at all, due to strong surface anchoring to

the alignment layer. This results in a splayed structure at both surfaces. These nonideal birefringence effects are especially pronounced during gray scale operation, because the optic axis of the nematic layer is at an oblique angle to the normal of the cell and the applied field. This nonideal behavior results in the asymmetric viewing-angle dependency of contrast, luminance, and chromaticity, due to interference effects and even to inversion of contrast in gray scale operation at large viewing angles. For example, for a typical TN-LCD cell, contrast ratios above 10 : 1 are limited to a maximum viewing angle of $\pm 45^\circ$ in the horizontal plane and $+60^\circ$ and -15° in the vertical plane [141]. This range is clearly unacceptable for large area displays (e.g., computer monitors).

The large viewing-angle dependency of TN-LCDs caused by the positive birefringence of the nematic layer can be compensated [141–151] to a large degree by using one or more optical retarders of positive or negative birefringence (See Sects. 3.1 and 7) in combination with the normally white (NW) mode (i.e., with crossed polarizers). The NW mode is especially important, because TN-LCDs with active addressing and video-rate compatibility are driven in this configuration. Compensation layers of negative birefringence used initially on either side of a TN-LCD cell with the optic axes in the plane of the cell led to an improvement in the horizontal plane, but did not improve the viewing-angle dependency in the vertical plane [141–144]. The compensation layers were replaced by compensation films [146], where the optic axis of the compensation layer of negative birefringence was also tilted and splayed with respect to the plane of the cell. If the optic axis of the compensation film of negative birefringence coincides with the optic axis of the nematic liquid crystal of positive birefringence, then unwanted birefringence effects are suppressed. The splay of the nematic layer is matched by the splay of the retardation film of opposite birefringence. The suppression of unwanted leakage of light in the on state leads to higher contrast at wider viewing angles and suppresses gray scale inversion. The twist of the nematic layer is compensated for by aligning the optic axis of the two compensation layers on either side of the cell at right angles to each other. This results in no retardation at normal incidence. Therefore, these optical compensation layers also improve the optical properties in the vertical as well as in the horizontal direction for nonnormal viewing angles, while maintaining good optical properties at normal viewing. These films are prepared from photopolymerizable columnar liquid crystals and are available commercially as a cross-linked anisotropic network referred to as Fuji WV Film Wide View A. A carrier film of cellulose triacetate also contributes to the compensation effect. Thus, these films are a hybrid of multiple compensation layers of positive and negative birefringence with the optic axis in the azimuthal plane of the cell, as well as configured with the optic axis tilted and splayed in the zenithal plane of the cell. Other approaches use a nematic anisotropic network with positive birefringence and a tilted optic axis [147] or holographic form birefringence [148]. The complex nature of the optics of these multiple anisotropic, birefringent layers means that it is essential to run computer simulations to find their optimal combination [149–151].

There are many other methods for improving the viewing angle dependency of TN-LCDs (e.g., pixel-divided cells [152] and multidomain cells [153]). However, these methods will not be discussed further.

13. NEMATIC MATERIALS OF POSITIVE DIELECTRIC ANISOTROPY

As the size and information content of TN-LCDs have increased, there has been a continual need to synthesize new classes of nematic liquid crystals to meet the ever more stringent requirements. In retrospect, the initial specifications were very undemanding. The major developments in the synthesis of nematic materials for the TN-LCDs are described next.

13.1. Nematics for Direct Addressing

The first TN-LCD prototypes [105] were constructed using a single nematic material [i.e., N-(4-ethoxybenzylidene)-4-aminobenzonitrile (**43**) of positive dielectric anisotropy ($\approx +14$)] [196, 197] and were prepared in the first decade of the 20th century [196]. The prototypes were operated in the nematic phase between the melting point (Cr–N = 106 °C) and the clearing point (N–I = 128 °C) (see Table VI). A tertiary mixture (**M1**), consisting of two 4-*n*-alkoxybenzylidene-4-aminobenzonitriles (**44** and **45**) [197]

and 4-heptanoylbenzylidene-4-aminobenzonitrile (**46**) [199] permitted operation at room temperature [200]. It was known that nematic mixtures usually exhibit a melting point much lower than that of the individual mixture components, whereas the clearing points are normally an average, although some deviation from ideal behavior is generally observed [200]. The binary mixture **M2**, consisting of the esters **47** and **48**, and the binary mixture **M3**, made up of the Schiff bases **49** and **50**, are also nematic at room temperature [201]. Furthermore, the threshold voltage of both of these mixtures is much lower than that of **M1**, due to an advantageous combination of elastic

Table VI. Transition Temperatures (°C), Dielectric Anisotropy, Threshold Voltage V , and Switching Times (s) for Nematic Mixtures **M1**, **M2**, and **M3** and Their Components **43–50**^a

Compound	Molecular structure	Crystal	Nematic	Isotropic	$\Delta\epsilon$	V_{th}	$t_{on}; t_{off}$	Ref.
43		• 106	• 128	•	+14			196, 197
44		• 63	• 111	•				198
45		• 55	• 101	•				198
46		• 54	• 98	•				199
47		• 66	(• 41)					199
48		• 46	• 55	•				199
49		• 65.5	• 77.5	•				199
50		• 33	• 64.5	•				199
M1	{ 44 : 33.3% 45 : 33.3% 46 : 33.3%	• 20	• 94	•	+14	3.5		105, 200
M2	{ 47 : 33.3% 48 : 66.6%	• 25	• 50	•	+14	0.9	0.2; 0.15	199
M3	{ 49 : 33.3% 50 : 66.6%	• -30	• 62	•	+14	1.1	0.1; 0.1	199

^aThe parentheses [()] represent a monotropic transition temperature.

constants [see Eq. (24)] the dielectric anisotropy of mixtures **M1**–**M3** is almost identical and the threshold voltage is independent of the cell gap. Moreover, because the values of the elastic constant ratio κ for **M2** and **M3** are very similar, the shorter switching times observed for **M3** also are due to a lower rotational viscosity γ_1 of the Schiff bases, compared with that of the esters [see Eqs. (25) and (26)]. The alkyl-substituted components of **M1** exhibit a lower viscosity than the alkoxy components of mixtures **M2** and **M3**.

The first commercial TN-LCDs utilized mixtures of Schiff bases and phenyl benzoate esters. They were manufactured by F. Hoffmann-La Roche and had to be handled with some care, due to the possibility of hydrolysis by atmospheric moisture. Researchers at the University of Hull realized that the chemical, photochemical, or electrochemical instabilities encountered for standard liquid crystals at that time were caused by the unsaturated linking unit between the aromatic rings. Therefore, the cyanobiphenyls [e.g., 4-cyano-4'-pentylbiphenyl (**51**); see Table VII], which do not contain a central linkage between the two phenyl rings [202], were designed and synthesized. Due to the absence of the unsaturated central linkage, they are chemically, photochemically, and electrochemically stable. The absence of the central linkage has the added advantage of lowering the viscosity and the melting point. Some homologues exhibit a nematic phase at room temperature. Mixtures of 4-*n*-alkyl-4'-cyanobiphenyls, 4-*n*-alkoxy-4'-cyanobiphenyls, and 4-*n*-alkyl-4''-cyano-*p*-terphenyls developed at Defense Evaluation and Research Agency (DERA) were made commercially available by BDH (now E. Merck, Darmstadt, Germany). Consequently, mixtures of 4-*n*-alkyl-4'-cyanobiphenyls, 4-*n*-alkoxy-4'-cyanobiphenyls, and 4-*n*-alkyl-4''-cyano-*p*-terphenyls over time replaced the mixtures of Schiff bases and phenyl benzoate esters in most commercially available TN-LCDs.

The pentyl homologues of the nitriles **51**–**73** [87, 203–221] listed in Tables VII–IX are representative of attempts to improve on the cyanobiphenyls [202]. The values of the dielectric anisotropy of 2-(4-cyanophenyl)-5-pentylpyridine (**52**) [203], 2-cyano-5-(4-pentylphenyl)pyridine (**53**) [204], and 2-(4-cyanophenyl)-5-pentylpyrimidine (**54**) [205] are higher than that of the 4-cyano-4'-pentylbiphenyl (**51**) due to the dipole moments along the long molecular axis associated with the lone pair of electrons on the nitrogen atoms (see

Table VII). If the dipole moments are in the opposite direction, $\Delta\epsilon$ is lower [e.g., 5-cyano-2-(4-pentylphenyl)pyrimidines (**55**) [205]. The 2-(4-cyanophenyl)-5-*n*-alkylpyrimidines [205] and related derivatives from F. Hoffmann-La Roche represent nematic liquid crystal replacements for the Schiff bases and phenyl benzoate esters.

Replacement of the phenyl ring attached to the alkyl group of the 4-cyano-4'-pentylbiphenyl (**51**) by a *trans*-1,4-disubstituted cyclohexane ring to create the *trans*-1-(4-cyanophenyl)-4-pentylcyclohexane (**17**) resulted in lower birefringence and lower viscosity without lowering the dielectric anisotropy substantially [87] (see Table VIII). This achievement led to the synthesis of a whole range of materials (e.g., compounds **56**–**67**) [206–216] with one aliphatic ring bearing a terminal alkyl group and one aromatic ring bearing a cyano group. Several types of nitriles collated in Table VIII, such as the dioxanes (**63**) [213] are also manufactured for TN-LCDs. This use was partially due to the large value of the dielectric anisotropy of the dioxanes, attributable, in part, to the dipole moments associated with the electronegative oxygen atoms. The high dielectric anisotropy gives rise to lower threshold and operating voltages. The other classes of aromatic nitriles suffer from at least one unattractive property, that prohibits their large-scale manufacture, such as photochemical instability (e.g., **61**), low resistivity values due to ionic impurities (e.g., **64**), and high viscosity (e.g., **67**).

If the cyano group is attached to a nonconjugated alicyclic ring, then the dipole moment of the cyano group is much lower than when it is attached to an aromatic ring, due to the absence of polarizable electron density (e.g., the aliphatic nitriles **68**–**73** collated in Table IX) [217–221]. Consequently, the value of the dielectric anisotropy is lower for aliphatic nitriles than for the corresponding structurally related aromatic nitriles (See Tables VII and VIII). However, the *trans*-1-(*trans*-4-cyanocyclohexyl)-4-pentylcyclohexane (**70**), with two cyclohexane rings instead of two phenyl rings in the corresponding 4-cyano-4'-pentylbiphenyl (**51**) or one cyclohexane ring and one phenyl ring in 4-(*trans*-4-pentylcyclohexyl)benzonitrile (**17**), still exhibits a moderately high value for the dielectric anisotropy [219]. Whereas the nematic clearing point is high and the birefringence and viscosity values are low, homologues of the aliphatic nitrile (**70**) are also used in nematic mixtures (e.g., by E. Merck). They are especially useful in nematic mixtures of low Δn for TN-LCDs with a cell gap

Table VII. Transition Temperatures (°C) and Some Values for the Dielectric Anisotropy ($\Delta\epsilon$ measured at $0.98 \times T_{N-1}$), Birefringence, and Bulk Viscosity (poise) of the Aromatic Nitriles **51**–**55**^a

Compound	Molecular structure	Crystal	Nematic	Isotropic	$\Delta\epsilon$	Δn	η	Ref.
51		• 22.5	• 35	•	+8.5	0.18	35	202
52		• 33.5	• 43.5	•				203
53		• 73	[• 31]	•	+9.4			204
54		• 71	(• 52)	•	+21	0.18	50	205
55		• 96	• 109 ^b	•	+3.4			205

^aThe parentheses ([]) represent a monotropic transition temperature and the square brackets ([]) represent an extrapolated “virtual” transition temperature.

^bSmectic A phase at 93.5 °C.

Table VIII. Transition Temperatures (°C) and Some Values for the Dielectric Anisotropy, Birefringence, and Bulk Viscosity (poise) of the Aromatic Nitriles **17** and **56–67**^a

Compound	Molecular structure	Crystal	Nematic	Isotropic	$\Delta\epsilon$	Δn	η	Ref.
17		• 31	• 55	•	+9.9 ^b	0.12	21	87
56		• 45.5	• 55.5	•				206
57		• 48	• 64	•				207
58		• 84	(• 36)	•				208, 209
59		• 70	• 98 ^c	•				208, 209
60		• 40	—	•				210
61		• 48	• 61	•				211
62		• 35	(• 5)	•				212
63		• 56	(• 52)	•	+11 ^d	0.8/9	46	213
64		• 48	—	•				214
65		• 74	(• 19)	•				215
66		• 98	—	•				215
67		• 62	• 100	•	−10 ^e	0.14	90	216

^aThe parentheses [()] represent a monotropic transition temperature.^b $\Delta\epsilon$ measured at $0.98 \times T_{N-I}$.^cSmectic B phase at 94 °C.^d $\Delta\epsilon$ measured at 42 °C.^e $\Delta\epsilon$ measured at 25 °C.

of $\approx 6.55 \mu\text{m}$ operated in the first minimum [21, 190] (See Fig. 27). The other aliphatic nitriles collated in Table IX generally exhibit a combination of high melting point, low nematic clearing point, and high viscosity.

The combination of a short alkyl chain, a *trans*-1,4-disubstituted cyclohexane ring, and a cyanobenzene in the *trans*-1-*n*-alkyl-4-(4-cyanophenyl)cyclohexanes (PCHs) appeared to be an optimal combination for TN-LCDs [87]. Therefore, it seemed potentially beneficial to investigate the incorporation of a stable central linkage between the two rings to form the compounds **74–83** collated in Table X [87, 222–226]. The chemists at E. Merck removed the central linkage from the 4-cyanophenyl *trans*-4-*n*-alkylcyclohexanoates [222] syn-

thesized earlier at the Martin Luther University (Halle, Germany), to yield the PCHs. These researchers were the first to investigate the effect of the *trans*-1,4-disubstituted cyclohexane ring on mesomorphic behavior. However, only the *trans*-1-*n*-alkyl-4-[2-(4-cyanophenyl)ethyl]cyclohexanes (PECHs) (e.g., **76**) [224], were found to be almost equivalent from the point of view of display devices. None of these materials is currently being manufactured, apart from the original esters (**74**) [222].

Changes in the terminal chains seemed to be one of the few remaining possibilities for modifying the properties of these core systems; see Table XI, where a series of *trans*-4-substituted-cyclohexylbenzonitriles (**17** and **84–99**) bearing a chain of fixed length

Table IX. Transition Temperatures (°C) and Some Values for the Dielectric Anisotropy ($\Delta\epsilon$ measured at $0.98 \times T_{N-1}$) and Birefringence of the Aliphatic Nitriles **68–73**^a

Compound	Molecular structure	Crystal	Nematic	Isotropic	$\Delta\epsilon$	Δn	Ref.
68		• < 25	• -25	•			217
69		• 113	(• 50)	•			218
70		• 62	• 85 ^b	•	+3 ~ 4	0.04/5	219
71		• 57	• 65	•			220
72		• 46	• 47	•			221
73		• 104	• 129	•			218

^aThe parentheses [()] represent a monotropic transition temperature.^bUnidentified smectic transitions at 43 and 52 °C.

(five units) is shown [87, 227–230]. In the series [227] of ethers (**84–87**), which differ only in the position of the oxygen atom, only the methoxypropyl-substituted-benzonitrile **87** with an oxygen atom at some distance from the core exhibits a nematic phase. However, because the melting point is higher than that of the unsubstituted benzonitrile **17**, the nematic range is narrower. Whereas the angle made by the carbon–oxygen–carbon bond (CH_2OCH_2) is very similar to that with a methylene unit instead of the oxygen atom ($\text{CH}_2\text{CH}_2\text{CH}_2$), it must be assumed that the effect of the oxygen atom on the clearing point is primarily of a polar and not a steric nature.

Substantial differences in the liquid crystal transition temperatures of benzonitriles **88–94** with a carbon–carbon double bond ($\text{C}=\text{C}$) in the terminal chain also were observed [228]. The elastic and dielectric constants also differ greatly, which is of real commercial and technological relevance for LCDs, especially supertwisted nematic liquid crystal displays (STN-LCDs) [24, 94] (See Sect. 14) [231–234]. Molecular modeling of ensembles of molecules indicates that steric effects due to different configurations of the terminal chain are primarily responsible for the very large differences in the transition temperatures [233]. The corresponding acetylene **95** derivative [227] exhibits a virtual nematic clearing point just above 0 °C. This is probably due to the nonaxial position of the acetylene group, which acts to increase the breadth of the molecule in this particular case.

The effect on the mesogenic tendencies of compounds [229] of combining two functional groups (i.e., one exerting polar effects and the other steric effects) is shown by reference to ethers **96** and **97**. For ether **96**, no liquid crystal behavior could be determined, whereas for ether **97**, a monotropic nematic phase could be detected at a temperature higher than that of the reference substance (**17**). Whereas ester **98** [230] is not mesomorphic, the related compound **99**, which contains an ester group (COO) and a carbon–carbon double bond exhibits very high nematic transition temperatures for two-ring systems [230]. This temperature is probably attributable to an advantageous combination of molecular rigidity and extended conjugation, despite the presence of the flexible cyclohexane ring.

13.2. Nematics for Multiplex Addressing

In simple displays (e.g., clocks and calculators), where the information content is limited, each pixel can be driven directly with a dedicated electrode contact and individual driver (See Sect. 5.1). With this type of addressing, the off voltage can be zero, and the on voltage can be several times the threshold voltage. Therefore, in a TN-LCD, where the electro-optical characteristic is relatively flat, a good contrast as well as low power consumption can be attained. The compounds described in the previous section satisfy these requirements. However, the need for displays with a higher information content (e.g., portable computers, personal organizers, and notebooks) requires more complex addressing schemes, due to the high cost of the many drivers required and an absence of space for the contacts. One way to resolve the problem is to use multiplex addressing (See Sect. 5.2).

In a TN-LCD with multiplex addressing, the number of addressable lines with good legibility is limited, although to a much lesser extent than direct addressing. Alt and Pleshko [93] showed that the maximum number of addressable lines (N) is given by the equation

$$\frac{V_{\text{ns}}}{V_s} = \sqrt{\frac{N-1}{N+1}}, \quad (29)$$

where V_s and V_{ns} are the select and nonselect voltages, respectively (See Sect. 5.2). Therefore, the more lines there are to be addressed, the smaller the permissible voltage change becomes. For example, there is only a difference of about 11% between the select and nonselect voltages for 64 addressable lines, which results in lower contrast, due to the inadvertent activation of neighboring pixels (i.e., crosstalk). To increase the number of addressable lines without reducing the contrast, it is essential that the electro-optical response curve have a very steep or, indeed, infinite slope. However, a steep electro-optic characteristic severely reduces the capacity for gray scale and, therefore, full color. Thus, multiplexed TN-LCDs are only capable of displaying a limited amount of black-on-white information with good

Table X. Transition Temperatures (°C) for the Compounds **17** and **74–83**^a

Compound	Molecular structure	Crystal	Nematic	Isotropic	Ref.
74		• 55	• 81	•	222
75		• 74	(• 67) ^b	•	223
17		• 30	• 59	•	87
76		• 45	• 55	•	224
77		• 74	(• 49)	•	224
78		• 54	• 107	•	225
79		• 41	• 73	•	225
80		• 51	(• 39)	•	226
81		• 40	(• 39)	•	226
82		• 63	(• 54)	•	226
83		• 64	(• 43)	•	226

^aThe parentheses [()] represent a monotropic transition temperature.^bMonotropic smectic X–smectic B transition at 58 °C.

contrast and legibility. In practice, a duty cycle of 1 : 64 is the upper limit; that is, 64 rows can be addressed in one frame.

To drive TN-LCDs with a relatively high information content with multiplex addressing, the nematic mixture used has to fulfill a new set of specifications. These requirements include a high $\Delta\epsilon$, for a low threshold voltage, a low viscosity for short response times, and low k_{33}/k_{11} , high k_{33}/k_{22} , and low $\Delta\epsilon/\epsilon_{\perp}$ for a steep electro-optic response curve (See Sect. 5.2). The birefringence, Δn , of the mixture depends on the cell gap and whether device operation is in the first or second transmission minimum. Furthermore, because the transmission curve also depends on temperature, a low rate of change is required (e.g., $\ll 1\%$ in threshold voltage per degree centigrade). This reduces the need to compensate for the change in operating voltages with temperature by electronic means. However, in practice, the variation of operating voltages with temperature is often compensated for electronically or by using an optically active dopant whose pitch decreases with increasing temperature [24].

The nematic liquid crystals shown in Tables VII–IX were found to exhibit strong antiparallel molecular correlation, probably due to the large dipole moment (≈ 4.0 D) of the cyano group attached to a

phenyl ring [235–239]. This structure corresponds to a binary mixture of virtually uncorrelated molecules (monomers) and pairs of associated molecules (dimers) [239] in a dynamic, temperature-dependent equilibrium. The effective resultant dipole moment and dielectric constants of the dimer will be much lower than those of the noncorrelated monomer, due to the antiparallel correlation of the terminal dipoles in the dimer. However, the effective molecular length of the dimer is greater (e.g., 1.4 times the molecular length of the monomer for 4-*n*-alkyl-4'-cyanobiphenyls) [235]. This length promotes the formation of a nematic phase at or just above room temperature for these short molecules. The degree and nature of the molecular association of polar nematic liquid crystals is described by the Kirkwood Froehlich factor *g* [236–239]. This factor can be calculated from macroscopic physical data, such as the refractive index, dielectric constants, and molecular dipole moments, obtained for the bulk nematic material [238, 239]. When $g = 1$, there is no correlation and when $g = 0$, there is complete correlation of the molecular dipoles. Thus, the Kirkwood Froehlich factor correlates directly with some bulk physical properties of a nematic phase, such as dielectric constants, elastic constants, clearing point, and viscosity.

Table XI. Transition Temperatures (°C) for Nitriles **17** and **84–99**^a

Compound	Molecular structure	Crystal	Nematic	Isotropic	Ref.
17		• 30	• 55	•	87
84		• 60	—	•	227
85		• 23	—	•	227
86		• 42	—	•	227
87		• 52	• 55	•	227
88		• 16	• 59	•	228
89		—	[• -144]	•	228
90		• 16	[• -67]	•	228
91		• -8	[• -54]	•	228
92		• 60	• 74	•	228
93		• 33	(• -14)	•	228
94		• 30	(• (10)	•	228
95		• 86	[• 1.5]	•	227
96		• 84	—	•	229
97		• 66	(• 59)	•	229
98		• 56	—	•	230
99		• 128	(• 119)	•	230

^aThe parentheses [()] represent a monotropic transition temperature and the square brackets ([]) represent a virtual (extrapolated) transition temperature.

Nematic mixtures, such as E7 (E. Merck, Darmstadt, Germany), consisting solely of components with a terminal cyano group (in this case, cyanobiphenyls and cyano-*p*-terphenyls), were found to be very difficult to multiplex to any significant degree. However, it was found [240] that mixtures of nematic compounds of low dielectric anisotropy, such as the esters **18**, **19**, and **100–107** [169, 241–246] shown in Table XII and the nitriles **17** and **51–73** shown in Tables VII–IX, consist of a larger number of unassociated polar and nonpolar monomers that not only give rise to a high value for the observed dielectric anisotropy of the mixture and, therefore, a lower threshold voltage, but also a low value of k_{33}/k_{11} . Thus, mixing apolar materials of low viscosity, weakly positive or negative dielectric anisotropy with polar nematic liquid crystals of high positive dielectric anisotropy creates nematic mixtures more suited to multiplexed

addressing of TN-LCDs than materials that consist solely of polar liquid crystals with terminal substituents with large dipole moments (e.g., the cyano group).

The aromatic phenyl benzoate esters **100–102** possess either a low nematic clearing point or narrow-range nematic phases of high viscosity [241–243]. The phenyl bicyclo[2.2.2]octane esters exhibit very low k_{33}/k_{11} values and high nematic clearing points, but possess high viscosity values and are synthetically complex [169, 245, 246]. Only the phenyl cyclohexyl esters **103–105** combine a good nematic range with a moderately high viscosity [241, 243, 244]. Although ester **106**, which has two cyclohexane rings, only possesses a smectic *B* phase, homologues with shorter chains also exhibit a nematic phase of relatively low viscosity and very low birefringence (See Table XIV) [244]. Although the presence of a fluorine atom in a lateral position in com-

Table XII. Transition Temperatures (°C) for Compounds **18**, **19**, and **100–107**^a

Compound	Molecular structure	Crystal	Smectic B	Nematic	Isotropic	Ref.
100		• 36	—	(• 26)	•	241
101		• 50	—	• 58	•	242
102		• 2	—	• 5	•	243
103		• 36	(• 29)	• 48	•	241
104		• 49	—	• 81	•	241
105		• 18	—	• 37	•	243
106		• 51	• 71	—	•	244
18		• 31	—	• 64.5	•	169, 245
107		• 42	—	• 100	•	245
19		• 26	—	• 65	•	169, 246

^aThe parentheses [()] represent a monotropic transition temperature.

pounds **102**, **105**, and **19** leads to a lower melting point (sometimes below room temperature) and the suppression of smectic phases, the viscosity of these esters is considerably higher than that of the nonfluoro-substituted analogues **100**, **103**, and **18**.

However, even the cyclohexyl esters shown in Table XII, used initially to produce multiplexable nematic mixtures, were found generally to induce unacceptably long response times, even in low-information-content TN-LCDs with multiplex addressing. Therefore, in attempts to produce apolar nematogens of low viscosity, a series of new materials that incorporate either (1) one *trans*-1,4-disubstituted cyclohexane ring or two *trans*-1,4-disubstituted cyclohexane rings and one or two aromatic ring (such as compounds **108–116** [247–251]; see Table XIII) or (2) only two *trans*-1,4-disubstituted cyclohexane rings (such as compounds **117–125** [244, 252–258]; See Table XIV), with a variety of different central linkages, were synthesized.

Most of the compounds (**108–116**) [247–251] collated in Table XIII exhibit a nematic phase, as well as an unwanted smectic B phase. However, only the compounds linked by the ethane linkage (e.g., **109**) [248] or linked directly (e.g., **114–116**) [250, 251], were found to exhibit the desired low values of the viscosity. The suppression of the highly viscous smectic B phase by mixture formulation is a difficult task, especially at low temperatures for mixtures with a wide temperature range. Therefore, compounds such as **108**, which only possess a smectic B phase, are not very suitable components of nematic mixtures with a wide nematic temperature range. Furthermore, the presence of a smectic B phase at elevated temper-

atures for such compounds also leads to a limited solubility at low temperatures in nematic mixtures. Therefore, mixtures of two-ring compounds, such as **113**, which are not mesomorphic at room temperature but exhibit a very low viscosity, are used in admixture with analogous three-ring and four-ring materials, such as compounds **114** and **115**, with very high nematic clearing points [250, 251]. The presence of a fluorine atom in a lateral position in compounds such as **116** leads to a greater molecular separation and a greater tendency for formation of the nematic phase [250, 251].

Nematic compounds that contain two cyclohexane rings possess very low values of birefringence, although they also exhibit a tendency for smectic B formation (e.g., compounds **117–125** [244, 252–258]; (See Table XIV)). Homologues of ether **119** [255] and ester **120** [244] also exhibit nematic phases, although unfortunately they are of high viscosity. Homologues with longer terminal chains exhibit predominantly smectic B phases (e.g., compound **121**) [256]. In spite of this, homologues of ester **120** [244, 94] have been manufactured for certain TN-LCD applications where low birefringence is required and very short response times are not essential. Of the classes of compounds shown in Tables XIII and XIV, only short-chain homologues of aliphatic ether **118** [253, 254] exhibit the desired combination of nematic phase and low viscosity, as well as a very low value of birefringence.

Studies of apolar aromatic liquid crystals have been much more limited, due to the preconception that the nematic phases of fully aromatic materials are intrinsically more viscous than those of the

Table XIII. Transition Temperatures (°C) for Compounds **108–116**^a

Compound	Molecular structure	Crystal	Smectic B	Nematic	Isotropic	Ref.
108		• 50	• 196	—	•	247
109		• 23	• 135	• 143	•	248
110		• 70	• 133	• 143	•	249
111		• 70	• 90	• 156	•	250
112		• 50	• 111	—	•	249
113		• 1	—	[• –70]	•	250, 251
114		• 13	• 164	• 170	•	250, 251
115		• 45	• 275 ^b	• 305	•	250, 251
116		• 37	—	• 117	•	250, 251

^aThe parentheses [()] represent an extrapolated transition temperature.

^bSeveral ordered smectic phases present.

Table XIV. Transition Temperatures (°C) for Compounds **117**–**125**^a

Compound	Molecular structure	Crystal	Smectic B	Nematic	Isotropic	Ref.
117		• 64	• 82 ^b	—	•	252
118		• 49	—	• 50	•	253, 254
119		• 7	• 8	• 17.5	•	255
120		• 23	—	• 37	•	244
121		• 52	• 72	—	•	244, 256
122		• 46	• 109	—	•	257
123		• 53	• 95	—	•	257
124		• 52	(• 50)	—	•	257
125		• 71	• 84	—	•	258

^aThe parentheses [()] represent a monotropic transition temperature.^bMonotropic smectic X–smectic B transition at 58 °C.

analogous cyclohexane derivatives. This concept has generally been found to be the case. However, liquid crystals that combine a high positive dielectric anisotropy with low k_{33}/k_{11} and $\Delta\epsilon/\epsilon_{\perp}$ ratios have been prepared by the incorporation of lateral substituents, especially fluorine, in polar molecules, such as compound **127** [237] collated in Table XV, which incorporates a terminal substituent with a strong dipole moment. Although the presence of a lateral fluorine atom results in lower absolute values for the elastic constants than do those of the nonlaterally substituted ester and results in a lower degree of molecular association, the relatively low value for the elastic constant ratio k_{33}/k_{11} does not improve the multiplexability of mixtures that contain such components. The viscosity of these fully aromatic esters is indeed very high.

However, fully aromatic apolar 5-*n*-alkyl-2(4-*n*-alkoxyphenyl)pyrimidines (e.g., compound **128**) [259] were found to give rise to very low k_{33}/k_{11} elastic constant ratios, high birefringence, and low viscosity in admixture with polar nematics, such as the compounds shown in Tables VII–IX (e.g., homologues of compound **17**) and related three-ring materials [87]. More examples of these pyrimidine materials are given in Sect. 19, because they are also used in ferroelectric smectic C* mixtures. Such pyrimidines are synthetically very accessible and, as a consequence of this attractive combination of properties, they are used on a large scale in nematic mixtures for

TN-LCDs with multiplexed addressing, especially where a higher Δn value is required.

13.3. Nematics for Active Matrix Addressing

The low contrast and brightness, as well as the very narrow viewing cone of TN-LCDs with even a moderate degree of multiplexing, renders the TN-LCD unsuitable for fast, high-information-content displays. These displays are presently achieved by using (1) versions of STN-LCDs [24] with a high degree of multiplexed addressing, (2) TN-LCDs [96–99] with active matrix addressing with a discrete thin film transistor (TFT-TN-LCDs) [99], or (3) diode metal-insulator-metal (MIM-TN-LCDs) [97] at each individual pixel on an amorphous or crystalline silicon substrate [98] (See Sect. 5.3). The advantages of active matrix addressed TN-LCDs include high contrast ratio, almost complete absence of cross-talk, gray scale, fast response times, a high information content, and large area. Major disadvantages are a direct consequence of the low brightness of the TN-LCD, that is, low luminosity or high power consumption. The high production cost associated with the silicon substrate and the low production yield due to pixel damage and subsequent repair initially hindered the market acceptance of active matrix addressed TN-LCDs. However, improved production equipment and processes

Table XV. Transition Temperatures (°C), Elastic Constant Ratio^a (k_{33}/k_{11}), Birefringence^a (Δn), Dipole Moment (μD), Kirkwood Froehlich Factor (g), and Dielectric Anisotropy ($\Delta \epsilon$) for Compounds **126–128**

Compound	Molecular structure	Crystal	Smectic A	Nematic	Isotropic	k_{33}/k_{11}	Δn	μ	g	$\Delta \epsilon$	Ref.
126		• 44	—	• 57	•	1.52	0.15	5.6	0.7	19.9	237
127		• 47	—	• 54	•	1.41		4.8	0.8	9.8	237
128		• 34	• 56	• 64	•	1.0			1.0	≈ 0	259

^aMeasured at $0.95 \times T_{N-I}$.

have reduced the price differential with comparative STN-LCDs substantially.

A TFT-TN-LCD is basically a memory effect; that is, the thin film transistor maintains the charge on the pixel capacitor until the pixel is readdressed in the following frame. Charge leakage from the pixel (e.g., into the nematic liquid crystal) decreases the effective voltage across the pixel, which leads to lower contrast. Consequently, the resistivity of the nematic liquid crystal mixture should be constant over time and also be orders of magnitude higher ($\approx 10^{12}$ – 10^{14} Ω cm) than that of commercial nematic mixtures for standard TN-LCDs without active-matrix addressing. The holding ratio HR represents the stability of the resistivity of the liquid crystal over time and is defined as

$$HR = \left[\left(1 - e^{-2T/\tau} \right) \left(\frac{\tau}{2T} \right) \right]^{1/2} \quad (30)$$

where T is the frame time and τ is the time constant for the pixel and storage capacitor. These requirements impose very demanding specifications on the purity, the stability (e.g., chemical, photochemical, and electrochemical), and the resistivity over time of each of the individual mixture components and the mixture itself.

Nitriles were found to be unsuitable for LCDs with active-matrix addressing, because the high polarity of the cyano group dissolves ions out of the layers on the LCD substrate. This leads to a lower value of resistivity and, therefore, a decrease in the effective holding voltage and contrast ratio. Hence, liquid crystals that contain halogen atoms, especially fluorine atoms (i.e., substituents with a much lower value for the permanent dipole moment than that of a cyano group), were synthesized. Typical examples are collated in Tables XVI–XIX for compounds **129–152** [260–274]. Many related derivatives have been reported [208, 226, 229, 249, 275, 276]. The two-ring compounds that correspond to those listed in these tables are also used in the same mixtures for TN-LCDs with active-matrix addressing as the

Table XVI. Transition Temperatures (°C), C–X Bond Length (\AA), Dipole Moment of C–X Bond (Debye), Birefringence (20 °C), Dielectric Anisotropy (extrapolated to 100% at 20 °C), and Viscosity (cP at 20 °C) for Compounds **129–133**

Compound	Molecular structure	Crystal	Smectic A	Nematic	Isotropic	C–X	μ	Δn	$\Delta \epsilon$	η	Ref.
129		• 67	—	• 82	•	1.10	≈ 0	0.15	≈ 0	22.7	260
130		• 76	—	• 125	•	1.39	1.47	0.17	+4.9	25.1	260
131		• 100	—	• 158	•	1.78	1.57	0.22	+7.5	46.6	260
132		• 125	—	• 163	•	1.93	1.59	0.24	+7.6	63.0	260
133		• 79	87	• 184	•	1.14	4.0	0.23	+13		261

Table XVII. Transition Temperatures (°C) and Dielectric Anisotropy (extrapolated to 100% at 20 °C) for Compounds **134–141**^a

Compound	Molecular structure	Crystal	Smectic <i>B</i>	Nematic	Isotropic	$\Delta\epsilon$	Ref.
134		• 58	• 81	• 98	•	0	262
135		• 98	• 123	• 178	•	0	262
136		• 100	—	• 152	•	+7.3	262
137		• 43	• 128	• 147	•	+9	263, 264
138		• 67	• 120	• 162	•	+9	265, 266
139		• 123	—	• 124	•	+13	265
140		• 96	—	• 222	•	+11	87
141		• 156	—	[• 60]	•	+27.1	267

^aThe parentheses [()] represent an extrapolated “virtual” transition temperature.Table XVIII. Transition Temperatures (°C) and Dielectric Anisotropy (extrapolated to 100% at 20 °C) for Compounds **142–147**^a

Compound	Molecular structure	Crystal	Smectic <i>B</i>	Nematic	Isotropic	$\Delta\epsilon$	Ref.
142		• 90	—	• 158	•	+7.3	268
143		• 46	—	• 124	•	+9.3	263
144		• 42	—	(• 33)	•	+12.6	269
145		• 64	—	—	•	+15.2	270
146		• 123	—	—	•	+20.5	270
147		• 49	• 65	• 159	•	+3.2 ^b	25, 271

^aThe parentheses [()] represent a monotropic transition temperature.^bExtrapolated at $T_{N-I} = 10$ °C.

Table XIX. Transition Temperatures (°C) and Dielectric Anisotropy (extrapolated to 100% at 20 °C) for Compounds **148**–**152**^a

Compound	Molecular structure	Crystal	Smectic A	Nematic	Isotropic	$\Delta\epsilon$	Ref.
148		• 84	—	• 105	•	+12.2	272
149		• 52	—	• 104	•	+12.5	272
150		• 124	—	• 156	•	+17.7	273
151		• 99	• 134	• 157	•	+20.8 ^b	274
152		• 71	—	(• 6)	•	+10.2	275

^aThe parentheses [()] represent a monotropic transition.^bExtrapolated at $T_{N-1} = 10$ °C.

three-ring analogues. Most of the two-ring compounds are not liquid crystalline and, therefore, they are not dealt with in any detail here.

The data in Table XVI indicate that a moderately high value of $\Delta\epsilon$ is indeed exhibited by compounds with a halogen atom in a terminal position (e.g., **130**–**132**) [260]. The value of $\Delta\epsilon$ increases with the dipole moment of the halogen–carbon bond. However, the largest value of $\Delta\epsilon$ exhibited by the halogenated compounds (i.e., **132**) is not as high as that of the corresponding nitrile (**133**) [261], due to the smaller dipole moment of the halogen–carbon bond. However, the viscosity increases drastically with the size of the terminal halogen atom [260]. Therefore, the fluorine atom in a terminal position appears to offer the best combination of a moderately high positive value of $\Delta\epsilon$ and a moderately low viscosity.

Significantly higher values of dielectric anisotropy can be achieved by using terminal groups that contain several halogen atoms bonded to the same carbon atom [e.g., trifluoromethoxy, difluoromethoxy, or trifluoromethyl groups (compounds **137**–**139**)] (See Table XVII) [87, 262–267]. The nematic clearing point and $\Delta\epsilon$ generally increase with polarity of the terminal substituent compared with the values of the nonterminally substituted reference compound **134**. The trifluoromethyl-substituted compound (**139**) possesses a $\Delta\epsilon$ value above that of corresponding nitrile (**140**). The effect on $\Delta\epsilon$ of the three fluorine atoms in compound **139** is seen by comparing its value with that of the analogous compound (**135**), with three hydrogen atoms in place of the fluorine atoms. A very high value of $\Delta\epsilon$ is observed for the sulfonyl fluoride (**141**), due to the added electron density and polarizability of the sulfonyl group. The trifluoromethoxy-, trifluoromethyl-, or difluoromethoxy-substituted compounds (**137**–**139**) are synthetically readily accessible. Therefore, these and related similarly substituted compounds are found

in commercial nematic mixtures for TN-LCDs with active-matrix addressing.

Very high values of the dielectric anisotropy are achieved for compounds that contain two or more fluorine atoms spread around the molecule (See Table XVIII) [25, 263, 268–271]. There is a clear additive effect for the dipole moments associated with the fluorine atom (e.g., compare the dielectric data for the polyfluorinated compounds **142**–**146**). However, the viscosity does not increase proportionately, because the molecular width does not increase with the addition of each supplementary fluorine atom. The nematic clearing point decreases with increasing number of lateral substituents. Compounds **145** and **146**, which have four and five fluorine atoms in terminal and lateral positions, respectively, are not mesomorphic. However, such compounds can be used as components of nematic mixtures to increase the positive value of the dielectric anisotropy to the desired value. The presence of a carbon–carbon double bond in a suitable position can help to compensate for the effect of the lateral substituents on the nematic clearing point e.g., compare the thermal data for compounds **143** and **147**.

Compounds such as **148** and **149** in Table XIX that combine a terminal group that contains halogen atoms with additional fluorine atoms in lateral positions can also exhibit values of $\Delta\epsilon$ comparable to that of aromatic nitriles [272]. Other combinations of heteroatoms can achieve similar effects. For example, the presence of electronegative heteroatoms other than halogen incorporated in aromatic or aliphatic rings, such as oxygen and nitrogen, can also give rise to high values of the dielectric anisotropy (e.g., the pyrimidine **150** [273] and the dioxane **151** [274]). There are many other possibilities [208, 226, 229, 249, 275, 276, 277] for combining different molecular building blocks to produce polar nematogens without a

ciano group or, indeed, for incorporating heteroatoms in different parts the molecular structure of organic molecules (e.g., compound **152** incorporates two fluorine atoms in the central linkage between two of the rings in the molecular core).

Many of the compounds shown in Tables XVI–XIX solvate ions to a much lesser degree than analogous nitriles, as indicated by the high stable holding ratios of nematic mixtures in which they are contained. Therefore, due to the advantageous combination of physical properties previously referred to, many of the polar compounds (without a terminal cyano group) shown in the Tables XVI–XIX are indeed used in commercial mixtures for TN-LCDs with active addressing, such as TFT-TN-LCDs.

14. SUPERTWISTED NEMATIC LCDs

It was evident in the early 1980s that the optical performance of highly multiplexed TN-LCDs was intrinsically insufficient for high-information-content displays for portable instruments, such as notebooks, personal digital assistants, and portable computers. Large-area, highly multiplexed TN-LCDs (e.g., the ones used in the first handheld televisions and portable computers) exhibited poor contrast, low brightness, and very strong viewing-angle dependency. However, it was found that a range of supertwisted nematic (STN) LCDs invented in the mid-1980s could fulfil these requirements. Competing technologies based on active-matrix addressed TN-LCDs see Sects. 5.3 and 13.3 and ferroelectric liquid crystals (see Sect. 19) were still in a development stage [24, 94, 109, 278–284].

The sharpness of the electro-optic contrast curve of applied voltage against optical transmission increases dramatically for twist angles, $\phi > 90^\circ$ up to values of $\approx 180^\circ$. For higher values ($180^\circ < \phi < 360^\circ$), hysteresis, bistability, and visible stripe textures [285] are observed. Under well-defined conditions, the stripe textures can be suppressed, and bistable displays with very steep electro-optic transmission curves can be produced. The steepness of the electro-optic transmission curve increases with increasing twist angle until a value with infinite slope is found for $\phi = 270^\circ$ (see Fig. 28). This allows the very high degree of multiplexing essential for high-information-content displays. Initially, STN-LCDs were addressed using rms voltages and Alt and Pleschko [93] driving schemes. Although such displays are adequate for high-information-content applications, such as notebooks, personal computers, and calculators, the long response times give rise to an unacceptably low contrast at the video rate (< 50 ms) required for television screens or computer monitors. So-called Active AddressingTM [286] of STN-LCDs can lead to substantially quicker response times and, therefore, of advantage contrast displays at video rate. Due to this combination of advantageous properties, STN-LCDs were manufactured in volume shortly after their invention. They contributed significantly to the market acceptance of laptop computers and thereby facilitated their large-scale manufacture. Although the market share for STN-LCDs is being eroded by TN-LCDs with active addressing (See Sect. 13.3) at the high end of the market, STN-LCDs are increasingly replacing TN-LCDs with multiplexed addressing for low-information-content applications.

15. STN-LCD CONFIGURATIONS

There are several kinds of STN-LCDs, not only with different optics, but also different operating principles. The common features that link these types of LCDs are a large twist of the chiral nematic medium within the cell and, at least in principle, the ability to display a large amount of digital and graphic information. The most important of these variants are described in the following subsections.

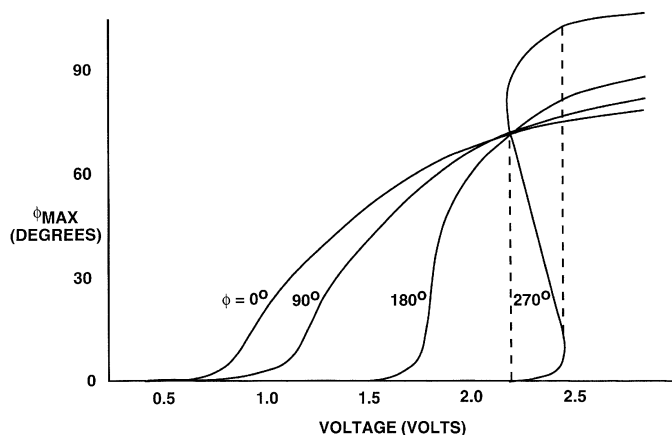


Fig. 28. A plot of the twist angle at the center of a cell versus applied voltage for a series of twist angles of nematic LCDs [24].

15.1. Bistable Liquid Crystal Twist LCDs

The first supertwisted nematic LCD was reported [287, 288] by researchers from Bell Laboratories in Murray Hill, NJ. Although not commercialized, these prototypes, the theory of cell operation that is associated with them, and related predictive computer programs laid the foundation for the discovery of the other commercially successful STN-LCD modes.

15.1.1. Device Configuration

A chiral nematic mixture of positive dielectric anisotropy is homogeneously aligned in a standard sandwich cell with a very high pretilt angle ($\theta \leq 45^\circ$), large cell gap ($d < 20 \mu\text{m}$), and crossed polarizers (See Fig. 29). The front polarizer is parallel to the nematic director in the off state. The large pretilt angle was produced by a vacuum-deposited SiO layer (1000 Å). The cell gap was generated by the use of mylar film at the edges of the device.

15.1.2. Off State

The nematic director is tilted at a high angle from the substrate surface at both substrates. Therefore, the molecules of the chiral

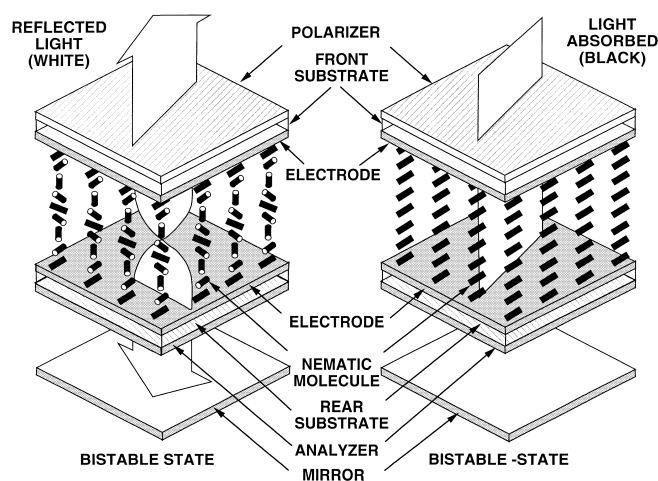


Fig. 29. Schematic representation of a bistable liquid crystal twist LCD [287, 288].

nematic phase are essentially parallel from the top to the bottom of the cell. In spite of the presence of a chiral dopant, there is no twisted structure in the cell. This leads to extinction between crossed polarizers and the nonaddressed parts of the display appear black.

15.1.3. On State

If a voltage, (e.g., 2 V) is applied above a threshold value and then removed quickly, the addressed pixel reverts to the original off-state orientation. However, if a higher voltage (e.g., 3 V) is applied and then removed, the nematic director twists through 360° at various angles to the cell normal to form a second stable state. In this orientation, two elliptically polarized modes are formed, and some light passes through the front polarizer and rear analyzer. Thus, information is displayed with negative contrast (i.e., a bright image against a black background). The on and the off states are both stable and, therefore, a bistable cell is formed under these conditions. This is due, in part, to the presence of the chiral dopant, which increases the energy barriers between the nontwisted and fully twisted states. Other metastable states can be eliminated by a judicious choice of device configurations, addressing schemes, and material properties. There are no disclinations in the activated areas. In principle, this opens up the possibility of producing high-information-content displays, due to the shorter refresh frame times associated with bistable displays (i.e., a memory effect). However, the growth of metastable twist states with intermediate twist, which degrade the optical performance of the device, is found to occur around dust particles in cells with a cell gap below a critical value ($d < 20 \mu\text{m}$). Therefore, whereas the response time is proportional to the square of the cell gap, very long response times (≈ 1 s) are observed. This phenomenon also precludes the use of distributed spacers, which, in turn, excludes the possibility of producing the uniform cell gap with very little variation that is essential for the manufacture of large-area LCDs. If the polarizers are removed and a dichroic dye is added, then a kind of supertwisted White and Taylor type guest-host (GH) LCD results [94, 112, 280, 290, 291]. The absorption of light by the dye depends on the direction of its polarization axis, which follows the LC director. In the off state, half the light (colored by the dye) is transmitted. Both elliptically polarized rays are absorbed in the twisted on state. This produces black information on a colored background; that is, the contrast is inverted from negative, as displayed by the nondyed mode, to positive. The contrast obtained is low, because the thick cells ($d > 20 \text{ mm}$) used in this STN-LCD result in a high optical retardation ($\Delta n d$).

15.2. Supertwisted Nematic Guest-Host LCDs

The supertwisted Nematic Guest-Host (STN-GH) LCD resolves many of the problems associated with the bistable liquid crystal twist (BLCT) LCDs, such as low contrast and optical instabilities. It also addresses the fact that nonsupertwisted GH-LCDs cannot be multiplexed to any significant degree [289]. At the Royal Signals and Radar Establishment (now DERA) in Malvern, U.K. in 1983 it was found [94, 112, 280, 290, 291] that supertwisted versions of the Heilmeyer and Zanoni GH-LCD [29, 30] that used one polarizer and a nematic liquid crystal of high birefringence or a White and Taylor type guest-host (GH) LCD [292–294] with no polarizers and a chiral nematic liquid crystal of low birefringence both exhibited very steep electro-optic transmission curves over a very short range of voltages [112, 280, 290, 291]. This observation offered the possibility of practical production of large-area, high-information-content GH-LCDs for the first time.

15.2.1. Display Configuration

The sandwich cell incorporates a chiral nematic host, a dichroic dye with positive dichroic ratio, and a relatively high concentration of

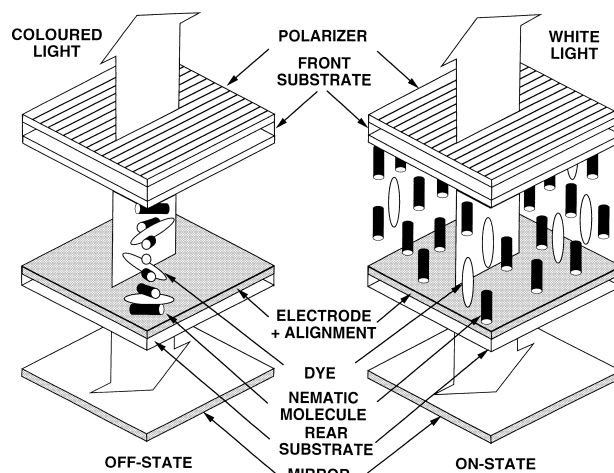


Fig. 30. Schematic representation of a supertwisted nematic guest-host LCD [24, 280, 112, 290, 291].

chiral dopant. This composition induces a large twist angle (270°) for a given cell gap ($0.5 < d/p < 1$). An alignment layer induces a high tilt angle, and one polarizer is fixed to the front substrate surface (See Fig. 30).

15.2.2. Off State

The incident polarized light is not wave guided, due to the highly twisted structure of the chiral nematic host. However, the transition moment of the dissolved dye, which follows the director orientation, has a component that is parallel to the electric vector of the propagated light, which is absorbed and then reemitted. Therefore, the nonaddressed areas of the display appear colored.

15.2.3. On State

Application of an operating voltage V_{op} just above the threshold voltage V_{th} causes the director to become strongly aligned with the electric field, due to the high pretilt angle and the highly twisted structure. The transition moment of the dye is now orthogonal to the direction of polarization of the light, which is transmitted without absorption taking place. Thus, white information is displayed against a colored background for reflective displays; that is, the contrast is negative. The transition from the on state to the off state is very sharp and occurs over a very short range of voltages ($V_{op}/V_{th} < 1.1$). Theoretically, this allows a very high degree of multiplexing (1 : 500) using standard Alt and Pleshko addressing schemes. However, practical displays operate at lower duty cycles (1 : 200), because the operating voltages are very sensitive to even marginal inhomogeneities in the cell gap (e.g., $\pm 0.1 \mu\text{m}$ over a gap of $9.0 \mu\text{m}$), due to insufficient planarity of the glass substrates. Furthermore, the temperature dependence of the threshold and operating voltages must be compensated for either through the drive electronics or through the use of optically active dopants. This situation also impacts negatively on the maximum degree of multiplexing possible. However, the viewing-angle cone is still very wide. A variant of this device configuration involves the use of a low tilt angle. However, the degree of multiplexing is considerably lower.

15.3. Superbirefringent Effect LCDs

Superbirefringent effect (SBE) LCD [24, 107, 282, 283] were reported by Scheffer and Nehring (Brown Boveri, Baden,

Switzerland), at more or less the same time as STN-GH-LCDs. Although the device configurations are very similar, the SBE-LCD differs in several important respects from the STN-GH-LCD. The most important difference is that the SBE device does not use a dichroic dye to produce an optical effect; rather, it utilizes the optical interference of two normal, elliptically polarized modes of transmitted light that are generated by a high-tilt, highly twisted nematic structure viewed between two crossed polarizers set in a nonstandard fashion. The input polarization direction is not parallel to the director at either substrate, and the polarizers are not crossed at 90° (See Fig. 31). It also differs from the related BLCT-LCDs (See Sect. 15.1), which also use birefringence effects, in that it is optically stable due to the fact that the cell gap is much thinner, the tilt angle is much lower, and the twist angle of the chiral nematic phase is also lower.

15.3.1. Device Configuration

Prototype SBE-LCDs, illustrated in Figure 32, combined a chiral nematic mixture with large twist angle ($\phi \approx 240\text{--}270^\circ$; $d/p \approx 0.75$), positive dielectric anisotropy ($\Delta\epsilon \approx +12$), high birefringence ($\Delta n \approx 1.4$), and a very large pretilt angle ($20^\circ < \theta < 30^\circ$). The high pretilt angle can be produced using vacuum-deposited SiO or SiO₂, rubbed polyimide, or polyphenylenes Imperial Chemical Industries (ICI). The polarization directions of the polarizer and analyzer are at angles α and β to the director at the front surfaces (See Fig. 31).

15.3.2. Off State

The highly twisted chiral nematic structure results in the production of two normal, elliptically polarized modes. The high optical retardation produced by the highly birefringent chiral nematic phase of positive dielectric anisotropy results in interference at the analyzer. Therefore, the display appears colored in the off state (blue or yellow). It was found that the highest contrast was obtained when the polarizers were positioned at 30° and 60° to the direction of alignment (nematic director) at the front and the rear surfaces, respectively. This gives a positive contrast display referred to as the yellow mode of black figures on a yellow background. Rotating one of the polarizers by 90° gives a negative contrast with white figures on a blue background (blue mode).

15.3.3. On State

Applying a voltage slightly above the threshold voltage results in a modest realignment ($\approx 10\%$) of the nematic director in the middle of the cell. This reduces the effective birefringence, the optical path difference, the degree of interference (color), and, therefore, the intensity of transmitted light. Thus, due to the highly twisted structure

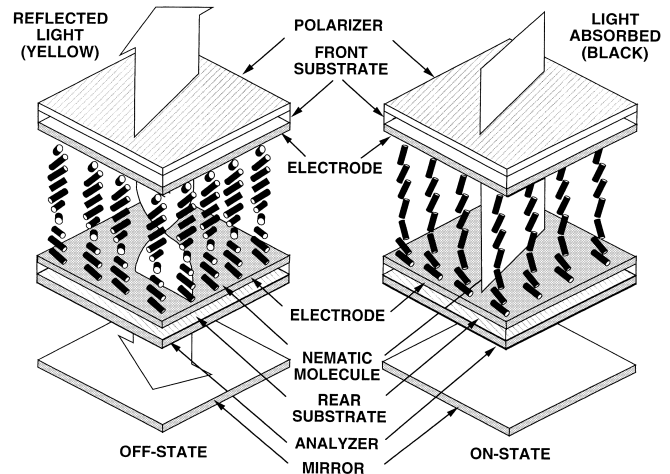


Fig. 32. Schematic representation of a superbirefringent effect LCD [24, 282, 283].

of the nematic phase, a large optical effect is generated by a small change in voltage, and a very steep slope of the distortion-voltage curve is produced. In practice, a twist angle ϕ is chosen so that the cell can be addressed at either side of a narrow bistable range in the distortion-voltage curve. In principle, this permits a very high degree of multiplexing (e.g., 1 : 600) using rms addressing and standard Alt and Pleshko driving schemes. However, device characteristics of practical displays, such as the lowering of applied voltage caused by the resistance of the electrode layers and the internal resistance of the drive electronics, as well as variations in the cell gap due to nonoptically flat surfaces, result in a lower, but still high, multiplexing rate [e.g., a duty cycle of 1 : 120, is obtained with a high contrast ratio (e.g., 10 : 1 for the yellow mode and 8 : 1 for the blue mode) when the display is directly viewed]. The contrast ratio is still relatively high (e.g., 4 : 1) for wide viewing angles (e.g., 45°) and is far superior to that observed for the GH-STN-LCDs and TN-LCDs at a comparable multiplex rate. The response time (90% transmission) was long (≈ 300 ms at 20°C) with normal rms addressing, which precludes use for applications where video frame rate addressing with short response times ($\approx 40\text{--}50$ ms) is required, such as television screens. The high tilt angle θ at the surfaces energetically favors the highly twisted and tilted nematic configurations in both the off state and the on state: That is, it suppresses a competing distortional structure and eliminates scattering stripe instabilities. It also results in a high

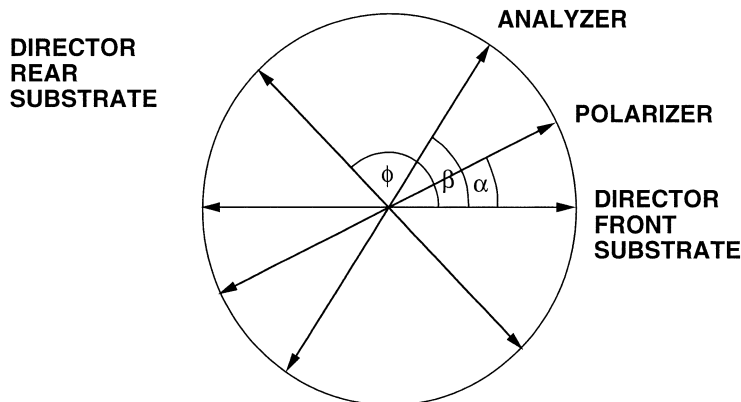


Fig. 31. Polarizer and analyzer orientation, as well as the director orientation, at the substrate surfaces for STN-LCDs [24].

transmission I when

$$\Delta n d \cos^2 \theta_{av} \approx 0.8 \mu\text{m}, \quad (31)$$

where θ_{av} is the average tilt angle in the nonselect state. The temperature dependence of the select and nonselect voltages can be compensated for either electronically or by using two optically active dopants of opposite twist sense [295]. As the pitch of one chiral dopant increases with temperature, the other decreases, resulting in an almost constant variation of pitch with temperature, at least over the operating temperature range of the display.

15.4. Supertwisted Nematic LCDs

The supertwisted nematic (STN) LCD reported by Kando, Nakagomi, and Hasagawa [108] in Japan is essentially a lower tilt-bias ($\theta \approx 5^\circ$) version of the SBE-LCD. It is otherwise very similar. Therefore, somewhat confusingly, both are often referred to as STN-LCDs, as are GH-STN-LCDs.

15.4.1. Device Configuration

The sandwich cell contains a chiral nematic mixture of positive dielectric anisotropy and a twist of 180° . The polarizer and analyzer are parallel to polarization directions at angles $\alpha, \beta = 45^\circ$ from the director at the substrates.

15.4.2. Off State

The two elliptically polarized rays give rise to a bright yellow background in the off state with a transmission I given by

$$I \propto \cos^2 \left\{ \pi \left[1 + \left(\frac{1.00}{\lambda} \right) \right]^2 \right\}^{1/2} \quad (32)$$

The transmission is optimized for yellow light when the optical path difference Ω is given by

$$\Omega = \Delta n d = 1 \mu\text{m} \quad (33)$$

15.4.3. On State

The application of an appropriate voltage above the threshold voltage gives rise to extinction. Thus, a positive contrast of black information on a yellow background is produced.

15.5. Optical Mode Interference LCDs

In 1987, an optical mode interference (OMI) LCD was reported by researchers at F. Hoffmann-La Roche in Basel, Switzerland. [296, 297] The OMI-LCD [109, 284] is a black and white display with a degree of multiplexability comparable with that observed for other STN-LCDs. However, it is much more tolerant of some other variable cell parameters. A larger pretilt angle (θ) can result in lower operating voltages, but much lower levels of multiplexability. Therefore, a low value of θ is preferred for high-information-content displays. Response times are also much shorter than those of comparable STN-LCDs. However, OMI-LCDs suffer from the major disadvantage of poor brightness. Although this can be improved to some extent by increasing the twist angle, the degree of brightness remains substantially lower than that of a comparable STN-LCDs or even TN-LCDs.

15.5.1. Device Configuration

The major difference between the configuration of the OMI sandwich cell and other STN-LCDs is that the optical path difference ($\Omega = \Delta n d \ll 1 \mu\text{m}$) is much lower than that for other STN-LCDs ($\approx 1 \mu\text{m}$). Other significant differences are that there is no requirement for a significant pretilt angle ($0 < \theta < 5^\circ$), the twist angle of the chiral nematic layer is lower (180°), the front polarizer is parallel to the nematic director ($\alpha = 0^\circ$), and the polarizers are crossed ($\beta = 90^\circ$) (see Fig. 33).

15.5.2. Off State

The 180° twist leads to strong interference between the two elliptically polarized rays generated by the highly twisted nematic structure. Whereas there is no wave guiding, if the optical path difference is small (e.g., $0.4 \mu\text{m}$), a bright, white, nondispersive off state is produced. The chiral nematic mixture has positive dielectric anisotropy, low birefringence, and a long pitch ($d/p \approx 0.3$).

15.5.3. On State

The effect of applying a voltage slightly above the threshold voltage is to realign the nematic director in the middle of the cell. This results in absorption of the propagated light at the analyzer. Thus, a positive contrast display of black information on a white background is produced. A very steep slope for the distortion-voltage curve is produced with a low dependence on temperature or inhomogeneity of the cell gap.

16. ELECTRO-OPTIC PERFORMANCE OF STN-LCDs

The cell construction and electro-optic response of SBE-LCDs and STN-LCDs (and, to a lesser degree, OMI-LCDs) exhibit strong similarities. The ways in which they differ were described in Section 15. Therefore, to a certain extent it is valid to generally discuss their electro-optic responses together. The general description is of a STN-LCD with a twist angle $240^\circ < \phi < 270^\circ$, pretilt angle $5^\circ < \theta < 10^\circ$, and a cell gap $\approx 5 \mu\text{m}$.

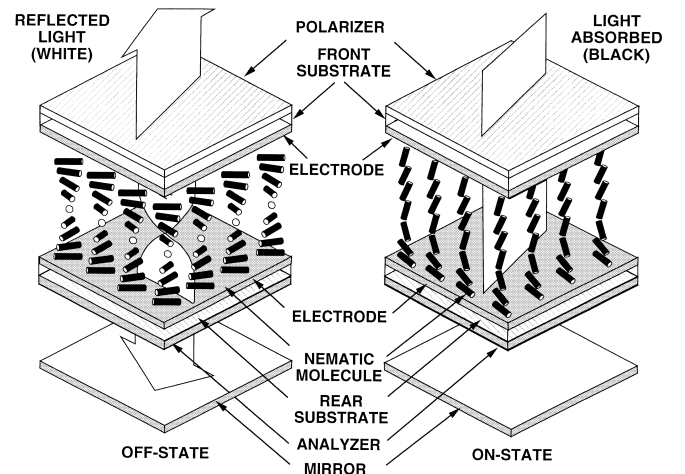


Fig. 33. Schematic representation of an optical mode interference LCD [109, 284, 296, 297].

16.1. General Electro-Optic Performance of STN-LCDs

The steepness γ of the electro-optic curve should be as low as possible to maximize the number of lines to be addressed [298], that is,

$$\gamma \propto \frac{\Delta \varepsilon k_{11}}{\varepsilon_{\perp} k_{33}} \quad (34)$$

Then ε_{\perp} and k_{33}/k_{11} should be as large as possible. A large value of $\Delta \varepsilon$ also gives rise to a low threshold voltage. However, because the overall response time is

$$t_{\text{on}} + t_{\text{off}} \propto \frac{\eta \varepsilon_{\perp} d^2}{\Delta \varepsilon^2} \left(\frac{k_{33}}{k_{11}} \right)^2 \quad (35)$$

a high value of the ratio k_{33}/k_{11} and a high value of ε_{\perp} lead to long response times. Therefore, if the cell gap d can be reduced and low viscosity nematic materials are used, then shorter response times will result. For STN-LCDs operating in the first minimum, because the product $\Delta n d$ is fixed (e.g., 0.85 for a 240° twist cell), then Δn should be as high as possible. A further complication is furnished by the fact that the elastic constant and the dielectric ratios also determine the upper limit of the ratio of cell thickness to the chiral nematic pitch, before the optically disruptive stripe texture appears [298]:

$$\left(\frac{d}{p} \right)_{\text{max}} \propto \frac{\Delta \varepsilon k_{11}}{\varepsilon_{\perp} k_{33}} \quad (36)$$

Therefore, a larger k_{33}/k_{11} ratio permits a greater tolerance of pitch variations for a given cell gap.

16.2. Temperature Dependence of Electro-Optic Performance of STN-LCDs

The temperature dependence of the electro-optic characteristics of multiplexed STN-LCDs is large and has to be compensated to avoid degradation of the optical performance of the display at temperatures significantly above or below room temperature. Initially, this was done electronically. However, a more sophisticated solution to this problem is based on the temperature dependence of the pitch of the chiral nematic mixture used in the display. The capacitive threshold voltage of a chiral nematic mixture that contains an optically active chiral dopant is dependent on the pitch of the mixture [299],

$$V_c^d = V_c^o \left(1 + \frac{d}{p} \frac{4k_{22}\phi_o}{\pi(k_{11} + (k_{33} - 2k_{22})/4)} \right)^{1/2} \quad (37)$$

where p is the pitch of the chiral nematic mixture, ϕ_o is the twist angle, and d is the cell gap. The temperature dependence of the first term in Eq. (37) is

$$V_c^o(T) = V_c^o(22^\circ\text{C}) + \frac{\partial V_c^o}{\partial T}(T - 22^\circ\text{C}) \quad (38)$$

It may be assumed that the optical threshold voltage is proportional to the capacitive threshold voltage. The twist angle and elastic constant ratios are almost temperature independent, and, because V_c^o decreases with temperature, the pitch of the chiral nematic mixture should also decrease with temperature according to Eq. (37), so that V_c^d is temperature independent. Therefore, optically active dopants are required to induce the desired twist in the STN-LCD cell, as well as a temperature-decreasing pitch, while increasing the viscosity and decreasing the nematic clearing point as little as possible. This prescription is usually achieved by using two chiral dopants of opposite twist sense [295]. They should both possess a high helical twisting power, because the viscosity of a nematic mixture increases substantially with increasing concentration of chiral dopant.

17. INTERFERENCE COLOR COMPENSATION

To produce full-color STN-LCDs, the interference colors must be suppressed. Suppression can be achieved in several ways, each of which has a series of advantages and disadvantages. The most common method utilized commercially involves the use of passive optical phase retarders [300].

17.1. Double-Layer Supertwisted Nematic LCDs

One method to compensate for optical retardation is to use double-layer STN-LCDs (DSTN-LCDs) [301, 302]. In addition to the active display STN cell, another nonaddressed, passive STN cell with opposite twist sense is stacked above it. This second cell, which is identical to the first, but not switched on or off, acts as a retardation compensation layer. Utilization of a second STN cell has the advantage of the same temperature dependence of the birefringence and the same dispersion, assuming that both cells are using an identical liquid crystal mixture. Note that it is important that the second STN cell does not have to be addressed; therefore, there is no increase in power consumption. However, the requirement for two almost identical cells increases the manufacturing cost and weight of the final product.

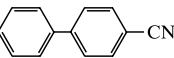
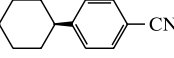
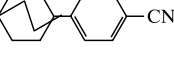
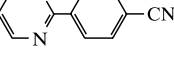
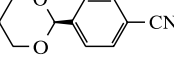
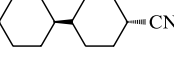
17.2. Film-Compensated STN-LCDs

A number of methods, such as selective polarizers and color filters, were developed to try to compensate for the interference colors manifested by STN-LCDs without the high cost and weight of DSTN-LCDs. However, a black and white appearance is produced most efficiently by utilizing polymer retardation layers with a high birefringence and an opposite twist sense to the STN-LCD (see Sect. 7). However, this also leads to a decrease in the display brightness, due to light absorption.

18. NEMATIC MATERIALS FOR STN-LCDs

It is known from studies of nematic materials for TN-LCDs [303–305] that nematic liquid crystals with a combination of terminal cyano group and a short alkyl chain exhibit not only a positive value for the dielectric anisotropy, but also relatively high ratio of k_{33}/k_{11} (see Table XX). Thus, the terminal cyano group present in compounds **17**, **51**, **54**, **63**, **67**, and **70** [87, 202, 205, 213, 216, 219] gives rise to a positive dielectric anisotropy combined with a moderate dielectric ratio, $\Delta \varepsilon/\varepsilon_{\perp}$, and a high bend to splay elastic constant ratio (i.e., $1.4 < k_{33}/k_{11} < 3.0$) [306, 307]. This combination should produce a steep electro-optic characteristic curve and a low threshold voltage for STN-LCDs (see Sect. 16.1). However, it also induces high values of the rotational and bulk viscosities [308–310]. Comparisons of values quoted in the literature for the physical properties of nematic liquid crystals are always somewhat open to interpretation, due to differences in measurement methods, different absolute temperatures (e.g., 22 or 25 °C) and reduced temperatures (e.g., $T_N = 10^\circ\text{C}$ or $0.95 \times T_N$) for the measurements and the use of extrapolated data from a variety of nematic mixtures at different concentrations. This variance of interpretation is especially the case for elastic constants, where the use of extrapolated data is common. Unfortunately, non-ideal behavior is common for such mixtures, and nonlinear behavior is not unusual; that is, the values extrapolated to 100% are often matrix and concentration dependent. However, although the absolute values of the data collated in Table XX [measured in the same way at the same reduced temperature ($0.96 \times T_N$)] are lower than those in the literature [25, 231, 311, 312] (usually measured at 22 °C), the trends and relative values are the same.

Table XX. Transition Temperatures (°C) [195, 354–358] and Some Values [307] for the Dielectric Anisotropy ($\Delta\epsilon$), the Ratio of the Dielectric Anisotropy and the Dielectric Constant Measured Parallel to the Director ($\Delta\epsilon/\epsilon_{\perp}$), and the Ratio of the Bend (k_{33}) and Splay (k_{11}) Elastic Constants for Nitriles **17**, **51**, **54**, **63**, **67**, and **70**^a

Compound	Molecular structure	Crystal	Smectic 2	Smectic 1	Nematic	Isotropic	$\Delta\epsilon$	$\Delta\epsilon/\epsilon_{\perp}$	k_{33}/k_{11}	Ref.
51		• 22.5	—	—	• 35	•	+13.3 ^b	2.0	1.43 ^b	202
17		• 31	—	—	• 55	•	+11.2 ^b	2.1	1.77 ^b	87
67		• 62	—	—	• 100	•	+10.0 ^b		2.35 ^b	216
54		• 71	—	—	(• 52)	•	+34.0 ^c	4.3	1.13 ^b	205
63		• 56	—	—	(• 52)	•	+17.4 ^c	2.2	1.36 ^b	213
70		• 62	• 43	• 52	• 85	•	+4.5 ^b	0.5	1.59 ^b	219

^aThe parentheses [()] represent a monotropic transition temperature.

^bMeasured at a reduced temperature of $0.96 \times T_{N-1}$.

^cExtrapolated value from a 10% concentration in a nematic mixture.

18.1. Polar Nematic Materials for STN-LCDs

A starting point for synthesizing new nematic materials with a high positive dielectric anisotropy, a high transverse dielectric constant, a low rotational and bulk viscosity, and, especially, a high k_{33}/k_{11} ratio came from mean-field theories [81, 313, 314] combined with molecular modeling [233]. These sources indicated that the elastic constant ratio k_{33}/k_{11} should be proportional to the length-to-breadth ratio of individual molecules; that is, long molecules with a narrow rotation volume about the molecular long axis should be synthesized. There is some indication that this may still be the case if ensembles of molecular dimers are taken into account [233]. Dimerization would increase the effective molecular length and, hence, would increase k_{33}/k_{11} .

This explanation seems to be confirmed to some extent by experimental data. It was found that nematic mixtures of apolar nematic compounds of low dielectric anisotropy and nitriles (See Sect. 132) consist of a larger number of unassociated polar and nonpolar monomers [233–240]. This composition not only gives rise to a high value for the observed dielectric anisotropy of the mixture, but also a low value of k_{33}/k_{11} , because the proportion of long molecular dimers is reduced. Thus, mixing apolar materials of low viscosity, weakly positive or negative dielectric anisotropy, and low k_{33}/k_{11} elastic constant ratio with polar nematic liquid crystals of high positive dielectric anisotropy and high k_{33}/k_{11} creates nematic mixtures suited to multiplexed addressing of TN-LCDs, which require a low ratio of k_{33}/k_{11} , but not for STN-LCDs. Therefore, a different approach to producing nematic mixtures with a high k_{33}/k_{11} ratio was required.

First attempts involved the synthesis of molecules with polar substituents in lateral positions. The dipole moment of the lateral substituents clearly gives rise to the required high ϵ_{\perp} value, low $\Delta\epsilon/\epsilon_{\perp}$ ratio, and, hopefully, high k_{33}/k_{11} elastic constant ratio. However, this projection is not consistent with the data collated in Table XXI for the phenyl benzoate esters **126**, **127**, and **153** [237]. The degree of molecular association of the 4-cyano-2-fluorophenyl 4-heptylbenzoate **127** and 4-cyano-3-fluorophenyl 4-heptylbenzoate **153**, which both possess a fluorine atom in a lateral position, is much lower than that of 4-cyanophenyl 4-heptylbenzoate **126**. The absence

of a molecular dimerization in the nematic phase of ester **153** ($g = 1$) means that the effective molecular length is much shorter than that of pairs of associated dimers. Therefore, a much lower clearing point results for this ester compared with that of the nonlaterally substituted ester **126** or 2-fluoro-substituted ester **127**. However, the ratio of k_{33}/k_{11} of compound **153** is found to be the highest of all three esters. Incidentally, the absence of association and the large dipole moment of 6.1 D of the 3-fluoro-substituted benzoate **153** result in the largest value for dielectric anisotropy observed for a liquid crystal ($\approx +50$). This fortuitous combination of properties led to the commercial production of ester **153** and other homologues of this ester on a large scale (by E. Merck in Germany and Dai Nippon Ink in Japan). These esters are used as components of nematic mixtures to significantly lower the threshold and operating voltages of STN-LCDs, while maintaining a steep electro-optic characteristic.

A breakthrough was achieved with the synthesis of alkenyl nematic materials (i.e., compounds with a carbon-carbon bond in the terminal alkyl or alkoxy chain). As long as the double bond is not conjugated with an aromatic ring, it absorbs in the near ultraviolet part of the spectrum below the cutoff frequency of the glass substrates used in most LCDs. Thus, alkenyl versions of commercial nematic materials with alkyl and alkoxy terminal chains can be just as chemically, electrochemically, and photochemically stable as other nematic mixtures. The elastic constants and other physical properties, such as the nematic clearing point, of materials that incorporate an alkenyl side chain were found to exhibit unusually high or low values [25, 231, 233, 312, 315]. However, these values varied greatly for (otherwise identical) isomers, depending on the position and the configuration [i.e. trans and cis, or (*E*) and (*Z*), respectively] of the double bond [25, 231, 233, 312, 315] (see Table XXII).

A trans carbon-carbon double bond at an odd number of carbon atoms away from the molecular core, such as in compounds **154** and **158**, shown in Table XXII, exhibits a high nematic clearing point [315]. The corresponding cis isomers **155** and **159** possess very low extrapolated clearing points, probably due to the nonlinear conformation of the alkenyl chain of the latter two materials. It is usually assumed that a linear, or at least completely antiperiplanar,

Table XXI. Transition Temperatures ($^{\circ}\text{C}$), Elastic Constant Ratio (k_{33}/k_{11}), Birefringence (Δn), Dipole Moment (μD), Kirkwood Froehlich Factor (g), and Dielectric Anisotropy ($\Delta \epsilon$) for Compounds **126**, **127**, and **153**

Compound	Molecular structure	Crystal	Nematic	Isotropic	k_{33}/k_{11}	Δn	μ	g	$\Delta \epsilon$	Ref.
126		• 44	• 57	•	1.52 ^a	0.15 ^a	5.6	0.7	19.9	237
127		• 47	• 54	•	1.41 ^a		4.8	0.8	9.8	237
153		• 28	• 28.5	•	1.71 ^a	0.14 ^a	6.1	1.0	48.9	237

^aMeasured at $0.95 \times T_{N-I}$.Table XXII. Transition Temperatures ($^{\circ}\text{C}$) for *trans*-1-(4-Cyanophenyl)-4-pentylcyclohexane **17** and Some Isomeric *trans*-1-(4-Cyanophenyl)-4-pentenylcyclohexanes **154–160**^a

Compound		Molecular structure	Crystal	Nematic	Isotropic	Ref.
17			• 30	• 55	•	87
154	(E)		• 16	• 59	•	315
155	(Z)		—	[• -144]	•	315
156	(E)		• 16	[• -67]	•	315
157	(Z)		• -8	[• -54]	•	315
158	(E)		• 60	• 74	•	315
159	(Z)		• 33	(• -14)	•	315
160			• 30	(• 10)	•	315

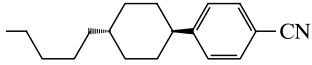
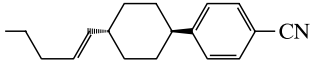
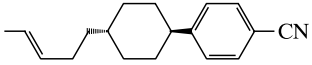
^aThe parentheses [()] represent a monotropic transition temperature and the square brackets ([]) represent a virtual (extrapolated) transition temperature.

conformation of a terminal aliphatic chain supports nematic phase formation by maintaining the rodlike shape of the molecule. The nematic clearing point of compounds **154** and **158** with a *trans* carbon–carbon double bond at an odd number of carbon atoms (1 and 3) away from the molecular core is higher than that of the reference material **17** [87], with no double bond in the terminal chain. This may be due to a greater rigidity of the alkenyl chain, which

allows less possible combinations with a nonlinear shape, a higher degree of molecular polarizability [315], or both.

The values of most of the physical properties of compounds **154** and **158** [315], with a *trans* carbon–carbon double bond at an odd number of carbon atoms away from the molecular core are equal or superior with respect to those of the reference material **17** [87] use as components in nematic mixtures for LCDs, especially STN-LCDs

Table XXIII. Transition Temperatures ($^{\circ}\text{C}$), Elastic Constants (k_{11}, k_{22}, k_{33} ; 10^{-12} N), Dielectric Anisotropy ($\Delta\epsilon$), Dielectric Constant Measured Perpendicular to the Molecular Long Axis (ϵ_{\perp}), birefringence (Δn), refractive index measured perpendicular to the director (n_o), rotational viscosity (γ_1 , poise), and Bulk Viscosity (η , poise) for *trans*-1-(4-Cyanophenyl)-4-pentylcyclohexane **17**, *trans*-1-(4-Cyanophenyl)-4-[(*E*)-pent-1-enyl]cyclohexane **154**, and *trans*-1-(4-Cyanophenyl)-4-[(*E*)-pent-3-enyl]cyclohexane **158** extrapolated to 100% at 22°C [312]

			
	17 [87]	154 [315]	158 [315]
Cr–N	30	16	60
N–I	55	59	74
k_{11}	8.98	9.40	9.41
k_{22}	4.73	6.15	5.74
k_{33}	18.3	22.8	24.1
k_{33}/k_{11}	2.03	2.42	2.56
$\Delta\epsilon$	12.22	13.03	13.13
ϵ_{\perp}	4.85	5.02	5.02
$\Delta\epsilon/\epsilon_{\perp}$	2.52	2.60	2.62
Δn	0.119	0.136	0.130
n_o	1.487	1.493	1.483
γ_1	1.28	1.34	
η	215	221	

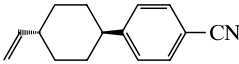
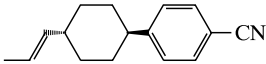
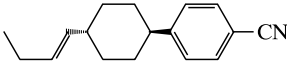
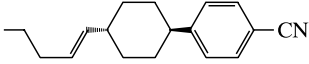
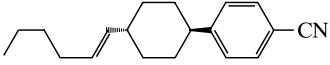
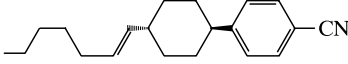
(see Table XXIII). The values of the elastic constant ratio k_{33}/k_{11} , the birefringence, and dielectric anisotropy of the alkenyl compounds **154** and **158** are all higher than the corresponding values of the reference commercial compound **17**. The viscosity is comparable. Thus, alkenyl-substituted compounds were found to be excellent components of nematic mixtures for use in STN-LCDs, due to a combination of very steep electro-optic curve, high nematic clearing point, and fast response times.

The thermal data collated in Table XXIV for compounds **154** and **161–165** [315] illustrate the effect of the length of the alkenyl chain on the liquid crystal transition temperatures. The nematic clearing point exhibits a clear odd–even effect, depending on the number of carbon atoms in the alkenyl chain. The higher clearing points are

those of compounds **162**, **154**, and **165** with an odd number of units in the chain. This is probably due to a higher degree of anisotropy of the molecular polarizability along the molecular long axis for the compounds **162**, **154**, and **165** compared to the corresponding materials **161**, **163**, and **164** with an even number of carbon atoms in the alkenyl chain. The unpredictability of the melting point of liquid crystals is demonstrated by comparing the melting point of the first three members of the series with that of the latter three members of the series. The latter three compounds exhibit a wide-range nematic phase at room temperature that could not have been predicted with any degree of certainty based on literature data.

The transition temperatures collected in Table XXV for compounds **161** and **166–170** [227, 315] reveal an odd–even effect for

Table XXIV. Transition Temperatures ($^{\circ}\text{C}$) for Some *trans*-1-Alkenyl-4-(4-cyanophenyl)cyclohexanes **154** and **161–165**^a

Compound		Molecular structure	Crystal	Nematic	Isotropic	Ref.
161			56	(• 29)	•	315
162	(<i>E</i>)		• 66	• 73	•	315
163	(<i>E</i>)		• 45	• 315	•	315
154	(<i>E</i>)		• 16	• 59	•	315
164	(<i>E</i>)		• 14	• 39	•	315
165	(<i>E</i>)		• 18	• 49	•	315

^aThe parentheses [()] represent a monotropic transition temperature.

Table XXV. Transition Temperatures (°C) for Some *trans*-1-Alkenyl-4-(4-cyanophenyl)cyclohexanes **160**, **161**, and **166–170**^a

Compound	Molecular structure	Crystal	Nematic	Isotropic	Ref.
161		• 56	(• 29)	•	315
166		• 29	• 31	•	315
167		• 50	• 53	•	315
160		• 30	(• 10)	•	315
168		• 46	• 53	•	227, 315
169		• 19	• 32	•	227, 315
170		• 38	• 53	•	227, 315

^aThe parentheses [()] represent a monotropic transition temperature.

the clearing point and at least one low melting point for the homologue **169** with a long alkenyl chain. Alkenyl chains with a terminal carbon–carbon double bond are attractive from a cost–performance point of view, due to the absence of *trans*–*cis* configurational isomers. Chemical reactions to form carbon–carbon double bonds normally give rise to a mixture of *trans* and *cis* isomers. The *cis* isomer can be converted by chemical or catalytic means into the more energetically favored *trans* isomer. However, this is costly and time consuming. Residual amounts of the unwanted isomer still have to be removed, usually by recrystallization from a suitable organic solvent. Alkenyl chains with a terminal double bond do not suffer from this problem, due to the absence of *trans* and *cis* isomers, because the terminal hydrogen atoms are equivalent. The physical properties of terminal alkenyl compounds with respect to use in mixtures for LCDs are usually inferior to those of corresponding isomers with a *trans* double bond at an odd number of atoms away from the central core, such as those shown in Tables XXIII and XXIV.

18.2. Apolar Nematic Materials for STN-LCDs

Apolar nematic compounds usually possess a low k_{33}/k_{11} ratio (typically $1.0 < k_{33}/k_{11} < 1.5$), partially due to the absence of molecular dimers. However, they are essential components of nematic mixtures for STN-LCDs, because they are used to lower the viscosity and melting point of the nematic mixture, as well as to improve the multiplexability of the mixture, partly due to reduction in the proportion of molecular dimers of associated polar molecules. Therefore, after the synthesis of the first polar alkenyl liquid crystals and the discovery of high values for the k_{33}/k_{11} ratio, a series of apolar compounds with a carbon–carbon double bond in various positions in the terminal chain were synthesized. Typical examples, such as compounds **171–180**, are shown in Table XXVI [227, 316].

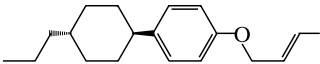
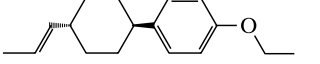
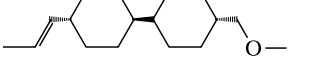
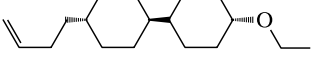
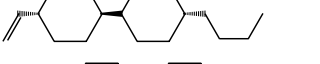
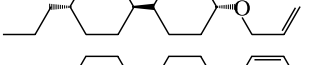
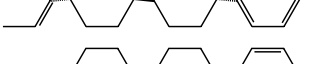
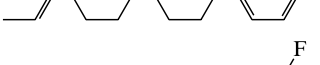
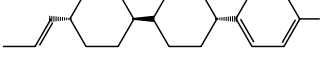
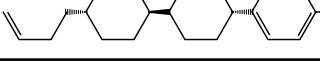
Based on the preceding evaluation of the results of physical measurements on polar alkenyl compounds, the position and configuration of the carbon–carbon double bond found in the apolar compounds are similar to those in the polar compounds (essentially for the same reasons). However, the combination of low melting point and high nematic clearing point in the bicyclohexane compounds

(**173**, **174**, and **176**) is remarkable. The birefringence and viscosity of these compounds is remarkably low [227].

The corresponding three-ring compounds (e.g., **177–180**) shown in Table XXVI exhibit higher melting and clearing points than those of the analogous two-ring materials, as expected [227, 316]. The low melting points of most of these kinds of alkenyl compounds and the absence of ordered smectic phases, such as the smectic B phase, render them very useful components of nematic mixtures. They can be used to increase the temperature range of the nematic phase by increasing the clearing point and lowering the melting point of the mixture. The presence of two cyclohexane rings and one phenyl ring gives rise to a low viscosity and a low birefringence for these three-ring materials [227, 316]. Fluoro- and methyl-substituted compounds are attractive from a synthetic point of view, due to the availability of cheap starting materials in an otherwise complex synthesis procedure. The short methyl group, being a terminal alkyl chain, also contributes to a low viscosity and the suppression of smectic phases.

The thermal data in the Tables XXI–XXVI show that the presence of a *trans* carbon–carbon double bond in a limited number of positions leads to a higher clearing point and a higher k_{33}/k_{11} ratio than those exhibited by the corresponding material without a double bond in the terminal chain. At the same time, smectic phases—especially the ordered smectic B phase—are strongly suppressed. This is advantageous for the formulation of nematic mixtures with a low melting point and a high clearing point, as well as a steep electro-optic transmission curve. The effect on the nematic clearing point and the suppression of smectic phases is additive to some extent (See Table XXVII) [317, 318]. Compound **181** [317, 318] exhibits only a smectic B phase. Compound **182**, with one carbon–carbon double bond, possesses a smectic B phase at a lower temperature, as well as a nematic phase. Compound **183**, with two double bonds, exhibits only a nematic phase with a higher clearing point than that of compounds **181** and **182**. No smectic phase could be observed. Compound **184** with three *trans* carbon–carbon double bonds exhibits the highest clearing point of all and is purely nematic [318]. However, the ratio of k_{33}/k_{11} is only slightly higher for compound **183** with two double bonds than that of the corresponding compound **182** with only one double bond. Thus, the effect of the presence of

Table XXVI. Transition Temperatures (°C) for Alkenyl-Substituted Cyclohexane Derivatives **171**–**180**

Compound	Molecular structure	Crystal	Smectic B	Nematic	Isotropic	Ref.
171		• 42	—	• 58	•	227
172		• 49	—	• 62	•	227
173		• 12	• 22	• 62	•	227
174		• 13	—	• 45	•	227
175		• -8	• 52	• 64	•	227
176		• 19	—	• 32	•	227
177		• 74	—	• 214	•	227, 316
178		• 105	—	• 194	•	227, 316
179		• 87	—	• 186	•	227, 316
180		• 52	• 104	• 177	•	227, 316

carbon–carbon double bonds on the elastic constants appears not to be additive, at least not in a linear or consistent way. The ratio of k_{33}/k_{11} for the compound with two carbon–carbon double bonds is still much lower than that exhibited by polar materials, such as the benzonitriles **17**, **51**, **54**, **63**, **67**, and **70** and phenyl benzoates **126**, **127**, and **153**, which have no double bond in the terminal chain, listed in Tables XX and XXI: they are very much lower than those of the alkenyl-substituted benzonitriles **154** and **158** shown in Table XXIII. The viscosity of the three compounds **182**–**184** increases with the number of carbon–carbon double bonds in the molecule. This is a general phenomenon for alkenyl compounds.

The three-ring alkenyl compounds **185** and **186** [318] shown in Table XXVII exhibit higher clearing points than those of the analogous two-ring materials. Although their melting points are low, Compounds **185** and **186** exhibit a smectic B phase at very high temperatures. The viscosity is also much higher than that of the analogous two-ring compounds, as expected. The k_{33}/k_{11} ratio is slightly lower than that of the corresponding two-ring materials **182** and **183**, perhaps due to a dilution effect attributable to the third cyclohexane ring.

The thermal data collated for the cyclohexane esters **106**, **187**, and **188** listed in Table XXVIII demonstrate that, as is often the case in liquid crystal research, it is not always valid to extrapolate from one series of compounds to another. The effect of the presence of one and then two trans carbon–carbon double bonds on the nematic and smectic transition temperatures of compounds **106**, **187**, and **188** is not as great as expected based on the data collated in Table XXVII for very similar cyclohexane materials. The fully saturated ester **106** [244] exhibits only a smectic B phase, as does the corresponding

ester **187** [319–321], with one trans carbon–carbon double bond in the terminal chain. Even the ester **188**, with a double bond in each of the terminal chains, possesses only a nematic phase over a temperature range of 2 °C. [319–321].

The combined effect of the presence of a trans carbon–carbon double bond and a nonconjugated heteroatom (e.g., an oxygen atom) in the terminal chain on the transition temperatures of compound **191** is shown in Table XXIX [322]. The thermal data for the corresponding compound **189** with just an oxygen atom in the chain and the related alkyl–alkenyl compound **190** without the oxygen atom are also shown in Table XXIX. The ether **189** exhibits only a smectic B phase, whereas the alkyl–alkenyl compound **190** exhibits both a smectic B and a nematic mesophase at elevated temperatures. However, the temperature range of the nematic phase of compound **190** is much narrower than that of ether **191**, which exhibits a particularly wide nematic temperature range (82 °C) with a melting point below room temperature. Thus, some synergetic effects, due to the presence of both an oxygen atom and a carbon–carbon double bond, can clearly lead to a wide nematic temperature range and a low melting point [322].

The effect of systematically introducing an oxygen atom, a carbon–oxygen double bond [i.e., a carboxy group (C=O)], and a carbon–carbon double bond (C=C) into the completely aliphatic compound **192** [323] to yield the intermediate compounds **193**–**195** [324] and then (*E*)-but-2-enoate **196** is shown in Table XXX. Increasing the polarity of the chain by introducing an oxygen atom or a carboxy group does not induce a nematic phase. The added stiffness of the chain due to the reduced number of nonlinear conformations and increased dispersion forces due to the presence of the

Table XXVII. Transition Temperatures (°C) and Some Values for the Viscosity (mPa s) and the Ratio of the Bend (k_{33}) and Splay (k_{11}) Elastic Constants for Apolar Cyclohexane Derivatives **181–186**

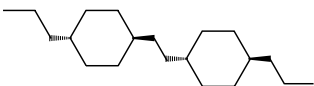
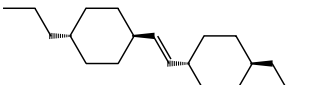
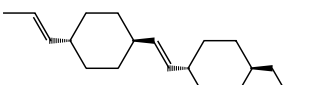
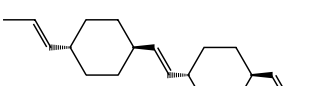
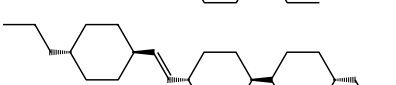
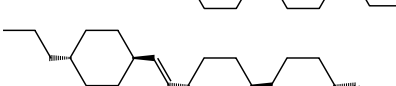
Compound	Molecular structure	Crystal	Smectic B	Nematic	Isotropic	γ_1	k_{33}/k_{11}	Ref.
181		• 36	• 83	—	•			317, 318
182		• 37	• 53	69	•	27	1.60	318
183		• 56	—	• 90	•	37	1.67	318
184		• 86	—	• 121	•	49		318
185		• 39	• 207	• 232	•	381		318
186		• 22	• 189	• 253	•	442	1.57	318

Table XXVIII. Transition Temperatures (°C) for Cyclohexane Esters **106**, **187**, and **188**

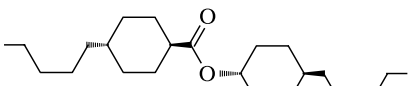
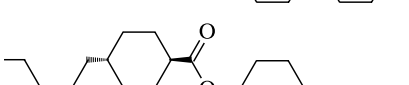
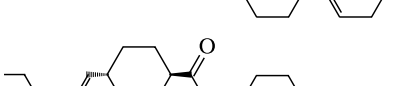
Compound	Molecular structure	Crystal	Smectic B	Nematic	Isotropic	Ref.
106		• 51	• 71	—	•	244
187		• 40	• 67	—	•	319–322
188		• 40	• 75	• 77	•	319–322

Table XXIX. Transition Temperatures (°C) for Bicyclohexanes **189–191**

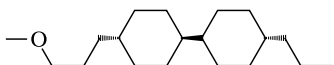
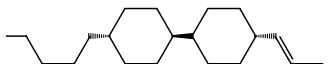
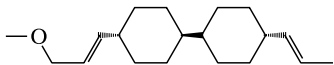
Compound	Molecular structure	Crystal	Smectic B	Nematic	Isotropic	Ref.
189		• 25	• 85	—	•	322
190		• 38	• 73	• 95	•	322
191		• 10	—	• 92	•	322

Table XXX. Transition Temperatures (°C) for Bicyclohexanes **192**–**196**

Compound	Molecular structure	Crystal	Smectic B	Nematic	Isotropic	Ref.
192		• 23	• 96	—	•	323
193		• 32	• 74	—	•	324
194		• 56	• 92	—	•	323
195		• 44	• 75	• 96	•	233
196		• 77	—	• 172	•	323

carbon–carbon double bond in the chain results in a nematic phase at elevated temperatures for the alkenyl compound **195**. However, a smectic B phase is still present at a high temperature. Only the combination of all these elements in compound **196** gives rise to a very high clearing point and a wide nematic phase without a smectic phase being present.

Thus, the data collated in Tables XXVII–XXX demonstrate clearly that the effects of individual molecular building blocks (such as nonconjugated oxygen atoms and double bonds) on the liquid crystal temperatures are clearly not additive. Therefore, some

cooperative effects due to the combination of exactly these groups in these positions and configurations must be responsible. These effects and the relationship between molecular structure and elastic constants are not understood currently. However, alkenyl compounds, such as those shown in Tables XX–XXVII, are used as components of nematic mixtures for STN-LCDs with high-information content (see Table XXXI) [25, 271, 298, 325, 326]. The data collated in the table are used only to give an indication of the general magnitude of the physical parameters of mixtures designed for STN-LCDs with different twist angles. The manufacturers of LCD mixtures offer a whole

Table XXXI. Transition Temperatures (°C), Elastic Constants (k_{11}, k_{22}, k_{33} ; 10^{-12} N), Dielectric Anisotropy ($\Delta\epsilon$), Dielectric Constant Measured Perpendicular to the Molecular Long Axis (ϵ_{\perp}), Birefringence (Δn), Refractive Index Measured Parallel and Perpendicular to the Director (n_e, n_o), Viscosity (γ_1 , $\text{mm}^2 \text{s}^{-1}$) Threshold Voltage (V), Rate of Change of Voltage with Temperature ($\% ^\circ\text{C}^{-1}$), and Twist Angle (degrees) Measured at 20 °C, Unless Otherwise Stated, for three typical nematic mixtures for STN-LCDs [298, 326]

	Low twist STN-LCD [326]	STN-LCD [298]	High twist STN-LCD [326]
Sm–N	< –30	< –40	< –30
N–I	79	100	71.5
k_{11}	13.1	13.1	
k_{22}	6.9	6.9	
k_{33}	21.1	21.1	
k_{33}/k_{11}	1.61	1.61	
k_{33}/k_{22}	3.1	3.1	
$\Delta\epsilon$	+24.3	+8.2	+7.39
ϵ_{\perp}	6.5	3.9	3.95
$\Delta\epsilon/\epsilon_{\perp}$	3.73	2.10	1.9
Δn	0.15	0.12	0.16
n_e	1.65	1.61	1.67
n_o	1.50	1.49	1.51
γ_1 (20 °C)	28	23	16.5
γ_1 (0 °C)	128	80	
γ_1 (–40 °C)	7100		
V_{10}	1.04	2.15	2.14
dV/dT	0.33		
Twist	180	220	270

range of mixtures, mostly customer-specific and confidential, with far superior properties than those quoted, and they are improved continually according to individual customer requirements.

19. SURFACE-STABILIZED FERROELECTRIC LCDs

The surface-stabilized ferroelectric (SSF) LCD [43], invented by Clark and Lagerwall at the Chalmers University in Gothenburg, Sweden, is based on switching the optic axis of a smectic C* phase between two degenerate directions separated by 45° in the plane of the cell between crossed polarizers. Following the prediction and discovery of ferroelectricity in smectic C* liquid crystals [41], it was postulated that if the helix of a smectic C* phase could be suppressed (e.g., by surface forces in very thin layers between two parallel substrates), then these surface forces would also pin the molecules in their positions with the molecular long axis in the plane of the cell [42]. This situation would give two energetically equivalent states on the smectic cone, separated by 2θ , where θ is the layer tilt angle. These states would have spontaneous polarizations of opposite polarity, pointing upward and downward out of the plane of the cell. The application of an electric field of appropriate polarity would switch uniformly between the two states, creating a bistable memory effect, because the switched state would remain after removal of the field [42]. If the director of one of the states was parallel to one of the absorption axes of two crossed polarizers, a switchable half-wave plate would be generated. Clark and Lagerwall demonstrated the validity of this hypothesis with the invention of the SSF-LCD.

20. SSF-LCD CONFIGURATION

The SSF cell contains a layer of liquid crystal in the ferroelectric smectic C* phase at the operating temperature. Ideally, the smectic layers should be orthogonal to the plane of the cell in the so-called bookshelf configuration (see Fig. 34). Therefore, the molecular long axes of the liquid crystal lie in the azimuthal plane with a small uniform pretilt angle in the zenithal plane. The polarizers are crossed (90°), with one polarizer parallel to the optic axis of one of the bistable states (as discussed here), or offset at a fixed angle (22.5°). If the cell gap (e.g., $d \approx 1 \sim 2 \mu\text{m}$) is considerably larger than the pitch of the smectic C* helix, then the helix is unwound by surface forces. The device is switched by dc pulses of appropriate polarity.

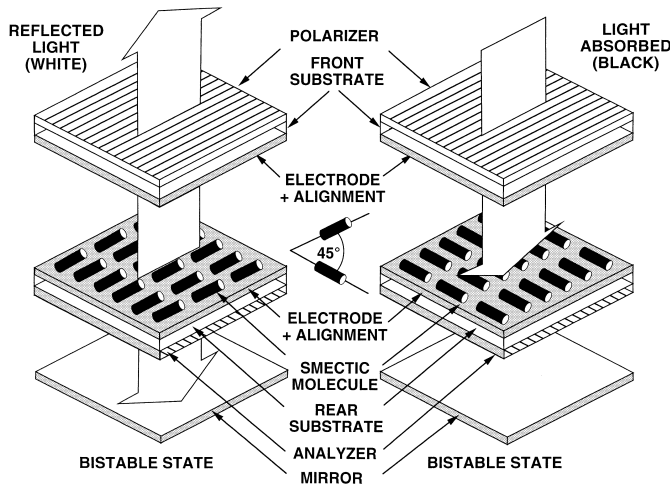


Fig. 34. Schematic representation of a surface-stabilized ferroelectric LCD [43, 92].

20.1. Dark State

When the axis of the input polarizer is parallel to the director direction of the cell, there can be no optical retardation. Then the incident polarized light travels through the smectic liquid crystal and is absorbed by the analyzer. Consequently, the cell appears dark.

20.2. Bright State

The application of a dc electric field of the appropriate polarity inverts the direction of the spontaneous polarization parallel to the field. The director rotates around the smectic cone to its second bistable state. The transmission I of the cell is given [43] by

$$I = I_o \sin^2 4\theta \sin^2 \frac{\pi \Delta n d}{\lambda} \quad (39)$$

where I_o is the incident light intensity of wavelength λ and Δn is the birefringence. Maximum transmission is obtained when θ is 22.5° , which is not unusual for the smectic C* phase. Then the input polarized light is divided into two components of equal amplitude, parallel and perpendicular to the director. If

$$\frac{\Delta n d}{\lambda} = \frac{1}{2} \quad (40)$$

on traversing the cell, the optical path difference between the components is $\lambda/2$, so that light is transmitted through the analyzer. Assuming a typical birefringence $\Delta n = 0.125$ and a median wavelength of visible light $\lambda = 550 \text{ nm}$, requires $d \approx 2 \mu\text{m}$ to maximize contrast and give a black and white display. The cell thickness tolerance must be less than 10%, a stringent requirement from a manufacturing aspect, considering the small cell gap.

The spontaneous polarization can be related to the tilt angle [91] by

$$P_s = P_o \sin \theta \quad (41)$$

where P_o is the maximum value for the spontaneous polarization. P_o is a constant molecular property characteristic for a particular dopant of a defined optical purity. An effective viscosity γ_{eff} can then be defined [90] as

$$\gamma_{\text{eff}} \frac{d\varphi}{dt} + P_s E \sin \varphi = 0 \quad (42)$$

where φ is the angle of rotation on the chiral smectic C cone and E is the applied electric field. This equation allows the definition of a characteristic response time:

$$\tau = \frac{\gamma_{\text{eff}}}{P_s E} \quad (43)$$

The experimental switching time is found to be proportional to τ . Geometrical considerations indicate that γ_{eff} is related to θ [90] by

$$\gamma_{\text{eff}} = \gamma_o \sin^2 \theta \quad (44)$$

where γ_o is independent of θ and represents the rotational viscosity of a hypothetical nematic-like smectic C structure with a tilt angle of 90° . Combining of Eqs. (42), (43), and (44) gives

$$\tau = \frac{\gamma_o}{P_o E} \sin \theta \quad (45)$$

Switching times ($\approx 100 \mu\text{s}$) are much shorter (i.e., 2 orders of magnitude) than those possible with standard LCDs using nematic liquid crystals. Furthermore, SSF-LCDs can be multiplexed to a significant degree (e.g., 400 lines), which would allow video-rate addressing for TV applications. The wide viewing angles are also an advantage.

However, several limitations have restricted market acceptance of SSF-LCDs, despite 20 years of research and development.

The ideal alignment for a SSF-LCD is the so-called bookshelf structure, whereby the smectic layer normal is parallel to the cell substrates [92, 327, 328]. Thus, good alignment of the smectic C* phase is usually achieved by cooling from the nematic into the layered smectic A phase and then into the smectic C* phase. However, the structure normally encountered is the chevron structure [328] with two opposite tilt angles. This structure corresponds to a curved layer with a kink in the middle. The chevron structure results in zigzag defects and lower contrast than expected, due to a nonideal and inhomogeneous orientation of the director throughout the cell. Furthermore, the two degenerate states are not completely bistable, and a degree of relaxation is observed at zero field. Moreover, the absence of intrinsic gray scale (i.e., full color) requires complex addressing schemes that involve spatial and temporal dither. A combination of these technical challenges, as well as complex alignment procedures and shock instability, have restricted the commercial acceptance of this display technology to niche products such as spatial light modulators or projection televisions.

21. SMECTIC C* MATERIALS

Although most tilted smectic phases fulfill the symmetry requirements for ferroelectricity, the smectic C* phase is used in SSF-LCDs, due to its low rotational viscosity γ . The achiral smectic C phase and the chiral smectic C* phase are tilted versions of the corresponding smectic A phase (see Sects. 1 and 3.5). In the smectic A phase, the time-averaged orientation of the director is perpendicular to the layer plane. Therefore, homogeneously aligned domains are optically uniaxial. In the smectic C* phase, the molecules are tilted at an azimuthal angle θ to the layer normal [329–331]. This gives rise to the observed optical biaxiality, [330] although the angle of tilt (θ) is temperature dependent and normally increases with decreasing temperature [331]. Many liquid crystals that exhibit the smectic C* phase, as well as its achiral counterpart, have been synthesized since the turn of the 20th century during investigations of the relationship between molecular structure and mesomorphic behavior [332–337]. However, the structure of the smectic C* phase was identified only in the early 1970s [338]. Theoretical studies had postulated that the molecular orientation (i.e., the director, in the smectic C* phase) should spiral around an axis normal to the layer plane, giving rise to a helical structure [339]. This was indeed found to be the case (See Sect. 8). There are many theories to explain the formation and structure of the smectic C and smectic C* phases [340–343]. Theories on the microscopic aspects of this structure suggested that aromatic compounds with two long terminal chains in a zigzag conformation and antiparallel lateral dipoles at the edge of the molecular core should lead to formation of the smectic C phase, due to a resultant torque [340]. Most compounds that exhibit a smectic C phase have such a molecular structure [344, 345], although it has been shown that such terminal outboard dipoles are not essential for smectic C formation [346–348].

21.1. Ferroelectric Smectic C* Mixtures of Optically Active Components

The first prototype SSF-LCD [43] was demonstrated using a Schiff base **197** [e.g., 4-decyloxybenzylidene-4-amino-2-methylbutylcinnamate (DOBAMBC) [41]]; [See Table XXXII]. This optically active liquid crystal was first synthesized specifically to test the validity of the postulate that the smectic C* mesophase would be ferroelectric. The first eight homologues of this series had been prepared earlier. Although some homologues were found retrospectively to exhibit the smectic C* phase, it was not recognized because the time

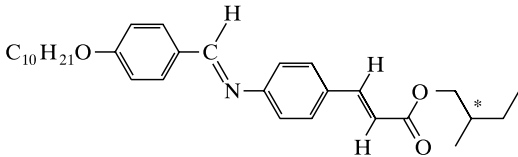
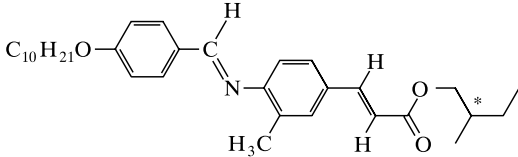
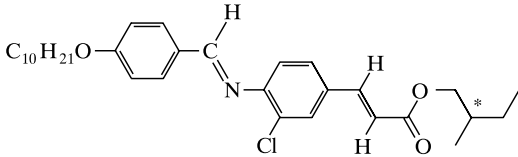
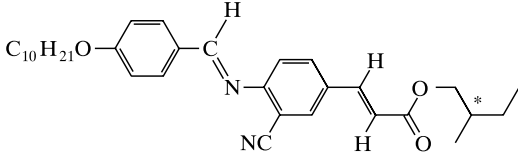
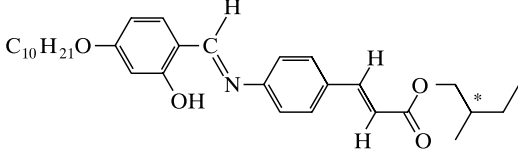
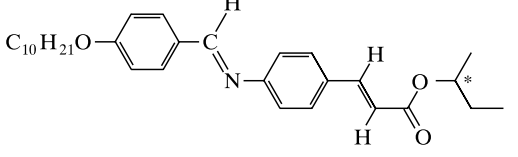
of their synthesis predated the discovery of ferroelectric properties in liquid crystals [334]. Consequently, many physical experiments and measurements were subsequently carried out on DOBAMBC as a single smectic C* compound.

Practical SSF-LCDs require eutectic mixtures of optically active chiral smectic C* materials with a low melting point (i.e., as far below room temperature as possible) and a high smectic C* transition temperature to allow device operation over the normal temperature range of LCDs [344, 345]. It was realized quickly that it is essential to mix smectic C* compounds with the same sign of spontaneous polarization, but opposing signs of pitch, so that the spontaneous polarization values are additive and the pitch values are compensated. Thus, both parameters are large, which should produce short switching times [see Eq. (45)] and suppression of the pitch in SSF-LCDs. Both the spontaneous polarization and the pitch depend on the polar character of the substituents at the chiral center and the position of the chiral center in the terminal chain, which permit a large degree of synthetic freedom and flexibility.

Therefore, in initial attempts to produce smectic C* materials with a lower melting point than DOBAMBC, analogous compounds with a lateral substituent in the phenyl ring next to the cinnamate group were prepared [41, 349], (e.g., compounds **197–201**; see Table XXXII). Except for the nitrile **200**, the presence of lateral substituents resulted in much lower melting point, smectic C* transition temperature, and clearing point compared with the transition temperatures of compound **197**, as well as in the suppression of ordered smectic phases. No significant effect on the spontaneous polarization was observed, although the presence of the lateral substituent should have had the effect of reducing the degree of rotation at the chiral center and increasing the lateral dipole moment in the core of the molecule [349]. This lack of effect is most probably attributable to the relatively large distance between the substituents and the chiral center in the (*S*)-2-methylbutyl moiety. The spontaneous polarization of these ester derivatives of naturally occurring (*S*)-2-methylbutanol is low. Therefore, the (*S*)-2-butyl ester **202** with an optically active center closer to the core and a polar carboxy function was prepared [41]. This combination increased the spontaneous polarization by a factor of 3 probably due to a higher degree of polar coupling and hindered rotation at the chiral center.

The presence of a hydroxy group in a lateral position in the Schiff bases **203–205** next to the central bond results not only in an improved electrochemical stability, but also in a low melting point and a wide smectic C* temperature range (See Table XXXIII) [350–353]. This result is caused by the formation of a pseudo six-membered ring at the core of the molecule, due to hydrogen bonding between the hydroxy group and the nitrogen atom of the central linkage, which causes a higher degree of planarity of the aromatic ring and, therefore, a higher degree of conjugation, without increasing the molecular rotation volume to any significant degree. The large dipole moment (2.58 D) of the hydroxy group in a lateral position does not lead to a significant increase in the spontaneous polarization. This observation is consistent with the supposition that a dipole moment in the core of the molecule, which is decoupled from the chiral center, should influence the observed value of the spontaneous polarization much less than a dipole moment of similar magnitude at the chiral center itself; this is not always the case, as we will see later. The smectic C* transition temperature is highest for compound **205**, which has the longest terminal chain and the chiral center furthest from the molecular core. This is because the steric effect of the methyl group at the point of branching on the transition temperatures decreases for positions further from the core, due to the greater number of nonlinear chain conformations possible. The spontaneous polarization, corrected for tilt angle differences, is also lower, due to the smaller energy differences between the various conformations of the dipole moment and the lower degree of coupling with the dipoles of the molecular core. The low value of the melting point and the wide smectic C* temperature range of such Schiff bases allowed

Table XXXII. Transition Temperatures ($^{\circ}\text{C}$) and Spontaneous Polarization (nC cm^{-2}) Measured 10°C below the Smectic C^* -Smectic A Transition of Ferroelectric Compounds **197–202**^a

Compound	Molecular structure	Crystal	Smectic C^*	Smectic A	Isotropic	P_s	Ref.
197		• 76	• 92	• 117	•	3	41, 349
198		• 45	• 68	• 99	•		41, 349
199		• 51	(• 45)	• 71	•		41, 349
200		• 92	(• 70)	• 104	•		41, 349
201		• 88	• 114	• 145	•	3	41, 349
202		• 82	• 91	• 106	•	10	351

^aThe parentheses [()] represent a monotropic transition temperature.

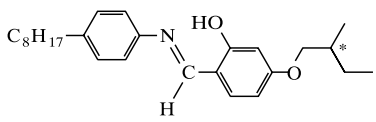
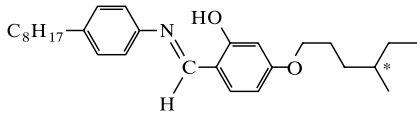
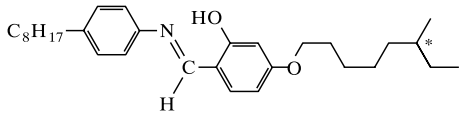
studies of the ferroelectricity in liquid crystals to be carried out at room temperature, even though the spontaneous polarization is low.

Schiff bases hydrolyze in the presence of moisture, which clearly imposes restrictions on the handling of these liquid crystals during the manufacture of LCDs, because hydrolysis generates ionic species that result in an unacceptably high value for the conductivity. Therefore, in attempts to prepare more stable smectic C^* liquid crystals with spontaneous polarization comparable to the Schiff bases, a diverse range of aromatic esters with alkyl-branched and, particularly, methyl-branched terminal chains were synthesized (See Table XXXIV) [195, 354–370]. Several series of optically active esters, which also happen to exhibit a smectic C^* phase, as well as the desired chiral nematic phase, had been reported previously as the result of research into chiral nematic liquid crystals for thermochromic applications [195]. The chiral part of the molecules was usually derived from the same commercially available optically active alcohols [such as (*S*)-2-methylbutanol, (*R*)-2-butanol, and (*R*)-2-pentanol] used in the preparation of the Schiff bases, shown in the

Tables XXXII and XXXIII. Similar dependencies of the transition temperatures, spontaneous polarization, and tilt angle on the nature of the methyl-branched chain were found. The value of spontaneous polarization increases with the number of carbon atoms in the chain after the point of branching, due to the dampening effect on the degree of rotation at the chiral center of the longer chain [344, 345]. Large substituents at the point of branching usually reduce the transition temperatures substantially due to steric effects.

The relationships between the absolute transition temperatures and mesomorphism of a wide variety of esters and their molecular structure, such as the direction of the ester linkage in the molecular core, the presence and nature of polar groups between the core and the terminal chain, and the number of rings in the core, have been established [344, 345]. Liquid crystals with two aromatic rings and one aliphatic ring in the core, such as *trans*-1,4-disubstituted cyclohexane [358–360], 1,4-disubstituted bicyclo(2,2,2)octane [361], *trans*-2,5-disubstituted dioxane ring [362], or *trans*-2,5-disubstituted dioxaborinane [363], exhibit a smectic C^* phase, although at much

Table XXXIII. Transition Temperatures (°C), Tilt Angle (degrees), Spontaneous Polarization (nC cm^{-2}), and Spontaneous Polarization Divided by Tilt Angle ($\text{nC cm}^{-2} \text{ rad}^{-1}$) Measured at 25 °C for Ferroelectric Compounds **203–205**

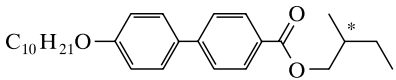
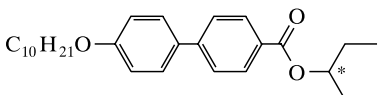
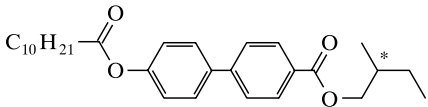
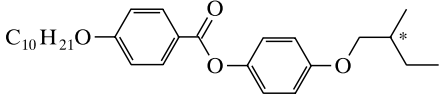
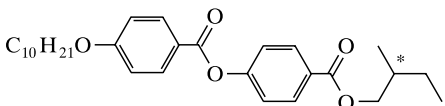
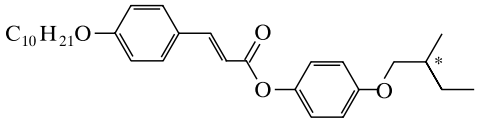
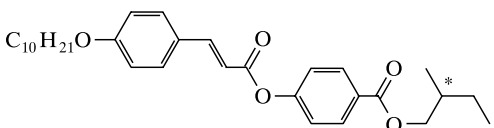
Compound	Molecular structure	Crystal	Smectic C*	Smectic A	Isotropic	θ	P_s	P_s/θ	Ref.
203		• 36	• 50	• 57	•	8	3	22.0	352, 353
204		• 20 ^a	• 77	—	•	40	2	2.9	352, 353
205		• 20	• 86	—	•	5	0.1	0.2	352, 353

^aUnknown smectic phase to smectic C* transition.

lower transition temperatures than those of the corresponding fully aromatic materials. The corresponding two-ring compounds with one aliphatic ring and one aromatic rings do not generally exhibit a smectic C* phase. However, the viscosity and birefringence of cyclohexane-containing smectic C* materials are lower than those

of the corresponding fully aromatic materials. This situation can be used to advantage in the formulation of mixtures for SSF-LCDs [364]. Mixtures with lower birefringence and viscosity result in shorter switching times or allow thicker cells to be used. It was also found that the presence of a cis carbon–carbon double bond or

Table XXXIV. Transition Temperatures (°C) for Ferroelectric Compounds **206–212**^a

Compound	Molecular structure	Crystal	Smectic C*	Smectic A	Isotropic	P_s	Ref.
206		• 48	(• 41)	• 66	•	12.0	354, 356
207		• 54	(• 30)	(• 50)	•	36.0	354, 356
208		• 44	• 50	• 62	•	5.0	354, 356
209		• 44	• 54	• 67	•	2.5	354, 356
210		• 52	(• 35)	• 60	•	5.0	354, 356
211		• 60	• 71	• 95	•		357
212		• 81	• 94	• 103	•		357

^aThe parentheses [()] represent a monotropic transition temperature.

Table XXXV. Comparison of the Transition Temperatures (°C), Dipole Moment (D), Relative and Absolute Spontaneous Polarization (nC cm⁻²), and Tilt Angle (degrees) measured 10 °C below the Smectic C*–Smectic A Transition of Ferroelectric Compounds **213–220**

Compound	Molecular structure	Crystal	Smectic C*	Smectic A	Nematic* N	Isotropic	μ	P_s	P_o	θ	Ref.
213		• 78	• 99	—	• 122	•	0	45	64	45	367
214		• 65	• 97	—	• 100	•	1.47	78	134	36	367
215		• 73	• 95	—	• 97	•	1.59	123	191	40	367
216		• 43	• 87	—	• 89	•	1.57	131	202	41	367
217		• 68	• 90	105	—	•	4.05	160	386	25	367
218		•	•	—	•	•	1.23	70	195		367
219		•	•	—	•	•	1.99	112	313		389
220		• 102	• 145	155	—	•			220		389

a terminal double bond in the alkoxy chains of two-ring and three-ring esters, in general, leads to lower transition temperatures and sometimes to a broad smectic C* phase close to room temperature [365, 366].

The three-ring esters **213–220** collated in Table XXXV all exhibit a chiral smectic C* phase at high temperatures [367, 368]. All the transition temperatures of compounds **214–217** decrease with increasing size of the lateral substituent compared with those of the nonlaterally substituted compound **213** [367]. In contrast, the values of the spontaneous polarization increase with increasing size of the lateral substituent, probably due to steric effects, because the energy difference between the most stable, time-dependent conformations of the chiral center are larger in the presence of larger substituents. This results in a higher degree of restriction of rotation of the chiral center. The higher value of spontaneous polarization for the bromo-substituted ester **216** appears to be caused by the greater size of the bromine atom compared to the chlorine atom, because the dipole moments are almost identical. Consequently, the pitch decreases and the rotational viscosity increases with the size of the lateral substituent [367, 368]. The advantage of a high spontaneous polarization is counterbalanced by the necessity of pitch compensation and high

viscosity. Thus, switching times of laterally substituted materials can actually be longer than those of analogous nonlaterally substituted compounds, in spite of the sometimes considerably higher spontaneous polarization. The presence of a large dipole moment in the form of a carbonyl function between the aromatic core and the chiral center to yield a number of alkanoyl-substituted (keto-) esters (e.g., compound **219**) [368], produces higher spontaneous polarization values than those of the corresponding ethers and esters [367]. The presence of a second optically active group in the second terminal chain can also lead to additive effects and a still higher spontaneous polarization, although the viscosity will be high, due to the presence of two branched chiral centers [367]. A strong dependence of the observed spontaneous polarization values on the number of carbon atoms in both terminal chains and the presence and position of various lateral substituents was also observed.

Large spontaneous polarization values were obtained by increasing the polarization at the chiral center by the introduction of an electronegative group, such as a cyano group (e.g. compound **220** [369]; see Table XXXV) or a heteroatom, such as an oxygen or halo-gen atom. Therefore, esters and ethers that are derivatives of naturally occurring alkyl L-(+)-lactates [alkyl (S)-2-hydroxypropanoates]

[370–375], readily accessible, synthetic alkyl (*R*)-3-hydroxybutanoates [372], or compounds with an alkoxy group and a methyl group at the chiral center in the terminal chain [373] were prepared. Lactate ethers [373] exhibit higher spontaneous polarization and are more viscous than comparable lactate ester mixtures with similar tilt angles (θ) and smectic C* transition temperatures. This results in almost equal switching times for similar mixtures that contain one or the other chiral dopant. The high smectic C* transition temperatures for the pure lactate esters [373] do not always induce high smectic C* transition temperature values for mixtures that incorporate them. This is indicative of the nonadditive and nonideal behavior often observed in the development of smectic C* mixtures for SSF-LCDs.

The presence of one or more nitrogen atom in aromatic rings was found to promote the formation of the smectic C or C* phase. Therefore, some two- and three-ring 2,5-disubstituted-pyrimidines, pyrazines, or pyridazines with optically active methyl-branched terminal chains [376–379] were found to exhibit a broad smectic C* phase, sometimes close to room temperature (e.g., compounds **221** and **222**; see Table XXXVI). The absence of a central linkage contributed to the low viscosity found for the smectic C* phase of many of these nitrogen heterocycles, especially pyrimidine derivatives. Alkenyloxy-substituted phenylpyrimidines with a *cis* carbon–carbon double bond or a carbon–carbon double bond in a terminal position were subsequently found to exhibit low melting points often close to room temperature [379]. The analogous three-ring compounds exhibit correspondingly higher transition temperatures. However, the melting point was still found to be relatively low for such compounds (e.g., compounds **223** and **224**). This is advantageous for mixture formulation.

A carbon–carbon double bond at or beyond position 3 in an alkenyl chain or position 2 in an alkenyloxy chain attached to an aromatic ring is nonconjugated and therefore sufficiently stable for LCD applications. A carbon–carbon double bond was introduced in a terminal position or in a *cis* configuration in the middle of an alkoxy chain of a wide variety of two-ring and three-ring phenyl benzoates [365, 366] and phenylpyrimidines [379], which exhibit a chiral smectic C phase. In all cases, this often led to a substantial decrease in the transition temperatures of all the observed mesophases. However, the melting point was often decreased more than the smectic C transition temperature, leading to a broadening of the smectic C temperature range (sometimes at or just above room temperature).

Either or both the ester group and the chain branching at the chiral center led to a high viscosity and relatively long response times [344, 345].

Most ferroelectric liquid crystals that incorporate halogen atoms at the optically active center are ester or ether derivatives of either naturally occurring lactic acid or amino acids as a consequence of ease of synthesis and cost considerations [380–387]. However, there is still a considerable degree of freedom of rotation at the chiral center, which reduces the observed value for the spontaneous polarization. To produce a large value of the spontaneous polarization, the dipole moments near the optically active center should be additive (e.g., compounds **225** and **227**; see Table XXXVII). For example, the dipole moments at the two chiral centers in the (2*S*, 3*R*)-2-chloro-3-methyl-pentanoyloxy-substituted ester **226** are additive and give rise to high values of spontaneous polarization [382–384]. The value of the spontaneous polarization measured in the enantiotropic smectic C* phase of the pure material and the corresponding values extrapolated from smectic C* mixtures are not identical, although they are of a similar magnitude. The extrapolated values are usually somewhat lower. The chiral smectic C* phase of compounds with a fluorine atom at the optically active center often exhibit a relatively high spontaneous polarization, but with a lower viscosity and higher smectic C* transition temperature than the corresponding chloro- or bromo-substituted compounds, due to the small van der Waals radius (1.47 Å) and relatively large dipole moment (1.41 D) of the fluorine atom [385–387].

21.2. Ferroelectric Guest–Host Chiral Dopant–Smectic C Host Mixtures

After much development of chiral smectic C* compounds and their mixtures, it was found that the rotational viscosity for mixtures that consist completely of optically active smectic C* components was intrinsically very high, despite the synthesis of a very wide variety of materials. The high viscosity of the smectic C* phase resulted in response times that were too long for commercially acceptable SSF-LCDs [see Eqs. (43) and (44)]. Therefore, the concept of doping an achiral smectic C mixture with a low viscosity, high smectic C transition temperature, negative dielectric anisotropy, and the low melting point with an optically active chiral dopant with a very high value of spontaneous polarization to produce a mixture with a chiral smectic C* phase with the desired values of the

Table XXXVI. Transition Temperatures (°C) of Ferroelectric Compounds **221**–**224**

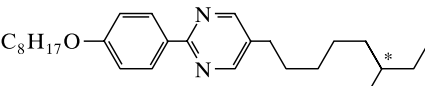
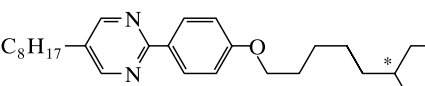
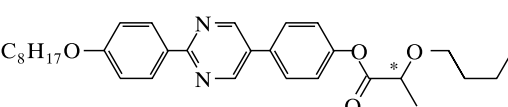
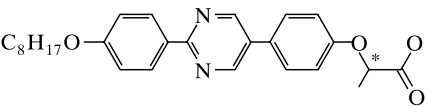
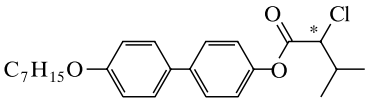
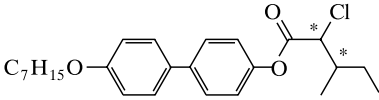
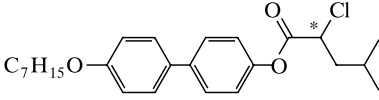
Compound	Molecular structure	Crystal	Smectic C*	Smectic A	Nematic*	Isotropic	Ref.
221		• 23	• 34	—	• 47	•	376
222		• 3	• 48	• 58	—	•	376
223		• 88	• 148	—	—	•	377, 378
224		• 51	• 69	—	• 91.5	•	377, 378

Table XXXVII. Transition Temperatures (°C) of Pure Ferroelectric Compounds **225–227** and Spontaneous Polarization (nC cm^{-2}) Measured 10 °C below the Smectic C*–Smectic A Transition of Mixtures of 10% of these Materials in 4,4' Diheptyloxyazobenzene (Cr–SmC = 74 °C; SmC–N = 94 °C; N–I = 124 °C)

Compound	Molecular structure	Crystal	Smectic C*	Smectic A	Isotropic	P_s	Ref.
225		• 72	• 74	• 82	•	140	382, 383
226		• 55	• 56	• 62	•	160	382, 383
227		• 54	• 57	• 68	•	70	382, 383

relevant physical properties was introduced [388–390]. An appropriate amount of the chiral dopant was added to induce the desired value of spontaneous polarization and a long pitch in the smectic C* mixture. Therefore, suitable chiral dopants were required, which induced the desired value of the spontaneous polarization, avoided the necessity for pitch compensation, and did not depress the smectic C* transition temperature or increase the viscosity or the birefringence of the mixture too much for practical SSF-LCDs. Ideally, the tilt angle of the resultant mixture should be 22.5° to produce good optical contrast. All the mixture components had to be chemically, thermally, and photo- and electrochemically stable. The resultant induced spontaneous polarization of the mixture should also not be too large to avoid space charge effects, which result in image sticking (“ghost images”). A large intrinsic value of the spontaneous polarization for the chiral dopant would allow smaller amounts to be used and would limit the potentially negative impact on the other physical properties of the mixture caused by the requirement of using optically active dopants. By definition, such materials nearly always incorporate a branched chiral center with four different substituents (sp^3 hybridization) to generate optical activity. Chiral dopants designed for SSF-LCDs do not necessarily have to exhibit a smectic C* phase themselves, as long as they do not lower the smectic C* transition temperature below the desired upper operating temperature.

However, it was soon found that the addition of a chiral dopant or, indeed, any other component to a liquid crystalline mixture often results in complex, nonideal behavior. Depending on the desired magnitude of the physical property, this may be advantageous. The spontaneous polarization induced by the addition of chiral dopants to achiral smectic C host mixtures was found to be concentration, tilt angle and order parameter dependent, as well as a function of temperature. It often reaches a maximum at a certain concentration and then remains constant or even decreases as more dopant is added [388–390]. A higher spontaneous polarization does not always induce shorter response times if the observed increase of spontaneous polarization is due to an increase in the smectic tilt angle [See Eq. (41)]. If both the response time and the spontaneous polarization increase (or decrease) upon changing the side chain within a homologous series of dopants, then this is probably a change of the tilt angle of the mixture caused by the dopant. If the response time decreases and the spontaneous polarization increases, this is probably due to a change of P_o , which is a constant characteristic of the dopant. This is usually valid at low dopant concentrations, where changes of viscosity are often small [348, 386].

21.2.1. Chiral Dopants

Many of the compounds synthesized for smectic C* mixtures can be used as chiral dopants as long as the spontaneous polarization is large [e.g., many of the compounds (**213–227**) shown in Tables XXXV–XXXVII]. However, the complexity involved in the successful development of chiral dopants for SSF-LCDs is illustrated by the data collated in the Table XXXVIII [386, 387]. The dopants that incorporate a *trans*-1,4-disubstituted cyclohexane ring shown in Table XXXVIII do not exhibit a chiral smectic C* phase. However, although the substitution of the aliphatic *trans*-1,4-disubstituted cyclohexane ring for the aromatic benzene ring of compound **228** to produce the compound **229** leads to a lower electron density at the chiral center and to a higher degree of conformational mobility of the dipole moment, the spontaneous polarization is only reduced by about 40% [386, 387]. The smectic C* transition temperature is acceptably high. Furthermore, the presence of the cyclohexane ring gives rise to lower values for Δn and viscosity γ , and a substantially longer pitch (p) than those of the fully aromatic material **229**.

Several of the optically active three-ring esters shown in Table XXXVIII (for example, compounds **232** and **233**) which incorporate the aliphatic cyclohexane ring, possess an enantiotropic smectic C* phase at elevated temperatures [386, 387]. However, the tendency to form the smectic C* phase is much reduced compared with the corresponding fully aromatic materials and the corresponding two-ring compounds, (e.g., **229–231**) that incorporate a cyclohexane ring do not exhibit a smectic C* phase. A number of dipole moments associated with heteroatoms, such as oxygen, nitrogen, and fluorine, in various parts of the molecular core are required to induce the formation of a smectic C phase. Therefore, the ether **230** [386] shown in Table XXXVIII, which differs only in the presence of a carbonyl group (CO) instead of a methylene unit (CH_2), **231** [387] from diester induces a lower smectic C* transition temperature in the host mixture. This result is consistent with the microscopic, dipole–dipole theory of the smectic C phase [20]. The spontaneous polarization is higher for the ester than for the ether, indicating a greater value for P_o , as indicated by the shorter response time.

The effect of an ester group in a central position of a chiral dopant can be elucidated by comparing the thermal data collated in Table XXXVIII for compounds **233** and **234** [387]. The smectic C* transition temperature for the mixture that contains the α -fluoro-substituted diester **233** with a second ester group in a central position is higher than that of the mixture that incorporates an equal amount

Table XXXVIII. Comparison of the Transition Temperatures ($^{\circ}\text{C}$), Spontaneous Polarization (nC cm^{-2}), and Response Times (μs ; $10 - V$ pp μm^{-1} square wave time to maximum current) Measured at 25°C for the Ferroelectric Smectic C^* Mixtures Consisting of 7-wt% Chiral Dopants **228–234** and 93 wt% the Same Achiral Host Smectic C Mixture ($\text{Cr-SmC}^* < 0^{\circ}\text{C}$; $\text{SmC}^*-\text{SmA} = 76^{\circ}\text{C}$; $\text{SmA-N}^* = 81^{\circ}\text{C}$; $\text{N}^*-\text{I} = 103^{\circ}\text{C}$)

Compound	Chiral dopant	Crystal	Smectic C*	Smectic A	Nematic*	Isotropic	P_s	τ	Ref.	
228							56 ^a	950	386, 387	
229							35 ^a	700	386, 387	
230		•	< 0	• 64.5	• 82.6	• 97.8	•	3.8	460	387
231		•	< 0	• 68.0	• 81.5	• 97.1	•	5.7	400	387
232		•	< 0	• 75.5	• 88.3	• 104.3	•	6.2	415	387
233		•	< 0	• 76.7	• 83.5	• 103.9	•	5.4	650	387
234		•	< 0	• 74.5	• 86.3	• 102.3	•	4.5	630	387

^aExtrapolated to 100% dopant; no mixture transition temperatures given.

of the α -fluoro-substituted monoester **232**. This is not surprising, because the α -fluoro diester **233** exhibits an enantiotropic smectic C^* phase at elevated temperatures in the pure state. However, the observed value for the spontaneous polarization, P_s , is higher for the monoester **232** than for the diester **233**, probably due to a change of the absolute value of the spontaneous polarization, P_o , as well as of the viscosity γ , because of the presence of the second carboxy (ester) group. Even if P_o were constant and the tilt angle (θ) were fully responsible for the increase of the spontaneous polarization, the viscosity (γ) of the monoester would still be substantially lower.

A comparison of the relative effects of either a fluorine or a chlorine atom attached directly to the optically active center of the chiral dopant is also shown in Table XXXVIII [387]. The transition temperatures and spontaneous polarization of the mixture that contains the α -fluoro ester **233** are all higher than those observed for the corresponding mixture that contains an equal amount of the otherwise identical α -chloro ester **234**. This may be attributable to the stronger electronegativity of the fluorine atom. Furthermore, the viscosity of the α -fluoro ester must also be lower than that of the α -chloro ester **234** as shown by the significantly lower switching time τ , which is only partially due to the higher value of P_o and is probably a consequence of the smaller size of the fluorine atom and the shorter carbon-fluorine bond compared to that of chlorine. It has been generally

found that the spontaneous polarization of analogous fluoro-alkyl- or alkoxy-substituted compounds, is lower than that of the corresponding chloro-substituted compounds due to the lower dipole moment at the optically active center [391–396]. The presence of the trifluoromethyl group at the chiral center in the side chain of three-ring compounds should lead to high spontaneous polarization values, due to the additive effects of three fluorine atoms. This is indeed found to be the case [397, 398]. Unfortunately, the presence of a trifluoromethyl group at the chiral center in the central linkage between two aromatic rings in the core of a similar three-ring phenylpyrimidine was found to give rise to very low transition temperatures and to the absence of a smectic C^* phase for the pure substance [397]. Consequently, mixtures that contain these chiral dopants exhibit a low smectic C^* transition temperature, although the values of the other physical properties are good [398]. This is probably due to the steric effect of the trifluoromethyl group, leading to a significant broadening of the molecular rotation volume.

The dipole moment of a cyano group is much larger than that of a fluorine atom or other halogen atoms bonded to the same group. Therefore, the spontaneous polarization should be larger. Furthermore, the steric bulk of a cyano group at the optically active center should give rise to a larger energy difference between the most probable time-averaged conformations of the chiral center. This should also contribute to a high spontaneous polarization value, although

Table XXXIX. Transition Temperatures ($^{\circ}\text{C}$) and Spontaneous Polarization (nC cm^{-2}) of Mixtures of 7.37-wt% Chiral Dopant **235** or 7.58-wt% Chiral Dopant **236** and a Host Chiral Smectic C* Compound ($\text{Cr-SmC}^* = 35\text{ }^{\circ}\text{C}$; $\text{SmC}^*\text{-SmA} = 70.5\text{ }^{\circ}\text{C}$; $\text{SmA-I} = 72\text{ }^{\circ}\text{C}$); 2.0-mol% Chiral Dopant **237** or Chiral Dopant **238** and a Host Achiral Smectic C Mixture ($\text{Cr-SmC}^* < 25\text{ }^{\circ}\text{C}$; $\text{SmC-SmA} = 51\text{ }^{\circ}\text{C}$; $\text{SmA-I} = 63\text{ }^{\circ}\text{C}$; $\text{N-I} = 69\text{ }^{\circ}\text{C}$); 2.0-mol% Chiral Dopant **239** or Chiral Dopant **240** and a Host Achiral Smectic C Mixture ($\text{SmCr-SmA} = 51\text{ }^{\circ}\text{C}$; $\text{SmA-I} = 61\text{ }^{\circ}\text{C}$; $\text{N-I} = 68\text{ }^{\circ}\text{C}$)

Compound	Chiral dopant	Crystal	Smectic C*	Smectic A	Nematic*	Isotropic	P_s	Ref.
235		• 53	• 66	• 70	—	•	+2	403, 404
236		• 25	• 61	• 66	—	•	-13	403, 404
237		•	• 52	• 61	• 68	•	<0.5	406
238		•	• 52	• 61	• 68	•	+5.3	406
239		• 2.5	• 53	• 60	• 67	•	-2.4	406
240		• 2.6	• 53	• 59	• 67	•	+4.2	407

low transition temperatures and a high viscosity should also be observed for the same steric reasons [399–402]. This is indeed found to be the case. As a consequence, only three-ring compounds possess enantiotropic liquid crystal phases (e.g., compound **220** shown in Table XXXV). However, used in small amounts, they are very effective chiral dopants [402].

If the degree of free rotation at the chiral center can be restricted (e.g., by incorporating the chiral center in a conformationally rigid cyclic system, such as in an oxirane), then the conformational averaging out of the dipole moment could be limited [403, 404]. This should lead to high spontaneous polarization. Whereas the molecular dipole of an epoxide is oriented normal to the tilt plane, the dipoles associated with the fluorine atoms and the epoxy moiety in the two diastereomeric oxiranes (**235** and **236**) shown in Table XXXIX [403, 404] point in the same direction and, consequently, a high value of the spontaneous polarization is observed (e.g., for compound **236**). If the dipole moments are of opposite polarity, they cancel each other out to some degree, and low spontaneous polarization value is observed (e.g., for compound **235**). Oxiranes can exhibit very different values of spontaneous polarization [403, 404], depending on the configuration at the second carbon atom of the epoxy group (i.e., trans or cis). For the cis-substituted oxirane, there is an enhanced stereo coupling between the polar chiral group and the lateral molecular dipole, and substantially higher spontaneous polarization values are observed [403, 404]. The cis configuration at the epoxy moiety leads automatically to a non-linear (i.e. fully extended) zigzag conformation of the terminal chain. Although this also leads to a substantially higher value for the viscosity, it does not compensate for the higher spontaneous polarization, and significantly shorter switching times are observed for the cis-substituted esters than those of the

corresponding trans-substituted esters. Replacing the oxygen atom in the epoxy moiety with a sulfur atom to produce the analogous thiiranes [405] results not only in lower transition temperatures, but also insignificantly lower values for the spontaneous polarization if the optically active unit is situated on the periphery of the molecule. The opposite is observed with respect to the spontaneous polarization if the chiral entity is situated between two mesogenic units, such as six-membered rings. A Walden inversion during the reaction results in an inversion of configuration at both asymmetric carbon atoms, resulting in an inverse absolute configuration. The thiiranes are significantly less thermally stable than the corresponding oxiranes.

In the optically active, five-membered γ -lactone ring, there are two asymmetric, chiral carbon atoms and a large dipole moment associated with the carboxy function. The dipole moments associated with the carbonyl and ether components of the ester linkage are in the same plane and point in the same direction perpendicular to the long axis of the molecule [406]. The degrees of free rotation of the chiral centers and the dipole moments are greatly reduced, and a large value for the spontaneous polarization is observed (see compounds **237** and **238** and Table XXXIX). The spontaneous polarization, tilt angle, and response times, but not the transition temperatures, are strongly dependent on the cis or trans configuration of the lactone ring [406]. This is also true for the related six-membered δ -lactone ring, and, therefore, similarly large values for the spontaneous polarization are found [407] (see compounds **239** and **240**). Large differences in the spontaneous polarization are observed for the cis and trans configurations, although the value for the trans isomer is greater than that of the cis isomer. The opposite is the case for the γ -lactones **237** and **238**. Whereas the concentration of the dopant is so low, the transition temperatures of the doped smectic C* mixtures

are little changed from those of the host smectic C mixtures [407]. Dopants that incorporate a series of optically active rings, such as 1,3-dioxolan-4-one [408], 1,3-dioxolan-2-one [409], 2-oxetanone [410, 411], oxazolidine [388], and proline [388], have also been prepared. These dopants generally induce lower spontaneous polarization values and/or higher response times and viscosity values, as well as lower transition temperatures in host mixtures than do the oxiranes, γ -lactones, and δ -lactones already discussed.

21.2.2. Smectic C Hosts

Studies of optically active compounds, that exhibit a smectic C* phase showed that aromatic compounds with two long terminal alkyl or alkoxy chains attached to an aromatic molecular core that incorporates one or two 1,4-disubstituted phenyl rings and a heterocyclic ring (such as 2,5-disubstituted pyrimidine, 2,5-disubstituted pyrazine, and 3,6-disubstituted pyridazine), linked by a direct bond give rise to smectic C* formation. The results of these studies were used as a starting point to develop new achiral materials with high smectic C transition temperature, low melting point, and low viscosity to act as components of host smectic C mixtures for guest chiral dopants.

The dependence of the formation of smectic and nematic phases and their transition temperatures in the presence of additional lateral dipoles in the form of nitrogen atoms is illustrated [376, 390, 412–418] in Table XL. The almost apolar 4-octyl-4'-octyloxybiphenyl **241** exhibits only an orthogonal smectic E phase, whereas the nitrogen heterocycles **242–246** all exhibit at least one tilted phase, especially the smectic C phase. The pyridine **242**, pyridazine **245**, and thiadiazole **246** with a resultant dipole moment across the molecular long axis are of negative dielectric anisotropy. They exhibit a higher smectic C phase transition temperature than that of the corresponding pyrimidine **243**. This is also true for the pyrazine **244**, which may be expected to have a small dielectric anisotropy, due to symmetry considerations. However, the dipole moments associated with the nitrogen atoms may be expected to exert a torque on the molecule. The higher transition temperature for the smectic C phase of these compounds may well be attributable to the torque exerted on these

molecules, due to the dipole moments [340]. The lateral component of the two nitrogen atoms in the pyrimidines should be almost compensated. The pyridazine **245** exhibits the largest negative value for the dielectric anisotropy (≈ -6 – -10) and, perhaps as a consequence, the highest smectic C transition temperature. The ethers **242–246** shown in Table XL generally exhibit a greater tendency than the corresponding esters to form the smectic C phase at higher temperatures [411].

The effect of introducing one or two oxygen atoms in various positions of a model system 5-nonyl-2-(4-nonylphenyl)pyrimidine **247** [415, 416, 418–421] on its liquid crystal transition temperatures is shown in Table XLI. Although the dialkyl material **247** only exhibits a smectic A phase at a lower temperature, the presence of an oxygen atom between the chain and the pyrimidine ring in compound **248** and the phenyl ring in compound **249** induces a smectic C phase below the smectic A phase. The dioctyloxy-substituted compound **250** with an oxygen atom between both terminal chains and the aromatic core exhibits the highest smectic C transition temperatures. The high transition temperature for the smectic C phase of the alkoxy-substituted compounds **248–250** may also be attributable to the torque exerted on these molecules, due to the dipole moments associated with the conjugated oxygen atoms (terminal outboard dipoles). A second, nonconjugated oxygen atom in the terminal chain of the diether **251** leads to lower smectic C and smectic A transition temperatures. However, the melting point is much lower, and a smectic C phase at room temperature is observed. There is a high degree of conformational freedom for the oxygen atom in the terminal chain, and a similar torque cannot be expected. This indicates that intermolecular dipole–dipole interactions are indeed responsible for these effects.

A similar investigation was carried out on the analogous esters **253–257** [418, 422–424] collated in Table XLI. The one nonconjugated oxygen atom in the chain of ester **256** leads to the absence of observable mesomorphism. The highest values for the liquid crystalline transition temperatures are observed for ester **257** with two polarizable carboxy groups attached directly to the molecular core. The esters **252–257** generally possess higher transition temperatures than the analogous ethers **248–251**.

Table XL. Transition Temperatures (°C) for Octyloxy-Substituted Ethers **241–246**^a

Compound	Molecular structure	Crystal	Smectic E	Smectic F	Smectic C	Smectic A	Nematic	Isotropic	Ref.
241		• 57	• 86	—	—	—	—	•	412
242		• 38	—	• 62	• 82	—	—	•	390, 413, 418
243		• 34	—	—	• 56	• 64	• 70	•	415, 416
244		• 65	—	(• 64)	• 79	—	•	376	
245		• 95	(• 90)	—	• 117	—	—	•	376
246		• 73	—	—	• 83	—	—	•	390, 417

^aThe parentheses [()] represent a monotropic transition temperature.

Table XLI. Transition Temperatures (°C) for Compounds **247**–**257**

Compound	R	Crystal	Smectic C	Smectic A	Nematic	Isotropic	Ref.
247		• 49	—	• 61	—	•	418, 419
248		• 36	• 52	• 85	—	•	418, 420
249		• 33	• 61	• 75	—	•	415, 416
250		• 51	• 91	• 100	• 101	•	421
251		• 8	• 47	• 69	—	•	418
252		• 82	—	—	—	•	418
253		• 53	• 64	• 65	—	•	422
254		• 74	• 90	• 93	• 94	•	423
255		• 69	• 85	—	• 96	•	423
256		• 70	—	—	—	•	418
257		• 81	• 93	—	• 97	•	423

More significant changes in the transition temperatures and other physical properties of relevance for SSF-LCDs were observed for achiral, alkenyloxy-substituted phenylpyrimidines, and pyridines [412], where the positions and configurations of the double bond were varied systematically [412]. This is illustrated by the thermal data collated in Table XLII for the hexenyloxy-substituted pyridines **259**–**265** and the reference compound **258** without a double bond in the chain. The trans carbon-carbon double bond at an even number of carbon atoms from the molecular core, (e.g., compounds **259** and **263**) usually results in higher smectic C and lower smectic A transition temperatures, an increase in θ and P_s , and a longer τ . A terminal carbon-carbon double bond or a cis double bond at an odd number of carbon atoms from the molecular core (e.g., compounds, **262** and **265**) tends to suppress the nematic phase, promote the formation of smectic phases, reduce θ and P_s , and shorten τ . The other combinations of position and configuration of the double bond all strongly reduce the liquid crystal transition temperatures. These observations are consistent with a requirement for a linear, alternating trans-cis configuration and conformation of the alkenyloxy chain [412]. However, the position and number of nitrogen atoms are also crucial in determining the types of phases observed, their absolute transition temperatures, and their temperature ranges (See also Table XL).

Very similar results have been found for analogous three-ring fully aromatic ethers [424].

The thermal data collated in Table XLIII [390, 415–418, 420, 424] show that the presence of three aromatic rings in molecular core in compounds **267**, **268**, **270**, **271**, and **273** leads to much higher transition temperatures than those exhibited by the corresponding two-ring compounds **266**, **269**, and **272**. This is of importance, because small amounts of three-ring compounds are often added to achiral smectic C mixtures to increase the smectic C transition temperature and lower the melting point without unduly increasing the viscosity of the mixture. They can also be used to induce a smectic A or a nematic phase over a narrow temperature range in the host mixture. This is generally considered essential for obtaining the required uniform orientation of the smectic C* phase in the chiral dopant mixture. The transition temperatures and the phases formed by the isomeric three-ring compounds depend on the order of the phenyl and pyrimidine rings (e.g., compare the transition temperatures for compounds **270** and **271**). The two-ring and three-ring phenylthiadiazoles **272** and **273** exhibit high smectic C transition temperatures, high birefringence, and low viscosity. However, their photochemical or electrochemical stability may not be sufficient for some applications.

Table XLII. Transition Temperatures (°C) of 2-[4-(Hexyloxy)-phenyl]-5-octylpyridine **258** and 2-[4-(Hexenyloxy)phenyl]-5-octylpyridine **259–265** [412]^a

Compound	Molecular structure	Crystal	Smectic G	Smectic I	Smectic C	Smectic A	Isotropic
258		• 30	(• 23)	• 58	• 77	—	•
259		(E) • 55	• 58	• 70	• 83	—	•
260		(Z) • 42	—	—	—	—	•
261		(E) • 33	—	—	—	• 42	•
262		(Z) • 47	—	—	• 62	—	•
263		(E) • 58	—	—	• 81	—	•
264		(Z) • 30	—	—	• 50	—	•
265		• 31	—	• 54	• 68	—	•

^aThe parentheses [()] represent a monotropic transition temperature.

The presence of the *trans*-1,4-disubstituted cyclohexane ring in a smectic C compound can give rise to low viscosity and low birefringence, as well as relatively high smectic C transition temperature [425]. The dependence of the mesomorphic behavior and some physical properties of a series of compounds **274–280** that contain the cyclohexane ring on the nature of the linkage between this ring and the aromatic core is shown in Table XLIV. All of the compounds possess an enantiotropic smectic C phase. The presence of an apolar flexible linkage in compounds **275** and **278** does not seem to affect the smectic C transition temperature greatly compared with that of the directly linked material **274**. The combination of a flexible linkage and a conjugated oxygen atom in compounds **276**, **279**, and **280** gives rise to a higher smectic C transition temperature than that of compound **274** with a direct carbon–carbon bond as linkage. These transition temperatures are higher than that of the corresponding compound **277** that contains the relatively rigid, polar carboxy linkage. The melting point of all of the materials is low for three-ring compounds, although the smectic C transition temperature is also much lower than those of analogous fully aromatic three-ring compounds. However, they also exhibit a nematic phase and several exhibit a smectic A phase. This is advantageous for the development of mixtures with the appropriate order of phases for good alignment. In mixtures, compounds **276**, **277**, **279**, and **280**, with an oxygen atom of the linkage attached to the benzene ring in the aromatic core, generally possess higher values for viscosity, tilt angle, and spontaneous polarization than those exhibited by the corresponding materials **274**, **275**, and **278**, with an apolar linkage.

The presence of ordered smectic phases in components of smectic C mixtures can limit the lower operating temperature of the mixture by inducing this phase in the mixture or by inducing crystallization. Lateral substituents are known to suppress ordered smectic phases more than the less ordered smectic C and smectic A phases, although all the transition temperatures are generally lower in laterally substituted compounds compared with the transition temperatures of the corresponding materials without a lateral substituent. To study this effect systematically on components of commercial chiral smectic C* mixtures and also to preferentially suppress the ordered smectic phases in esters (such as compound **281**) [358], a series of related esters **282–296** [426, 427] with at least one, but up to four, fluorine atoms were prepared (See Table XLV). Except for the melting point, which is generally higher, all of the other liquid crystal transition temperatures of esters **282–296**, which incorporate a fluorine atom in a lateral position, are lower than those of the nonlaterally substituted ester **281**. The extent to which the transition temperatures are lower generally increases with the number of fluorine atoms. Only two monosubstituted esters **282** and **283** exhibit the ordered smectic phase, although at a much lower transition temperature than that of the standard ester **281**. The smectic C transition temperature is lowered to a much smaller extent for most of the fluorinated esters. This results in a smectic C phase over a wider temperature range for several of the difluoro-substituted esters (e.g., **289** and **290**) at lower absolute temperatures. This helps to generate a low melting point for smectic C mixtures that contain them. The presence of more than two fluorine atoms in esters **292–296** generally results in low smectic C transition temperatures, although compound

Table XLIII. Transition Temperatures (°C) of Heterocyclic Ethers **266–273**

Compound	Molecular structure	Crystal	Smectic F	Smectic C	Smectic A	Nematic	Isotropic	Ref.
266		• 34	—	• 56	• 64	• 70	•	415, 416
267		• 80	—	• 85	• 195	—	•	424
268		• 91	—	• 114	—	• 183	•	424
269		• 39	—	• 58	84	—	•	418, 420
270		• 98	—	• 159	—	• 187	•	424
271		• 69	• 129	• 172	• 205	—	•	424
272		• 64	—	• 75	—	—	•	390, 417
273		• 80	—	• 167	—	• 182	•	390, 417

Table XLIV. Transition Temperatures (°C) of Phenyl Pyrimidines **274–280** and the Tilt Angle (degrees), Viscosity (mPa s), and Spontaneous Polarization (nC cm⁻²) of Mixtures that Contain Them (13 wt%) [425]

Compound	Molecular structure	Crystal	Smectic B	Smectic C	Smectic A	Nematic	Isotropic	θ	$\gamma \sin^2 \theta$	P_s
274		• 60	• 83	• 93	• 131	• 152	•	18.7	26.6	5.64
275		• 84	—	• 98	• 118	• 132	•	20.0	30.0	5.66
276		• 87	—	• 118	—	• 142	•	23.2	38.8	6.44
277		• 64	• 85	• 104	—	• 161	•	25.8	45.2	7.05
278		• 66	• 71	• 86	• 102	• 109	•	19.3	31.9	4.97
279		• 69	—	• 110	—	• 130	•	25.1	51.1	6.31
280		• 69	—	• 110	—	• 134	•			

Table XLV. Transition Temperatures (°C) of Nonfluoro-Substituted Ester **281** [358] and Fluoro-Substituted Esters **282–296** [426, 427]^a

Compound	X ₁	X ₂	X ₃	X ₄	Crystal	Smectic 3	Smectic C	Smectic A	Nematic	Isotropic
281	H	H	H	H	• 58	• 78	• 118	• 132	• 147	•
282	F	H	H	H	• 72	(• 56)	• 110	• 125	• 135	•
283	H	F	H	H	• 52	(• 44)	• 98	—	• 137	•
284	H	H	F	H	• 71	—	• 79	—	• 133	•
285	H	H	H	F	• 59	—	• 96	• 120	• 133	•
286	F	H	F	H	• 48	—	• 80	—	• 119	•
287	H	F	F	H	• 44	—	• 55	—	• 122	•
288	F	H	H	F	• 62	—	• 102	• 115	• 124	•
289	H	F	H	F	• 40	—	• 91	• 104	• 125	•
290	F	F	H	H	• 64	—	• 114	—	• 138	•
291	H	H	F	F	• 60	—	• 82	—	• 128	•
292	F	F	F	H	• 64	—	• 83	—	• 120	•
293	F	F	H	F	• 66	—	• 112	—	• 127	•
294	F	H	F	F	• 58	—	• 82	—	• 116	•
295	H	F	F	F	• 48	—	• 69	—	• 119	•
296	F	F	F	F	• 71	—	• 90	—	• 118	•

^aThe parentheses [()] represent a monotropic transition temperature.

293 is an exception. Therefore, it is clear from the data collated in Table XLV that the presence of two fluorine atoms in a lateral position is the optimal number for suppression of ordered smectic phases, low melting point and formation of the smectic C phase at elevated temperatures. Although all of the esters exhibit a smectic C phase and a nematic phase, a smectic A phase is observed only for two monofluoro-substituted esters **282** and **285** and two difluoro-substituted esters **288** and **289**. Thus, these esters can be used to generate a smectic A or a nematic phase over a narrow temperature range to improve the alignment characteristics of a mixture to which they are added.

A sophisticated driving scheme for SSF-LCDs [428–430] requires high smectic C materials with a large degree of biaxiality (i.e., with a large transverse dipole moment) [431]. Difluoro-substituted materials such as compounds **297–302** in Table XLVI were found [432–435] to suit these requirements. All of the difluoro-substituted three-ring materials **297–302** exhibit an enantiotropic smectic C phase, whereas the corresponding nonfluoro-substituted compound **297** exhibits only the orthogonal smectic E and smectic A phases over a narrow temperature range at very high temperatures. The presence of the two fluorine atoms in a peripheral position in compounds **297** and **300**, rather than a central position in compound **299**, gives rise to a higher value for the transition temperature for the smectic C phase. All of these correlations seem to be consistent with previous findings and the standard theory of the smectic C phase. The presence of a *trans*-2,5-disubstituted dioxane ring [435] or a *trans*-1,4-disubstituted cyclohexane ring [436] in compounds **301** and **302** leads to a lower smectic C transition temperature than that of the corresponding compound **300** with a 1,4-disubstituted phenyl ring in place of either of the alicyclic rings.

The axially substituted cyclohexane compound **303** is also suited to this driving scheme, although it was used originally in commercial mixtures for prototype SSF-LCDs with standard addressing schemes.

The dipole moment of the cyano group is orthogonal to the molecular long axis. This gives rise to a large negative value (≈ -10) of the dielectric anisotropy. Unfortunately, the viscosity is also high. However, the combination of an axially cyano-substituted cyclohexane ring appears to correspond to a difluorophenyl ring in terms of the tendency for smectic C formation.

The combination of a fluorine atom in a lateral position and a heterocyclic ring should give rise to a large lateral dipole moment across the molecular long axis and promote smectic C formation. This is indeed the case as illustrated by the thermal data collated in Table XLVII for the compounds **304–309** [434, 437, 438]. The position of the nitrogen atom next to the oxygen atom in compound **304** gives rise to an ordered smectic phase. The additional presence of a fluorine atom next to the nitrogen atom in compound **305** leads to a smectic A phase at a low transition temperature. A smectic C phase is not observed for either compound. In contrast, the isomers **306–307** exhibit a very high value for the smectic C transition temperature. The presence of a fluorine atom in a lateral position in monofluoro-substituted pyrimidine **307** leads to a lower transition temperature for the smectic C phase than that of the corresponding nonfluoro-substituted material **306**. However, the ordered smectic phase found for the former compound **306** is missing from the latter compound **307**. The monofluoro-substituted pyrimidine **308** possesses a lower transition temperature for the smectic C phase than that of the corresponding difluoro-substituted pyrimidine **309**.

22. CONCLUSIONS

Liquid crystal displays are well set to overtake the Cathode ray tube in the overall displays market in terms of total value, units shipped, and market share. Despite the emergence of competing technologies in flat panel displays, such as light-emitting polymers,

Table XLVI. Transition Temperatures (°C) of Compounds **297–303**

Compound	Molecular structure	Crystal	Smectic X	Smectic C	Smectic A	Nematic	Isotropic	Ref.
297		• 195	• 211	—	• 222	—	•	432–434
298		• 89	—	• 155	• 165	• 166	•	432–434
299		• 49	—	• 95	—	• 142	•	432–434
300		• 94	—	• 144	• 148	• 159	•	432–434
301		• 53	—	• 58	• 127	• 142	•	434
302		• 62	—	• 86	• 134	—	•	435
303		• 81	(• 52)	• 118	• 150	• 151	•	436

^aThe parentheses [()] represent a monotropic transition temperature.

Table XLVII. Transition Temperatures (°C) of Compounds **304–309** [434]^a

Compound	Molecular structure	Crystal	Smectic X	Smectic C	Smectic A	Nematic	Isotropic
304		• 50	• 69	—	—	—	•
305		• 48	—	—	(• 40)	—	•
306		• 76	(• 75)	• 110	—	—	•
307		• 81	—	• 89	—	—	•
308		• 42	—	• 52	—	• 77	•
309		• 48	—	• 76	—	• 77	•

^aThe parentheses [()] represent a monotropic transition temperature.

LCDs will remain the dominant display device in the flat panel part of the displays market, at least for the near future and especially for handheld devices. New technologies will probably complement LCD technology and serve to expand the overall displays market (e.g., plasma-addressed LCDs and LCDs with light-emitting polymer backlighting). LCDs can be expected to dominate in the portable instrument segment of the market (e.g., notebook computers, personal organizers, and cellular telephones). However, the market position of LCDs will be maintained and, indeed, expanded only if significant progress in research and development across a range of technologies and scientific disciplines is maintained. A crucial contribution to this progress will be the design and synthesis of new liquid crystals with a physical property spectrum to match the continually changing requirements of new types of LCDs and optimized versions of standard LCDs.

Acknowledgments

We gratefully acknowledge the Engineering and Physical Sciences Research Council for support of an advanced fellowship (S. M. K.). We thank Dr. W. L. Duffy for a critical reading of the manuscript. This work was produced with the permission of Her Britannic Majesty's Stationery Office.

REFERENCES

1. D. Demus, J. W. Goodby, G. W. Gray, H.-W. Spiess, and V. Vill, Eds., "Handbook of Liquid Crystals." Wiley, New York, 1997.
2. V. Vill, *Liq. Cryst.* 24, 21 (1998).
3. V. Vill, "LiqCryst. 1—Database of Liquid Crystalline Compounds for Personal Computers." LCI Publisher, Hamburg, 1996.
4. D. Blunk, K. Praefcke, and V. Vill, in "Handbook of Liquid Crystals" (D. Demus, J. W. Goodby, G. W. Gray, H.-W. Spiess, and V. Vill, Eds.), Vol. 3, p. 305. Wiley, New York, 1998.
5. C. Fairhurst, S. Fuller, J. Gray, M. C. Holmes, and G. J. T. Tiddy, in "Handbook of Liquid Crystals" (D. Demus, J. W. Goodby, G. W. Gray, H.-W. Spiess and V. Vill, Eds.) Vol. 3, p. 341, Wiley, New York, 1998.
6. H. Andree and B. Middehaue, *Tenside Surf. Det.* 28, 413 (1991).
7. D. Balzer, *Tenside Surf. Det.* 28, 419 (1991).
8. K. Hill, in "Carbohydrates as Raw Materials." (G. Descotes, Ed.), Vol. 2, p. 163. VCH, Weinheim, 1993.
9. D. Chapman, R. M. Williams, and B. D. Ladbroke, *Chem. Phys. Lipids* 1, 445 (1967).
10. V. Percec and C. Pugh, in "Side Chain Liquid Crystalline Polymers" (C. B. McArdle, Ed.), p. 30. Blackie, Glasgow/London, 1989.
11. H. Finkelmann, *Angew. Chem. Int. Ed. Engl.* 26, 816 (1987).
12. H. Coles and R. Simon, *Polymer* 26, 180 (1985).
13. C. Noël and P. Navard, *Prog. Polym. Sci.* 16, 55 (1991).
14. J. C. Dubois, P. le Barny, M. Mauzac, and C. Noel, in "Handbook of Liquid Crystals." (D. Demus, J. W. Goodby, G. W. Gray, H.-W. Spiess, and V. Vill, Eds.), Vol. 3, p. 207. Wiley, New York, 1998.
15. D. Demus, J. W. Goodby, G. W. Gray, H.-W. Spiess, and V. Vill, Eds., "Physical Properties of Liquid Crystals." Wiley, New York, 1999.
16. V. Fréedericks and V. Zolina, *Trans. Faraday Soc.* 29, 919 (1933).
17. V. Zwetkoff, *Acta Physico. Chem. (USSR)* 6, 885 (1937).
18. P. Chatelain, *Bull. Soc. Fr. Mineral Cristallogr.* 66, 105 (1943).
19. R. Williams, *J. Chem. Phys.* 39, 384 (1963).
20. W. Helfrich, *Mol. Cryst. Liq. Cryst.* 21, 187 (1973).
21. G. Baur, *Mol. Cryst. Liq. Cryst.* 63, 45 (1981).
22. L. M. Blinov, in "Handbook of Liquid Crystal Research." (P. J. Collings and J. S. Patel, eds.). Oxford Univ. Press, London, 1997.
23. V. G. Chigrinov, in "The Physics of Liquid Crystal Display Devices." Springer-Verlag, New York, 1998.
24. T. J. Scheffer and J. Nehring, *Annu. Rev. Mater. Sci.* 27, 555 (1997).
25. M. Schadt, *Annu. Rev. Mater. Sci.* 27, 305 (1997).
26. I. C. Sage, in "Handbook of Liquid Crystals." (D. Demus, J. W. Goodby, G. W. Gray, H.-W. Spiess, and V. Vill, Eds.), Vol. 1, p. 731. Wiley, New York, 1998.
27. L. M. Blinov, in "Handbook of Liquid Crystals." (D. Demus, J. W. Goodby, G. W. Gray, H.-W. Spiess, and V. Vill, Eds.), Vol. 1, p. 477. Wiley, New York, 1998.
28. L. M. Blinov and V. G. Chigrinov, in "Electro-Optic Effects in Liquid Crystal Materials." Springer-Verlag, New York, 1994.
29. G. H. Heilmeyer and L. A. Zanon, *Appl. Phys. Lett.* 13, 91 (1968).
30. G. H. Heilmeyer, L. A. Zanon, and L. A. Barton, *Proc. IEEE* 56, 1162 (1968).
31. E. F. Carr, *Mol. Cryst. Liq. Cryst.* 7, 253 (1969).
32. W. Helfrich, *J. Chem. Phys.* 51, 4092 (1969).
33. P. A. Penz, *Phys. Rev. Lett.* 24, 1405 (1970).
34. P. G. de Gennes, in "The Physics of Liquid Crystals." Oxford Univ. Press, London, 1974.
35. P. G. de Gennes and J. Prost, in "The Physics of Liquid Crystals." Oxford Univ. Press, London, 1993.
36. R. B. Meyer, *Phys. Rev. Lett.* 22, 918 (1969).
37. D. Schmidt, M. Schadt, and W. Helfrich, *Z. Naturforsch.* 27a, 277 (1972).
38. J. S. Patel and R. B. Meyer, *Phys. Rev. Lett.* 58, 1538 (1987).
39. I. Dozov, M. Nobili, and G. Durand, *Appl. Phys. Lett.* 70, 1179 (1997).
40. G. P. Bryan-Brown, C. V. Brown, J. C. Jones, E. L. Wood, I. C. Sage, P. Brett, and J. Rudin, *Proc. SID '97 Dig.* 37 (1997).
41. R. B. Meyer, L. Liebert, L. Strzelecki, and P. Keller, *J. Phys. (Paris)* 36, L69 (1975).
42. R. B. Meyer, *Mol. Cryst. Liq. Cryst.* 40, 33 (1977).
43. N. A. Clark and S. T. Lagerwall, *Appl. Phys. Lett.* 36, 899 (1980).
44. J. Fünfschilling and M. Schadt, *J. Appl. Phys.* 35, 5765 (1996).
45. A. Fukuda, *J. Mater. Chem.* 4, 997 (1994).
46. S. Garoff and R. B. Meyer, *Phys. Rev. Lett.* 38, 848 (1997).
47. D. J. Broer, R. A. M. Hikmet, and G. Challa, *Makromol. Chem.* 190, 3201 (1989).
48. J. Lub, D. J. Broer, R. A. M. Hikmet, and K. G. J. Nierop, *Liq. Cryst.* 18, 319 (1995).
49. S. M. Kelly, *J. Mater. Chem.* 5, 2047 (1995).
50. D.-K. Yang and J. W. Doane, *SID '92 Dig.* 759 (1992).
51. U. Behrens and H.-S. Kitzerow, *Polym. Adv. Technol.* 5, 433 (1994).
52. R. A. M. Hikmet, H. M. J. Boots, and M. Michielson, *Liq. Cryst.* 19, 65 (1995).
53. R. A. M. Hikmet, *Adv. Mater.* 4, 679 (1992).
54. J. L. Ferguson, *SID Dig. Tech. Papers* 16, 68 (1985).
55. D. Coates, *J. Mater. Chem.* 5, 2063 (1995).
56. G. P. Crawford, J. W. Doane, and S. Zumer, in "Handbook of Liquid Crystal Research." (P. J. Collings and J. S. Patel, Eds.) p. 347. Oxford Univ. Press, London, 1997.
57. F. Reinitzer, *Monatsh. der Wiener Chem. Ges.* 9, 421 (1888).
58. O. Lehmann, *Z. Phys. Chem. (Leipzig)* 4, 462 (1889).
59. D. Vorländer, "Kristalline Flüssigkeiten und Flüssige Kristalle." Engelmann, Leipzig, Germany, 1905.
60. D. Demus, in "Handbook of Liquid Crystals" (D. Demus, J. W. Goodby, G. W. Gray, H.-W. Spiess, and V. Vill, Eds.), Vol. 1, p. 134. Wiley, New York, 1998.
61. H. Sackmann, *Liq. Cryst.* 5, 43 (1989).
62. G. W. Gray, "Molecular Structure and the Properties of Liquid Crystals." Academic Press, London, 1962.
63. G. W. Gray, in "Advances in Liquid Crystals." Vol. 2, p. 1. Academic Press, New York, 1976.
64. G. W. Gray, *Philos. Trans. R. Soc. London Ser. A* 309, 77 (1983); 330, 73 (1990).
65. J. A. Castellano, J. E. Goldmacher, L. A. Barton, and J. S. Kane, *J. Org. Chem.* 33, 3501 (1968).
66. A. Aviram, R. J. Cox, and W. R. Young, *Angew. Chem. Int. Ed. Engl.* 10, 410 (1971).

67. A. Aviram, I. Haller, and W. R. Young, *Mol. Cryst. Liq. Cryst.* 13, 357 (1971).
68. R. E. Rondeau, M. A. Berwick, R. N. Steppel, and M. P. Servé, *J. Amer. Chem. Soc.* 94, 1096 (1972).
69. R. Steinsträsser, *Z. Naturforsch.* 27b, 774 (1972).
70. O. Lehmann, *Z. Phys. Chem.* 4, 462 (1889).
71. R. Steinsträsser and L. Pohl, *Z. Naturforsch.* 26b, 577 (1971).
72. M. Rosenberg and R. A. Champa, *Mol. Cryst. Liq. Cryst.* 11, 191 (1970).
73. H. Kelker and B. Scheurle, *Angew. Chem. Int. Ed. Engl.* 8, 884 (1969).
74. H. Zocher, *Trans. Faraday Soc.* 29, 931 and 945 (1933).
75. C. W. Oseen, *Trans. Faraday Soc.* 29, 883 (1933).
76. F. C. Frank, *Discuss. Faraday Soc.* 25, 19 (1958).
77. J. L. Eriksen, *Art. Rat. Mech. Anal.* 9, 371 (1962).
78. J. L. Eriksen, *Trans. Soc. Rheol.* 5, 23 (1961).
79. F. M. Leslie, *Art. Rat. Mech. Anal.* 28, 265 (1968).
80. F. M. Leslie, in "Physical Properties of Liquid Crystals." (D. Demus, J. W. Goodby, G. W. Gray, H.-W. Spiess, and V. Vill, Eds.), p. 25. Wiley, New York, 1999.
81. W. Maier and A. Saupe, *Z. Naturforsch.* 13a, 564 (1958); 14a, 882 (1959); 15a, 287 (1960).
82. R. Alben, *Mol. Cryst. Liq. Cryst.* 13, 193 (1971).
83. P. J. Flory and G. Ronca, *Mol. Cryst. Liq. Cryst.* 54, 311 (1979).
84. M. A. Cotter, *Philos. Trans. R. Soc. London Ser. A* 309, 127 (1983).
85. M. A. Osipov, in "Physical Properties of Liquid Crystals." (D. Demus, J. W. Goodby, G. W. Gray, H.-W. Spiess, and V. Vill, Eds.), p. 40. Wiley, New York, 1999.
86. U. Finkenzeller, *Kontakte* 2, 7 (1988).
87. R. Eidenschink, D. Erdmann, J. Krause, and L. Pohl, *Angew. Chem.* 89, 103 (1977).
88. P. Chatelain, *Bull. Soc. Fr. Mineral Cristallog.* 77, 353 (1954).
89. M. Miezowicz, *Nature* 158, 27 (1946).
90. C. Escher, T. Geelhaar, and E. Bohm, *Liq. Cryst.* 3, 469 (1988).
91. K. Siemensmeier and H. Stegemeier, *Chem. Phys. Lett.* 148, 409 (1988).
92. S. T. Lagerwall, in "Handbook of Liquid Crystals." (D. Demus, J. W. Goodby, G. W. Gray, H.-W. Spiess, and V. Vill, Eds.), Vol. 2B, p. 515. Wiley, New York, 1998.
93. P. M. Alt and P. Pleshko, *IEEE Trans. Electron. Devices* ED-21, 146 (1974).
94. E. P. Raynes, in "The Optics of Thermotropic Liquid Crystals." (S. Elston and R. Sambles, Eds.), p. 289, Taylor and Francis, London 1998.
95. S. Kobayashi, H. Hori, and Y. Tanaka, in "Handbook of Liquid Crystal Research." (P. J. Collings and J. S. Patel, Eds.), Oxford Univ. Press, London, 1997.
96. B. J. Lechner, *Proc. IEEE* 59, 1566 (1971).
97. D. E. Castlebury, *IEEE Trans. Electron. Devices* ED-26, 1123 (1979).
98. D. Dixon, *IEEE Trans. Electron. Devices* ED-20, 995 (1973).
99. T. P. Brody, J. T. Asars, and G. D. Dixon, *IEEE Trans. Electron. Devices* ED-20, 995 (1973).
100. E. Kaneko, in "Handbook of Liquid Crystals." (D. Demus, J. W. Goodby, G. W. Gray, H.-W. Spiess, and V. Vill, Eds.), Vol. 2A, p. 230. Wiley, New York, 1998.
101. J. Cognard, *Mol. Cryst. Liq. Cryst.* 51, 1 (1982).
102. D. Berreman, *Phys. Rev.* 28, 1683 (1972).
103. L. Janning, *Appl. Phys. Lett.* 21, 173 (1972).
104. F. J. Kahn, *Appl. Phys. Lett.* 22, 386 (1973).
105. M. Schadt and W. Helfrich, *Appl. Phys., Lett.* 18, 127 (1971).
106. S. Morozumi, T. Ohta, R. Araki, K. Kubota, Y. Ono, T. Nakazawa, and H. Ohara, *SID '84 Dig.* 404 (1983).
107. T. J. Scheffer and J. Nehring, *Appl. Phys. Lett.* 45, 1021 (1984).
108. Y. Kando, T. Nakagomi, and S. Hawasaga, German Patent DE-3 503 259 A1, 1985.
109. M. Schadt and F. Leenhouts, *Proc. SID* 28, 275 (1987).
110. K. Katoh, Y. Endo, M. Akatsuka, M. Ohgawara, and K. Sawada, *Jpn. J. Appl. Phys.* 26, L1784 (1987).
111. O. Okumura, M. Nagata, and K. Wada, *ITEJ Tech. Rep.* II, 27 (1987).
112. C. Waters, V. Brimmel, and E. P. Raynes, *Proc. Jpn Display '83* 396 (1983).
113. W. M. Gibbons, P. J. Shannon, S.-T. Sun, and B. J. Swetlin, *Nature* 351, 49 (1991).
114. S.-T. Sun, W. M. Gibbons, and P. J. Shannon, *Liq. Cryst.* 12, 869 (1992).
115. W. M. Gibbons, P. J. Shannon, and S.-T. Sun, *Mol. Cryst. Liq. Cryst.* 251, 191 (1994).
116. K. Ichimura, N. Hamada, S. Kato, and I. Shinohara, *J. Polym. Sci., Polym. Chem. Ed.* 21, 1551 (1983).
117. Y. Iinura, J. Kusano, S. Kobayashi, and Y. Aoyagi, *Jpn. J. Appl. Phys.* 32, L93 (1993).
118. K. Ichimura, Y. Suzuki, T. Seki, A. Hosoki, and N. Aoki, *Langmuir* 4, 1214 (1988).
119. K. Ichimura, in "Photochemical Processes in Organized Molecular Systems." (K. Honda, Ed.), p. 343. Elsevier, Amsterdam, 1991.
120. K. Ichimura, Y. Hayashi, Y. Kawanishi, T. Seki, T. Tamaki, and N. Ishizuki, *Langmuir* 9, 857 (1993).
121. K. Ichimura, Y. Hayashi, and N. Ishizuki, *Chem. Lett.* 1063 (1992).
122. A. Dyadyusha, V. Kozenkov, T. Marusii, Y. Reznikov, V. Reshetnyak, and A. Khizhnyak, *Ukr. Fiz. Zh.* 36, 1059 (1991).
123. M. Schadt, K. Schmitt, V. Kozinkov, and V. G. Chigrinov, *Jpn. J. Appl. Phys.* 31, 2135 (1992).
124. K. Ichimura, Y. Akita, K. Akiyama, K. Kudo, and Y. Hayashi, *Macromolecules* 30, 903 (1997).
125. G. P. Bryan-Brown and I. C. Sage, *Liq. Cryst.* 20, 825 (1996).
126. M. Schadt, H. Seiberle, A. Schuster, and S. M. Kelly, *Jpn. J. Appl. Phys.* 34, L764 (1995).
127. M. Schadt, H. Seiberle, A. Schuster, and S. M. Kelly, *Jpn. J. Appl. Phys.* 34, 3240 (1995).
128. Y. Iimura, S. Kobayashi, T. Hashimoto, T. Sugiyama, and K. Katoh, *IEICE Trans. Electron.* E79-C, 1040 (1996).
129. R.-P. Herr, F. Herzog, and A. Schuster, *WO* 96/10049 (1996).
130. M. Schadt, H. Seiberle, and A. Schuster, *Nature* 381, 212 (1996).
131. M. Schadt, *Mol. Cryst. Liq. Cryst.* 292, 235 (1997).
132. M. Schadt and H. Seiberle, *Proc. SID* 5/4, 367 (1997).
133. S. M. Kelly, P. Hindmarsh, G. J. Owen, P. O. Jackson, P. J. Taylor, and M. O'Neill, *SID EID '98 Dig.* 5.1 (1998).
134. P. Hindmarsh, G. J. Owen, S. M. Kelly, P. O. Jackson, M. O'Neill, and R. Karapinar, *Mol. Cryst. Liq. Cryst.* 332, 439 (1999).
135. P. O. Jackson, R. Karapinar, M. O'Neill, P. Hindmarsh, G. J. Owen, and S. M. Kelly, *Proc. SPIE* 3635, 48 (1999).
136. M. Hasegawa and Y. Taira, *IRDC '94 Dig.* 213 (1994).
137. J. L. West, X. Wang, Y. Ji, and J. R. Kelly, *SID '95 Dig.* 703 (1995).
138. C. J. Newsome, M. O'Neill, and G. P. Bryan Brown, *Proc. SPIE* 3618, 132 (1999).
139. P. J. Bos, *Proc. SID '94* 118 (1994).
140. Y. Fujimura, *SID Dig.* 397 (1992).
141. S. Kaneko, Y. Hirai, and K. Sumiyoshi, *SID Dig.* '93 265 (1993).
142. H. L. Ong, *Jpn. Display '92* 247 (1992).
143. J. P. Eblen, W. J. Gunning, J. Beedy, D. Taber, L. Hale, P. Yeh, and M. Khoshnevisan, *SID '94 Dig.* 245 (1994).
144. A. Shimizu, *Asia Display '98* 207 (1998).
145. S. Stallinga, J. M. van den Eerenbeemd, and J. A. M. M. van Haaren, *Jpn. J. Appl. Phys.* 37, 560 (1998).
146. H. Mori, Y. Itoh, Y. Nisiura, T. Nakamura, and Y. Shinagawa, *AM-LCD '96/IDW '96 Digest* 189 (1996).
147. P. van de Witte, J. van Haaren, J. Tuijtelars, S. Stallinga, and J. Lub, *Jpn. J. Appl. Phys.* 38, 748 (1999).
148. C. Joubert and J.-C. Leheureau, *Asia Display '98* 1119 (1998).
149. R. Brinkley, G. Xu, A. Abileah, and J. Vanderploeg, *SID '98 Dig.* 471 (1998).
150. A. Lien, *Appl. Phys. Lett.* 57, 2767 (1990).

151. M. Jones and G. Xu, *SID '98 Dig.* 475 (1998).
152. K. R. Sarma, H. Franklin, M. Johnson, K. Frost, and A. Bernot, *SID '89 Dig.* 148 (1989).
153. K. H. Yang, *IDRC '91 Dig.* 68 (1991).
154. M. F. Schiekel and K. Fahrenschoen, *Appl. Phys. Lett.* 15, 391 (1971).
155. H. Mailer, K. L. Likins, T. R. Taylor, and J. L. Ferguson, *Appl. Phys. Lett.* 118, 105 (1971).
156. M. Hareng, G. Assouline, and F. Leiba, *Appl. Opt.* 11, 2920 (1972).
157. F. J. Kahn, *Appl. Phys. Lett.* 20, 199 (1972).
158. G. Labrunie and J. Robert, *J. Appl. Phys.* 44, 4869 (1973).
159. Hp. Schad, *SID '82 Dig.* 244 (1982).
160. V. Fréedericksz and V. Zolina, *Trans. Faraday Soc.* 29, 919 (1933).
161. W. Helfrich, *Mol. Cryst. Liq. Cryst.* 21, 187 (1973).
162. L. M. Blinov, in "Handbook of Liquid Crystal Research." (P. J. Collings and J. S. Patel, Eds.), Chap. 5, p. 125. Oxford Univ. Press, London, 1997.
163. S. T. Wu, *Appl. Phys. Lett.* 57, 986 (1990).
164. S. T. Wu, *Mol. Cryst. Liq. Cryst.* 207, 1 (1991).
165. A. Rapini and M. Papoular, *J. Phys. (Paris)* 30, C4-54 (1969).
166. F. Gharadjedaghi, *Disp. Technol.* 1, 95 (1986).
167. R. Steinsträsser and F. Del Pino, German Patent DE-24,500,088, 1974.
168. T. Inukai, H. Inoue, K. Furukawa, S. Saito, S. Sugimori, and K. Yokohama, German Patent DE-2,937,700, 1979.
169. G. W. Gray and S. M. Kelly, *Mol. Cryst. Liq. Cryst.* 75, 109 (1981).
170. M. A. Osman, *Mol. Cryst. Liq. Cryst.* 82, 295 (1982).
171. S. M. Kelly and Hp. Schad, *Mol. Cryst. Liq. Cryst.* 110, 239 (1984).
172. S. M. Kelly and T. Huynh-Ba, *Helv. Chim. Acta* 66, 1850 (1983).
173. M. A. Osman and T. Huynh-Ba, *Mol. Cryst. Liq. Cryst. Lett.* 92, 57 (1983).
174. S. M. Kelly and Hp. Schad, *Helv. Chim. Acta* 68, 813 (1985).
175. Hp. Schad and S. M. Kelly, *Mol. Cryst. Liq. Cryst.* 75, 133 (1986).
176. M. A. Osman and T. Huynh-Ba, *Mol. Cryst. Liq. Cryst. Lett.* 82, 339 (1983).
177. M. A. Osman, *Mol. Cryst. Liq. Cryst.* 128, 45 (1985).
178. M. A. Osman, *Helv. Chim. Acta* 68, 606 (1985).
179. M. Schadt, *Proc. Jpn Display '83, Kobe* 220 (1983).
180. M. Schadt, M. Petrzilka, P. R. Gerber, A. Villiger, and G. Trices, *Mol. Cryst. Liq. Cryst.* 94, 139 (1983).
181. M. P. Burrow, G. W. Gray, D. Lacey, and K. J. Toyne, *Z. Chem.* 26, 21 (1986).
182. R. Eidenschink, O. Haas, M. Römer, and B. S. Scheuble, *Angew. Chem.* 96, 151 (1984).
183. B. S. Scheuble, G. Weber, and R. Eidenschink, "Proceedings of EuroDisplay '84," Paris, 1984, p. 65.
184. R. Eidenschink and B. S. Scheuble, *Mol. Cryst. Liq. Cryst. Lett.* 3, 33 (1986).
185. V. Reiffenrath, J. Krause, H. J. Plach, and G. Weber, *Liq. Cryst.* 5, 159 (1989).
186. V. Reiffenrath and M. Bremer, *Angew. Chem. Int. Ed. Engl.* 33, 87 (1994).
187. S. M. Kelly, *Liq. Cryst.* 10, 261 (1991).
188. C. H. Gooch and H. A. Tarry, *Electron. Lett.* 10, 2 (1974).
189. Ch. Maugin, *Bull. Soc. Fr. Mineral. Cristallogr. Phys. Z.* 12, 1011 (1911).
190. L. Pohl, G. Weber, R. Eidenschink, G. Baur, and W. Fehrenbach, *Appl. Phys. Lett.* 38, 497 (1981).
191. J. van der Veen, W. H. de Jeu, A. H. Grobbsen, and J. Boven, *Mol. Cryst. Liq. Cryst.* 17, 291 (1972).
192. E. Jakeman and E. P. Raynes, *Phys. Lett.* 39A, 69 (1972).
193. F. M. Jaeger, *Recueil Trav. Chim. Pays-Bas* 26, 311 (1907).
194. G. W. Gray and D. G. McDonnell, *Mol. Cryst. Liq. Cryst. Lett.* 34, 211 (1977).
195. G. W. Gray and D. G. McDonnell, *Mol. Cryst. Liq. Cryst.* 37, 189 (1976).
196. E. Froehlich, Dissertation, Halle, 1910.
197. G. H. Heilmeyer, L. A. Zanon, and J. E. Goldmacher, in "Liquid Crystals and Ordered Fluids." (J. F. Johnson and R. S. Porter, Eds.). Plenum, New York, 1970.
198. J. A. Castellano, German Patent Application DE-OS, 1,928,003, 1971.
199. L. Pohl and R. Steinsträsser, German Patent Application DE-OS, 2,024,269, 1971.
200. R. Steinsträsser, *Z. Naturforsch.* 27b, 774 (1972).
201. A. Boller, H. Scherrer, M. Schadt, and P. Wild, *Proc. IEEE* 60, 1002 (1972).
202. G. W. Gray, K. J. Harrison, and J. A. Nash, *Electron. Lett.* 9, 130 (1973).
203. A. I. Pavluchenko, V. V. Titov, and N. I. Smirnova, in "Advances in Liquid Crystal Research and Applications" (L. Bata, Ed.), p. 1007. Pergamon, Oxford, 1980.
204. L. A. Karamysheva, E. I. Kovsky, A. I. Pavluchenko, K. V. Roitman, V. V. Titov, S. I. Torgova, and M. F. Grebyonkin, *Mol. Cryst. Liq. Cryst.* 67, 241 (1981).
205. A. Boller, M. Cereghetti, M. Schadt, and H. Scherrer, *Mol. Cryst. Liq. Cryst.* 42, 1225 (1977).
206. A. I. Pavluchenko, N. I. Smirnova, V. F. Petrov, M. F. Grebyonkin, and V. V. Titov, *Mol. Cryst. Liq. Cryst.* 209, 155 (1991).
207. M. F. Grebyonkin, V. F. Petrov, and B. I. Ostrovsky, *Liq. Cryst.* 7, 367 (1990).
208. V. Petrov, S. I. Torgova, L. A. Karamysheva, and S. Tanenaka, *Liq. Cryst.* 26, 1141 (1999).
209. A. Boller, M. Schadt, and A. Villiger, UK Patent Application GB 208 2085877.
210. J. Bartulin, C. Zuniga, H. Muller, T. R. Taylor, and W. Haase, *Mol. Cryst. Liq. Cryst. Sci. Technol., Sect. B* 150, 237 (1987).
211. T. Inukai, H. Inoue, and H. Sato, U.S. Patent, 4,211,666, 1978.
212. M. A. Osman and L. Revesz, *Mol. Cryst. Liq. Cryst.* 82, 41 (1982).
213. H. Sorkin, *Mol. Cryst. Liq. Cryst.* 56, 279 (1980).
214. V. S. Bezborodov, *Zh. Org. Khim.* 25, 2168 (1989).
215. Y. Haramoto and H. Kamogawa, *Chem. Lett.* 79 (1985).
216. G. W. Gray and S. M. Kelly, *Angew. Chem. Int. Ed. Engl.* 20, 393 (1981).
217. A. Villiger, A. Boller, and M. Schadt, *Z. Naturforsch.* 34, 1535 (1979).
218. G. W. Gray, "12th Arbeitstagung Flüssigkristalle," Freiburg, Germany, 1978, abstract.
219. R. Eidenschink, D. Erdmann, J. Krause, and L. Pohl, *Angew. Chem.* 90, 133 (1978).
220. W. Sucrow and W. Schatull, *Z. Naturforsch.* 37b, 1336 (1982).
221. M. Petrzilka and M. Schadt, U.S. Patent 4,565,425, 1986.
222. H.-J. Deutscher, F. Kuschel, S. König, H. Kresse, D. Pfeiffer, A. Wiegeleben, J. Wulf, and D. Demus, *Z. Chem.* 17, 64 (1977).
223. S. Sugimori, H. Sato, T. Inukai, and K. Furakawa, German Patent Application DE-OS 3,029,378, 1981.
224. N. Carr, G. W. Gray, and D. G. McDonnell, *Mol. Cryst. Liq. Cryst.* 97, 13 (1983).
225. M. Petrzilka, *Mol. Cryst. Liq. Cryst.* 111, 329 (1984).
226. S. M. Kelly, *Liq. Cryst.* 10, 273 (1991).
227. R. Buckecker and M. Schadt, *Mol. Cryst. Liq. Cryst.* 149, 359 (1987).
228. M. Petrzilka and M. Schadt, *Mol. Cryst. Liq. Cryst.* 131, 109 (1985).
229. S. M. Kelly, A. Germann, R. Buckecker, and M. Schadt, *Liq. Cryst.* 16, 67 (1994).
230. S. M. Kelly, M. Schadt, and H. Seiberle, *Liq. Cryst.* 18, 581 (1995).
231. M. Schadt, R. Buckecker, A. Villiger, F. Leenhouts, and J. Fromm, *Trans. IEEE Electron. Devices* ED-33, 1187 (1986).
232. M. Schadt, M. Petrzilka, P. R. Gerber, and A. Villiger, *Mol. Cryst. Liq. Cryst.* 122, 241 (1985).
233. M. Schadt, R. Buckecker, and K. Müller, *Liq. Cryst.* 5, 293 (1989).
234. G. W. Gray and S. M. Kelly, *J. Mater. Chem.* 9, 2037 (1999).
235. A. J. Leadbetter, R. M. Richardson, and C. N. Collings, *J. Phys. (Paris)* 36, 37 (1975).

236. H. Schad and M. A. Osman, *J. Chem. Phys.* 75, 880 (1981); 79, 5710 (1983).
237. H. Schad and S. M. Kelly, *J. Chem. Phys.* 81, 1514 (1984).
238. C. J. F. Boettcher and P. Bordwijk, "Theory of Electric Polarization," Vol. 2. Elsevier, Amsterdam, 1978.
239. P. Bordwijk, *J. Chem. Phys.* 73, 595 (1980).
240. M. J. Bradshaw and E. P. Raynes, *Mol. Cryst. Liq. Cryst.* 91, 145 (1983).
241. H.-J. Deutscher, B. Laaser, W. Dölling, and H. Schubert, *J. Prakt. Chem.* 320, 194 (1978).
242. M. E. Neubert, L. T. Carlino, D. L. Fishel, and R. M. D. Sidocky, *Mol. Cryst. Liq. Cryst.* 59, 253 (1980).
243. G. W. Gray, C. Hogg, and D. Lacey, *Mol. Cryst. Liq. Cryst.* 67, 1 (1981).
244. M. A. Osman and L. Revesz, *Mol. Cryst. Liq. Cryst.* 56, 157 (1980).
245. G. W. Gray and S. M. Kelly, *Mol. Cryst. Liq. Cryst.* 75, 95 (1981).
246. N. Carr, G. W. Gray, and S. M. Kelly, *Mol. Cryst. Liq. Cryst. Lett.* 1, 53 (1985).
247. M. A. Osman, *Mol. Cryst. Liq. Cryst.* 128, 45 (1985).
248. H. Takatsu, K. Takeuchi, and H. Sato, *Jpn Display '83* 228 (1983).
249. S. M. Kelly, *Mol. Cryst. Liq. Cryst.* 204, 27 (1991).
250. R. Eidenschink, *Kontakte (Darmstadt)* 1, 15 (1979); *Mol. Cryst. Liq. Cryst.* 123, 57 (1985).
251. R. Eidenschink, M. Römer, and F. V. Allen, in "Liquid Crystals and Ordered Fluids." (A. C. Griffin and J. F. Johnson, Eds.), p. 737. Plenum, New York, 1984.
252. M. A. Osman, *Z. Naturforsch.* 38a, 693 (1983).
253. R. Eidenschink, *Mol. Cryst. Liq. Cryst.* 113, 57 (1985).
254. R. Eidenschink, M. Römer, G. Weber, G. W. Gray, and K. J. Toyne, German Patent 3,321,373, 1983.
255. M. A. Osman, *Mol. Cryst. Liq. Cryst.* 72, 291 (1982).
256. H.-J. Deutscher, M. Körber, and H. Schubert, in "Advances in Liquid Crystal Research and Applications" (L. Bata, Ed.), p. 1075. Pergamon, Oxford, 1980.
257. K. Praefcke, D. Schmidt, and G. Heppke, *Chem. Zeit.* 104, 269 (1980).
258. K. Praefcke, D. Schmidt, and G. Heppke, *Istr. J. Chem.* 18, 195 (1979).
259. B. S. Scheuble "Proceedings of the 16th Freiburger Arbeitstagung Flüssigkristalle," Freiburg, Germany, 1987.
260. H. Takatsu, K. Takeuchi, and H. Sato, *Mol. Cryst. Liq. Cryst.* 100, 345 (1983).
261. G. W. Gray and D. G. McDonnell, *Mol. Cryst. Liq. Cryst.* 53, 147 (1979).
262. R. Eidenschink and M. Römer, "Proceedings of the 13th Freiburger Arbeitstagung Flüssigkristalle," Freiburg, Germany, 1983.
263. U. Finkenzeller, A. Kurmeier, and E. Poetsch, "Proceedings of the 18th Freiburger Arbeitstagung Flüssigkristalle," Freiburg, Germany, 1989.
264. E. Bartmann, D. Dorsch, and U. Finkenzeller, U. Kurmeier, and E. Poetsch, "Proceedings of the 19th Freiburger Arbeitstagung Flüssigkristalle," Freiburg, Germany, 1990.
265. B. Rieger, E. Poetsch, and V. Reifenrath, "Proceedings of the 19th Freiburger Arbeitstagung Flüssigkristalle," Freiburg, Germany, 1990.
266. A. I. Pavluchenko, N. I. Smirnova, V. F. Petrov, Y. A. Fialkov, S. V. Shelyazhenko, and L. M. Yagupolsky, *Mol. Cryst. Liq. Cryst.* 209, 225 (1991).
267. E. Bartmann, D. Dorsch, and U. Finkenzeller, *Mol. Cryst. Liq. Cryst.* 204, 77 (1991).
268. Y. Goto, T. Ogawa, S. Sawada, and S. Sugimori, *Mol. Cryst. Liq. Cryst.* 209, 1 (1991).
269. Y. Onji, M. Ushioda, S. Matsui, T. Kondo, and Y. Goto, European Patent Application EPA 0,647,696, A1, 1993.
270. K. Tarumi, M. Bremer, and T. Geelhaar, *Annu. Rev. Sci.* 27, 423 (1997).
271. H. Takatsu, K. Takeuchi, M. Sasaki, and H. Onishi, *Mol. Cryst. Liq. Cryst.* 206, 159 (1991).
272. E. Bartmann, J. Krause, and K. Tarumi, "Proceedings of the 23rd Freiburger Arbeitstagung Flüssigkristalle," Freiburg, Germany, 1994.
273. M. Bremer, *Adv. Mater.* 7, 867 (1995).
274. R. Buchecker, G. Marck, and M. Schadt, *Mol. Cryst. Liq. Cryst.* 260, 93 (1995).
275. E. Bartmann, *Adv. Mater.* 8, 570 (1996).
276. M. Goulding, S. Greenfield, O. Parri, and D. Coates, *Mol. Cryst. Liq. Cryst.* 265, 27 (1995).
277. S. Greenfield, D. Coates, M. Goulding, and R. Clemitson, *Liq. Cryst.* 18, 665 (1995).
278. D. W. Berreman and W. R. Heffner, *J. Appl. Phys.* 122, 1 (1985).
279. E. P. Raynes, *Mol. Cryst. Liq. Cryst. Lett.* 4, 1 (1986).
280. E. P. Raynes and C. M. Waters, *Displays* 59 (1987).
281. E. P. Raynes, *Mol. Cryst. Liq. Cryst. Lett.* 4, 69 (1987).
282. T. J. Scheffer and J. Nehring, *Z. Naturforsch.* 45a, 867 (1990).
283. T. J. Scheffer, J. Nehring, M. Kaufmann, H. Amstutz, D. Heimgartner, and P. Eglin, *SID '85 Dig.* 120 (1985).
284. M. Schadt and F. Leenhouts, *J. Appl. Phys.* 50, 236 (1987).
285. V. G. Chigrinov, V. V. Belyaev, S. V. Belyaev, and M. F. Grebenkin, *Sov. Phys. JETP* 50, 994 (1979).
286. T. J. Scheffer, B. Clifton, D. Prince, and A. R. Connor, *Displays* 14, 74 (1993).
287. D. W. Berreman and W. R. Heffner, *J. Appl. Phys.* 52, 3032 (1981).
288. R. N. Thurston, *Mol. Cryst. Liq. Cryst.* 122, 1 (1985).
289. Y. Nara, S. Kobayashi, and A. Miyaji, *J. Appl. Phys.* 49, 4277 (1978).
290. C. M. Waters, E. P. Raynes, and V. Brimmell, *Proc. SID* 25, 261 (1984).
291. C. M. Waters, E. P. Raynes, and V. Brimmell, *Mol. Cryst. Liq. Cryst.* 123, 303 (1985).
292. F. Gadjedaghi, *Mol. Cryst. Liq. Cryst.* 68, 127 (1981).
293. T. Uchida and M. Wada, *Mol. Cryst. Liq. Cryst.* 63, 19 (1981).
294. D. L. White and G. N. Taylor, *J. Appl. Phys.* 45, 4718 (1974).
295. A. Göbl-Wunsch, G. Heppke, and F. Oestereicher, *J. Phys. (Paris)* 40, 773 (1979).
296. F. Leenhouts and M. Schadt, *Mol. Cryst. Liq. Cryst.* 158B, 241 (1988).
297. F. Moia, M. Schadt, and H. Seiberle, *SID '93* 1 (1993).
298. S. Naemura, T. Oyama, H. Plach, G. Weber, and B. Scheuble, and E. Merck, "Liquid Crystal Seminar Data," Tokyo, Japan (1995).
299. D. W. Berreman, *Appl. Phys. Lett.* 25, 12 (1974).
300. P. J. Bos, *SID '94*, 118 (1994).
301. N. Kimura, T. Shinomiya, K. Yamamoto, Y. Ichimura, K. Nakagawa, Y. Ishi, and M. Matsuura, *Proc. SID* 49 (1988).
302. H. Watanabe, O. Okumura, H. Wada, A. Ito, M. Yazaki, M. Nagata, H. Takeshita, and S. Morozumi, *Proc. SID* 416 (1988).
303. M. Schadt and P. R. Gerber, *Z. Naturforsch.* 37a, 165 (1982).
304. W. H. de Jeu and W. A. P. Claasen, *J. Chem. Phys.* 67, 3705 (1977).
305. Hp. Schad, G. Baur, and G. Meier, *J. Chem. Phys.* 70, 2770 (1979).
306. M. Schadt, *Liq. Cryst.* 14, 73 (1993).
307. V. Petrov, S. I. Torgova, L. A. Karamysheva, and S. Tanenaka, *Liq. Cryst.* 26, 1141 (1999).
308. M. Schadt and F. Müller, *Rev. Phys. Appl.* 14, 265 (1979).
309. J. Constant and E. P. Raynes, *Mol. Cryst. Liq. Cryst.* 62, 115 (1980).
310. M. Schadt and P. R. Gerber, *Z. Naturforsch.* 37a, 179 (1982).
311. J. Constant and E. P. Raynes, *Mol. Cryst. Liq. Cryst.* 62, 115 (1980).
312. M. Schadt and M. Petrzilka, *Jpn Display '84* 53 (1984).
313. R. G. Priest, *Phys. Rev. A* 7, 720 (1973).
314. J. P. Straley, *Phys. Rev. A* 8, 2181 (1973).
315. M. Petrzilka, *Mol. Cryst. Liq. Cryst.* 131, 109 (1985).
316. H. Ohnishi, H. Takatsu, K. Takeuchi, F. Moia, and M. Schadt, *SID '92 Dig.* 17 (1982).
317. K. Praefcke, D. Schmidt, and G. Heppke, *Chem. Zeit.* 104, 269 (1980).
318. E. Poetsch, V. Reiffenrath, and B. Rieger, "Proceedings of the 24th Arbeitstagung Flüssigkristalle," Freiburg, Germany, 1995, p. 1.
319. M. Petrzilka, R. Buckecker, S. Lee-Schmiederer, M. Schadt, and A. Germann, *Mol. Cryst. Liq. Cryst.* 148, 123 (1987).

320. M. Petrzilka, U.S. Patent 4,676,604, 1987.
321. M. Schadt, R. Buckecker, and A. Villiger, *Liq. Cryst.* 79, 519 (1990).
322. S. M. Kelly, A. Germann, and M. Schadt, *Liq. Cryst.* 16, 491 (1994).
323. S. M. Kelly, *Liq. Cryst.* 17, 211 (1994).
324. R. Eidenschink, G. W. Gray, K. J. Toyne, and A. E. F. Waechter, *Mol. Cryst. Liq. Cryst. Lett.* 5, 177 (1988).
325. S. Kawakami, K. Kotani, S. Shirokura, H. Ohnishi, Y. Fujita, T. Ohtsuka, H. Takatsu, and F. Moia, *Proc. SID '92* 487 (1992).
326. H. Seiberle, F. Moia, M. Schadt, H. Takatsu, and K. Kotani, "Proceedings of the 20th Freiburger Arbeitstagung Flüssigkristalle," Freiburg, Germany, 1992.
327. T. P. Rieker, N. A. Clark, G. S. Smith, D. S. Parmar, D. S. Sirota, and E. B. Safinya, *Phys. Rev. Lett.* 59, 2658 (1987).
328. D. C. Ulrich and S. J. Elston, in "The Optics of Thermotropic Liquid Crystals" (S. J. Elston and R. Sambles, Eds.), p. 195. Taylor and Francis, London, 1998.
329. S. L. Arora, J. L. Ferguson, and A. Saupe, *Mol. Cryst. Liq. Cryst.* 10, 243 (1970).
330. T. R. Taylor, J. L. Ferguson, and S. L. Arora, *Phys. Rev. Lett.* 24, 359 (1970).
331. T. R. Taylor, S. L. Arora, and J. L. Ferguson, *Phys. Rev. Lett.* 25, 722 (1970).
332. F. M. Jäger, *Recueil Trav. Chim. Pays Bas* 25, 334 (1906).
333. W. Urbach and J. Billard, *C. R. Hebd. Seances. Acad. Sci.* 274B, 1287 (1972).
334. G. W. Gray, *Mol. Cryst. Liq. Cryst.* 7, 127 (1969).
335. M. Leclercq, J. Billard, and J. Jacques, *Mol. Cryst. Liq. Cryst.* 8, 367 (1969).
336. G. W. Gray, *J. Chem. Soc.* 43, 59 (1955).
337. S. L. Arora, T. R. Taylor, J. L. Ferguson, and A. Saupe, *J. Am. Chem. Soc.* 91, 3671 (1969).
338. W. Helfrich and C. S. Oh, *Mol. Cryst. Liq. Cryst.* 14, 289 (1971).
339. A. Saupe, *Mol. Cryst. Liq. Cryst.* 7, 59 (1969).
340. W. L. McMillan, *Phys. Rev. A* 8, 1921 (1973).
341. A. Wulf, *Phys. Rev. A* 11, 365 (1975).
342. R. G. Priest, *J. Chem. Phys.* 65, 408 (1976).
343. A. Wiegeleben and D. Demus, *Liq. Cryst.* 11, 111 (1972).
344. J. W. Goodby, in "Ferroelectric Liquid Crystals." (G. W. Taylor, Ed.), p. 99. Gordon and Breach, Philadelphia, 1991.
345. J. W. Goodby and T. M. Leslie, in "Liquid Crystals and Ordered Fluids." (A. C. Griffin and J. F. Johnson, Eds.), Vol. 4, p. 1. Plenum, New York, 1984.
346. J. W. Goodby, G. W. Gray, and D. G. McDonnell, *Mol. Cryst. Liq. Cryst. Lett.* 34, 183 (1977).
347. J. W. Goodby, and G. W. Gray, *Ann. Phys.* 3, 123 (1978).
348. S. M. Kelly and J. Fünfschilling, *J. Mater. Chem.* 4, 1673 (1994).
349. P. Keller, L. Liebert, and L. Strzelecki, *J. Phys. (Paris) Colloq.* 37, C3 (1976).
350. B. I. Ostrovski, A. Z. Rabinovitch, A. S. Sonin, and E. L. Sorkin, *Ferroelectrics* 24, 309 (1980).
351. K. Yoshino and T. Sakurai, in "Ferroelectric Liquid Crystals." (G. W. Taylor, Ed.), p. 317. Gordon and Breach, Philadelphia 1991.
352. A. Hallsby, M. Nilsson, and B. Otterholm, *Mol. Cryst. Liq. Cryst. Lett.* 82, 61 (1982).
353. B. Otterholm, M. Nilsson, S. T. Lagerwall, and K. Skarp, *Liq. Cryst.* 2, 757 (1987).
354. J. W. Goodby and J. S. Patel, *Proc. SPIE* 684, 52 (1986).
355. J. W. Goodby, E. Chin, J. M. Geary, J. S. Patel, and P. L. Finn, *J. Chem. Soc. Faraday Trans.* 1, 83, 3429 (1987).
356. J. W. Goodby, *Science* 231, 350 (1986).
357. T. M. Leslie, *Ferroelectrics* 58, 9 (1984).
358. S. M. Kelly, R. Buchecker, H.-J. Fromm, and M. Schadt, *Ferroelectrics* 85, 385 (1988).
359. S. M. Kelly and R. Buchecker, *Helv. Chim. Acta* 71, 451 (1988).
360. S. M. Kelly and R. Buchecker, *Helv. Chim. Acta* 71, 461 (1988).
361. R. Dabrowski, J. Dziaduszek, J. Szulc, K. Czuprynski, and B. Sosnowska, *Mol. Cryst. Liq. Cryst.* 209, 201 (1991).
362. Y. Haramoto and H. Kamogawa, *Mol. Cryst. Liq. Cryst.* 182, 195 (1990).
363. H. Matsubara, S. Takahashi, K. Seto, and H. Imazaki, *Mol. Cryst. Liq. Cryst.* 180, 337 (1990).
364. F. Leenhouts, S. M. Kelly, and A. Villiger, *Displays* 40 (1990).
365. S. M. Kelly, R. Buchecker, and M. Schadt, *Liq. Cryst.* 3, 1115 (1988).
366. S. M. Kelly, R. Buchecker, and M. Schadt, *Liq. Cryst.* 3, 1125 (1988).
367. A. Yoshizawa, I. Nishiyama, M. Fukumasa, T. Hirai, and M. Yamane, *Jpn. J. Appl. Phys.* 28, L1269 (1989).
368. K. Furakawa, K. Terashima, M. Ichihashi, S. Saitoh, K. Miyazawa, and T. Inukai, *Ferroelectrics* 85, 451 (1988).
369. L. K. M. Chan, G. W. Gray, D. Lacey, R. M. Scowston, I. G. Shenouda, and K. J. Toyne, *Mol. Cryst. Liq. Cryst.* 172, 125 (1989).
370. K. Yoshino, M. Osaki, K. Nakao, H. Taniguchi, N. Yamasaki, and K. Satoh, *Liq. Cryst.* 5, 1203 (1989).
371. S. Sugita, S. Toda, T. Yamashita, and T. Teraji, *Bull. Chem. Soc. Jpn.* 66, 568 (1993).
372. E. Chin, J. W. Goodby, and J. S. Patel, *Mol. Cryst. Liq. Cryst.* 157, 163 (1988).
373. S. Sugita, S. Toda, T. Yoshiyasu, and T. Teraji, *Mol. Cryst. Liq. Cryst.* 237, 399 (1993).
374. J. Nakauchi, Y. Kageyama, S. Hayashi, and K. Sakashita, *Bull. Chem. Soc. Jpn.* 62, 1685 (1989).
375. C. Sekine, T. Tani, Y. Ueda, K. Fujisawa, T. Higashi, I. Kurimoto, S. Toda, N. Takano, Y. Fujimoto, and M. Minai, *Ferroelectrics* 148, 203 (1993).
376. S. Takehara, M. Osawa, K. Nakamura, and T. Kuriyama, *Ferroelectrics* 148, 185 (1993).
377. M. Murakami, S. Miyake, T. Masumi, T. Ando, and A. Fukami, *Jpn Display '86* 344 1986.
378. S. Matsumoto, A. Murayama, H. Hatoh, Y. Kinoshita, H. Hirai, M. Ishikawa, and S. Kamagami, *SID '88 Dig.* 41 (1988).
379. S. M. Kelly and A. Villiger, *Liq. Cryst.* 3, 1173 (1988).
380. P. Keller, S. Jugé, L. Liebert, and L. Strzelecki, *C. R. Acad. Sci.* 282, C639 (1976).
381. T. Sakurai, N. Mikami, R. Higuchi, M. Honma, and K. Yoshino, *Ferroelectrics* 85, 469 (1988).
382. C. Bahr and G. Heppke, *Mol. Cryst. Liq. Cryst.* 148, 29 (1987).
383. G. Heppke, D. Lötsch, N. K. Sharma, D. Demus, S. Diele, K. Jahn, and M. Neundorff, *Liq. Cryst.* 241, 275 (1994).
384. S. Arakawa, K. Nito, and J. Seto, *Mol. Cryst. Liq. Cryst.* 204, 15 (1991).
385. J. Bömelburg, G. Heppke, and A. Ranft, *Z. Naturforsch.* 44b, 1127 (1989).
386. R. Buchecker, S. M. Kelly, and J. Fünfschilling, *Liq. Cryst.* 8, 217 (1990).
387. S. M. Kelly, R. Buchecker, and J. Fünfschilling, *J. Mater. Chem.* 4, 1689 (1994).
388. H. R. Dübal, C. Escher, D. Günther, W. Hemmerling, Y. Inoguchi, I. Müller, M. Murikami, D. Ohlendorf, and R. Wingen, *Jpn. J. Appl. Phys.* 27, L2241 (1988).
389. F. Leenhouts, J. Fünfschilling, R. Buchecker, and S. M. Kelly, *Liq. Cryst.* 5, 1179 (1989).
390. T. Geelhaar, *Ferroelectrics* 85, 329 (1988).
391. S. Nakamura and H. Nohira, *Mol. Cryst. Liq. Cryst.* 185, 199 (1990).
392. H. Nohira, S. Nakamura, and M. Kamei, *Mol. Cryst. Liq. Cryst.* 180, 379 (1990).
393. D. M. Walba, H. A. Razavi, N. A. Clark, and D. S. Parma, *J. Am. Chem. Soc.* 110, 8686 (1988).
394. M. D. Wand, R. Vohra, D. M. Walba, N. A. Clark, and R. Shao, *Mol. Cryst. Liq. Cryst.* 202, 183 (1991).
395. K. Yoshino, M. Ozaki, H. Taniguchi, M. Ito, K. Satoh, N. Yamasaki, and T. Kitazume, *Jpn. J. Appl. Phys.* 26, L77 (1987).
396. Y. Suzuki, T. Hagiwara, I. Kawamura, N. Okamura, T. Kitazume, M. Kakimoto, Y. Imai, Y. Ouchi, H. Takezoe, and A. Fukuda, *Liq. Cryst.* 6, 167 (1989).

397. A. Sakaigawa, Y. Tashiro, Y. Aoki, and H. Nohira, *Mol. Cryst. Liq. Cryst.* 206, 147 (1991).
398. Y. Aoki and H. Nohira, *Chem. Lett.* L113 (1993).
399. L. A. Beresnev and L. M. Blinov, *Ferroelectrics* 33, 129 (1981).
400. I. Sage, *Ferroelectrics* 85, 351 (1988).
401. D. M. Walba, K. F. Eidman, and R. C. Haltiwanger, *J. Org. Chem.* 54, 4939 (1989).
402. C. J. Booth, J. W. Goodby, J. P. Hardy, O. C. Lettington, and K. J. Toyne, *Liq. Cryst.* 16, 925 (1994).
403. D. M. Walba, R. T. Vohra, N. A. Clark, M. A. Handschy, J. Xue, D. S. Parma, S. T. Lagerwall, and K. Skarp, *J. Am. Chem. Soc.* 108, 724 (1986).
404. D. M. Walba and N. A. Clark, *Ferroelectrics* 84, 65 (1988).
405. G. Scherowsky and J. Gay, *Liq. Cryst.* 5, 1253 (1989).
406. K. Sakaguchi and T. Kitamura, *Ferroelectrics* 114, 265 (1991).
407. K. Sakashita, M. Shindo, J. Nakauchi, M. Uematsu, Y. Kageyama, S. Hayashi and T. Ikemoto, *Mol. Cryst. Liq. Cryst.* 199, 119 (1991).
408. G. Scherowsky and M. Sefkow, *Mol. Cryst. Liq. Cryst.* 202, 207 (1991).
409. G. Scherowsky, J. Gay, and M. Gunaratne, *Liq. Cryst.* 11, 745 (1992).
410. G. Scherowsky and M. Sefkow, *Liq. Cryst.* 12, 355 (1992).
411. S. Takehara, M. Osawa, K. Nakayama, T. Kusumoto, K. Sato, A. Nakayama, and T. Hiyama, *Ferroelectrics* 148, 195 (1993).
412. S. M. Kelly and J. Fünfschilling, *Ferroelectrics* 180, 269 (1996).
413. A. Maedicke, D. Demus, A. I. Pavluchenko, V. V. Titov, and N. I. Smirnova, *Cryst. Res. Tech.* 21, 111 (1986).
414. S. M. Kelly, J. Fünfschilling, and A. Villiger, *Liq. Cryst.* 14, 1169 (1993).
415. S. M. Kelly, *Liq. Cryst.* 14, 675 (1993).
416. H. Zäschke, *J. Prakt. Chem.* 317, 617 (1975).
417. K. Dimitrova, J. Hauschild, H. Zäschke, and H. Schubert, *J. Prakt. Chem.* 322, 933 (1980).
418. S. M. Kelly and J. Fünfschilling, *Mol. Cryst. Liq. Cryst.* 260, 139 (1995).
419. K. Terashima, M. Kikuchi, and K. Murashiro, EPA, U.S. Patent 0,454,157, 1991.
420. S. Saito, K. Kitano, K. Ohno, H. Inoue, and M. Ushido, European Patent Application 0,293,764, 1998.
421. H.-R. Dübal, C. Escher, W. Hemmerling, I. Müller, D. Ohlendorf, and R. Wingen, European Patent Application 0,307,880, 1988.
422. H., Zäschke and R. Stolle, *Z. Chem.* 15, 441 (1975).
423. T. Saurai, T. Yakota, E. Komatsu, N. Mikami, R. Higuchi, and K. Takeuchi, European Patent Application 0,260,077, 1987.
424. S. M. Kelly and J. Fünfschilling, *Liq. Cryst.* 19, 519 (1995).
425. S. M. Kelly, J. Fünfschilling, and F. Leenhouts, *Liq. Cryst.* 10, 243 (1991).
426. S. M. Kelly, *Liq. Cryst.* 5, 171 (1989).
427. S. M. Kelly, *Helv. Chim. Acta* 72, 594 (1989).
428. J. C. Jones, M. J. Towler, and J. R. Hughes, *Displays* 14, 86 (1993).
429. J. C. Jones, E. P. Raynes, M. J. Towler, and J. R. Sambles, *Mol. Cryst. Liq. Cryst. Lett.* 7, 91 (1990).
430. J. C. Jones and E. P. Raynes, *Mol. Cryst. Liq. Cryst.* 11, 199 (1992).
431. A. J. Slaney, V. Minter, and J. C. Jones, *Ferroelectrics* 178, 65 (1996).
432. G. W. Gray, M. Hird, D. Lacey, and K. J. Toyne, *J. Chem. Soc., Perkin Trans. 2*, 2041 (1989).
433. M. Hird, G. W. Gray, and K. J. Toyne, *Liq. Cryst.* 11, 531 (1992).
434. M. Hird and K. J. Toyne, *Mol. Cryst. Liq. Cryst.* 323, 1 (1999).
435. C. C. Dong, P. Styring, J. W. Goodby, and L. K. M. Chan, *J. Mater. Chem.* 9, 1669 (1999).
436. R. Eidenschink, R. Hopf, B. S. Scheuble, and A. E. F. Wächtler, "Proceedings of the 16th Freiburger Arbeitstagung Flüssigkristalle," Freiburg, Germany, 1986. p. 48.
437. V. Reiffenrath and M. Bremer, *Angew. Chem. Int. Ed. Engl.* 33, 1386 (1994).
438. U. Finkenzeller, A. E. Pausch, E. Poetsch, and J. Suermann, *Kontakte (Darmstadt)* 2, 3 (1993).